

South Dakota State University

Open PRAIRIE: Open Public Research Access Institutional Repository and Information Exchange

Electronic Theses and Dissertations

2019

Evaluation of the Effect of Carvedilol on the Thioredoxin Pathway in H9C2 Rat Cardiomyocytes

Metab Alharbi
South Dakota State University

Follow this and additional works at: <https://openprairie.sdstate.edu/etd>



Part of the [Pharmacy and Pharmaceutical Sciences Commons](#)

Recommended Citation

Alharbi, Metab, "Evaluation of the Effect of Carvedilol on the Thioredoxin Pathway in H9C2 Rat Cardiomyocytes" (2019). *Electronic Theses and Dissertations*. 3179.
<https://openprairie.sdstate.edu/etd/3179>

This Dissertation - Open Access is brought to you for free and open access by Open PRAIRIE: Open Public Research Access Institutional Repository and Information Exchange. It has been accepted for inclusion in Electronic Theses and Dissertations by an authorized administrator of Open PRAIRIE: Open Public Research Access Institutional Repository and Information Exchange. For more information, please contact michael.biondo@sdstate.edu.

EVALUATION OF THE EFFECT OF CARVEDILOL ON THE THIOREDOXIN
PATHWAY IN H9C2 RAT CARDIOMYOCYTES

BY
METAB ALHARBI

A dissertation submitted in partial fulfillment of the requirements for the

Doctor of Philosophy

Major in Pharmaceutical Sciences

South Dakota State University

2019

EVALUATION OF THE EFFECT OF CARVEDILOL ON THE THIOREDOXIN
PATHWAY IN H9C2 RAT CARDIOMYOCYTES

METAB ALHARBI

This dissertation is approved as a creditable and independent investigation by a candidate for the Doctor of Philosophy in Pharmaceutical Sciences degree and is acceptable for meeting the dissertation requirements for this degree. Acceptance of this does not imply that the conclusions reached by the candidate are necessarily the conclusions of the major department.

Teresa M. Seefeldt, Pharm. D., Ph.D. Date
Dissertation Advisor

Omathanu Perumal, Ph.D. Date
Head, Department of Pharmaceutical Sciences

Dean, Graduate School Date

الحمد لله حمدا يليق بجلاله، الحمد لله حمدا تستديم به النعم، الحمد لله على تيسيره وعونه على إتمام دراستي.

اهدي هذا العمل المتواضع الى

أمي وأبي الغاليين، فمهما كانا الامل الذي دفعني لإنجاز هذا العمل
 أجدادي وجداتي وأخص جدتي عائشة رحمها الله
 أخوتي وأخواتي عيدة وأسماء وسعود وليلى وهيفاء وعبد المحسن وأمجاد وعبد الرحمن وأبناء اخوتي فهم دافعي
 للإنجاز
 أقاربي وأخص عمي فالح وعمي محمد العيسى لتأثري وإعجابي الشديد بشخصياتهم منذ كنت طفلاً صغير.
 أصدقائي، وبالأخص هزاع العتيبي وعبد العزيز العنزي و يحيى هزازي و ماجد الموسى.
 أصدقائي من تعرفت عليهم في بلد الغربة وبالأخص جيسيك هرناندز

ACKNOWLEDGEMENTS

Finding a mentor for PhD dissertation is always hard and challenging, and it was more challenging for me when two of my best friends who came with me to the United States decided to change schools. That time was hard for me till January 23, 2015 when Dr. Seefeldt and I agreed to join her lab for my thesis dissertation. Till this day, and for the rest of my life, I will know that this was one of the best decisions I made. Dr. Seefeldt resolved all concerns and stresses I encountered regarding my school and research. Although Dr. Seefeldt was involved in many obligations at SDSU, I felt like I was on the top of the priority list. Dr. Seefeldt, with her own unique, passionate and motivating character, pushed me to excel and strive for success. Dr. Seefeldt always was considerate of all my needs, personally and professionally, leading me to succeed, improve and raise to the highest peaks on both levels. Her help and inspiration for me throughout my study was a big part of my success, and for that I am thankful and grateful.

I would like to thank and appreciate Dr. Xiangming Guan, Dr. Jayarama Gunaje, Dr. Becky Kuehl, Dr. Feng Li, Dr. Christophina Lynch, and Dr. Rakesh Dachineni for their constant help and support for this work. I also would like to thank Dr. Dennis D. Hedge, the former dean of the College of Pharmacy and Allied Health Professions, Dr. Jane Mort, the current Dean of the College of Pharmacy and Allied Health Professions, and Dr. Omathanu Perumal, Pharmaceutical Sciences Department Head, for providing the opportunity for me to pursue my PhD study and research in the College of Pharmacy and Allied Health Professions at South Dakota State University.

I would also want to thank my friends who contributed significantly to my study and research. First, Sami Alzarea for his tremendous contribution from his experience and broad knowledge. Yue Huang, Yahya Alqahtani, Shenggang Wang, Asim Najmi Ibrahim Abusulot, Abdulsalam Alqahtani and Ghalab Alotaibi who helped me in my day to day work in the lab throughout my study.

Finally, I would like to thank King Saud University and Saudi Arabian Culture Mission for the scholarship and fund support. I would also like to thank South Dakota State University and the Brookings community for accepting me to complete my study and for all of the life time memories that I got during my stay in United States.

CONTENTS

ABBREVIATIONS.....	xi
LIST OF FIGURES.....	xiii
LIST OF TABLES	xvii
ABSTRACT.....	xviii
CHAPTER 1. INTRODUCTION AND BACKGROUND.....	1
1.1 Thiol Redox State.....	1
1.2 Pathways Regulating Thiol Redox State.....	2
1.2.1 Thioredoxin	2
1.2.2 Thioredoxin Reductase.....	3
1.2.3 Thioredoxin-Interacting Protein	4
1.2.4 Glutathione	6
1.3 Free Radicals and Oxidative Stress	7
1.4 Oxidative Stress and Cardiovascular Disease	9
1.4.1 Heart Failure (HF).....	9
1.4.2 Atherosclerosis.....	10
1.4.3 Hypertension.....	11
1.5 TXNIP in Cardiovascular Disease.....	12
1.6 TXNIP and Glucose Regulation.....	13
1.7 Current Approaches to Modulate TXNIP	14

1.8 Carvedilol.....	15	
1.9 Doxorubicin.....	17	
1.10 Research Objectives.....	19	
CHAPTER 2: THE EFFECT OF CARVEDILOL ON THE THIOREDOXIN		
PATHWAY IN H9C2 CELLS.....		21
2.1 Introduction	21	
2.2 Materials and Methods.....	23	
2.2.1 Reagents and Antibodies	23	
2.2.3 Cell Culture.....	23	
2.2.4 Evaluation of Proteins in the Thioredoxin Pathway by Western Blot.....	24	
2.2.5 Rt-PCR	25	
2.2.6 Proteasomal Inhibition	25	
2.2.7 Isolation of Mitochondrial Fractions from H9c2 Cells.....	25	
2.2.8 Cell Fractionation and Nuclear Isolation	26	
2.2.9 Immunoprecipitation.....	26	
2.2.10 Thioredoxin Activity Assay.....	27	
2.2.11 Statistical Analysis.....	27	
2.3 Results.....	28	
2.3.1 Carvedilol’s Impact on Major Thioredoxin Proteins: Trx1, TrxR1, Trx2, TrxR2 and TXNIP	28	

2.3.2 Comparison with Other Beta-Blockers	28
2.3.3 Investigation of the mechanism of TXNIP Reduction.....	29
2.3.4 Impact of Carvedilol on TXNIP Localization in Nucleus and Mitochondria ..	29
2.3.5 Effect of carvedilol on TXNIP-PARP and TXNIP-Trx1 Protein Complexation	30
2.3.6 Effect of Carvedilol on Trx1 activity.....	30
2.4 Discussion	44
CHAPTER 3. THE EFFECT OF GLUCOSE CONCENTRATION AND OXIDATIVE STRESS ON TXNIP LEVEL IN H9C2 CELLS.	47
3.1 Introduction	47
3.2 Materials and Methods.....	50
3.2.1 Reagents and Antibodies	50
3.2.2 Cell Culture.....	50
3.2.3 Cell Viability	50
3.2.4 Glucose Effect on TXNIP Protein Expression in H9c2 Cells	51
3.2.5 Doxorubicin Treatment	51
3.2.6 Hypoxia and Reoxygenation	52
3.2.7 Radiation Procedure.....	52
3.2.8 Statistical Analysis.....	52
3.3 Results.....	53

3.3.1 Glucose Concentration Effect on Cell Viability	53
3.3.2 Impact of Glucose Concentration on TXNIP Expression	53
3.3.3 Impact of Doxorubicin Treatment on TXNIP Expression	53
3.3.4 Effect of Hypoxia Reoxygenation on TXNIP Expression	54
3.3.5 Effect of Radiation on TXNIP Expression.....	54
3.4 Discussion	61
CHAPTER 4. THIOREDOXIN PATHWAY MODULATION BY CARVEDILOL AND DOXORUBICIN TOXICITY IN H9C2 CELLS.....	65
4.1 Introduction.....	65
4.2 Materials and Methods.....	68
4.2.1 Reagents and Antibodies.....	68
4.2.2 Cell Culture.....	68
4.2.3 Cell Viability	69
4.2.4 Reactive Oxygen Species (ROS) Production	70
4.2.5 Examination of TXNIP, Trx1, TrxR1 and c-PARP Proteins in H9c2 Cells by Western Blot.....	70
4.2.6 Isolation of Mitochondrial Fractions from H9c2 Cells.....	71
4.2.7 Cell Fractionation and Nuclear Isolation	71
4.2.8 Immunoprecipitation.....	72
4.2.9 Statistical Analysis.....	73

4.3 Results.....	74
4.3.1 Cell viability	74
4.3.2 Effect of Carvedilol Pretreatment on Doxorubicin-Induced ROS Production.	74
4.3.3 Carvedilol and Doxorubicin Combination Impact on Major Thioredoxin Proteins: Trx1, TrxR1, Trx2, TrxR2 and TXNIP.....	75
4.3.4 Impact of Carvedilol on TXNIP Localization in Nucleus and Mitochondria ..	75
4.3.5 Carvedilol and Doxorubicin Combination Impact on PARP, cleaved PARP and ASK1 Level.....	76
4.3.6 Effect of carvedilol on Trx1-ASK1 and TXNIP-PARP Protein Complexation	76
4.4 Discussion	99
CHAPTER 5. CONCLUSIONS.....	105
Bibliography	110

ABBREVIATIONS

ASK1:	Apoptosis signal-regulating kinase 1
ATCC:	American Type Culture Collection
BSA:	Bovine serum albumin
Carv:	Carvedilol
CVD:	Cardiovascular diseases
Dox:	Doxorubicin
DMSO:	Dimethyl sulfoxide
EDTA:	Ethylenediamine tetraacetic acid
FBS:	Fetal bovine serum
GRx:	Glutaredoxin
GR:	Glutathione reductase
GS:	Glutathione synthetase
GSH:	Glutathione
GSSG:	Glutathione disulfide
GCS:	γ -glutamylcysteine synthase
GPx:	Glutathione peroxidase
HF:	Heart failure
H ₂ O ₂ :	Hydrogen peroxide
HDAC:	Histone deacetylase
HCl:	Hydrochloric acid
LDL:	Low-density lipoprotein
MTT:	3-(4,5-dimethylthiazolyl-2)-2, 5-diphenyltetrazolium bromide

NADPH:	Reduced nicotinamide dinucleotide phosphate
PARP:	Poly (ADP-ribose) polymerase
PBS:	Phosphate buffered saline
ROS:	Reactive oxygen species
SOD:	Superoxide dismutase
TRS:	Thiol redox state
TXNIP	Thioredoxin interacting protein
TBP-2:	Trx-binding protein 2
Trx:	Thioredoxin
Trx1:	Thioredoxin 1
Trx2:	Thioredoxin 2
TrxR1:	Thioredoxin reductase 1
TrxR2:	Thioredoxin reductase 2

LIST OF FIGURES

Figure 1. Redox cycle of thioredoxin.....	4
Figure 2. TXNIP-Trx Complexation.....	6
Figure 3. Reduced glutathione (GSH) and oxidized glutathione (GSSG).....	6
Figure 4. Carvedilol structure.....	17
Figure 5. Doxorubicin structure.....	18
Figure 6. Effect of 10 μ M carvedilol treatment on TXNIP in H9c2 cells after 24 and 48 hours of treatment. 100 μ M Verapamil was used as a positive control.	31
Figure 7. Effect of 10 μ M carvedilol treatment on Trx1 and TrxR1 in H9c2 cells after 24 and 48 hours of treatment.	32
Figure 8. Effect of 10 μ M carvedilol treatment on Trx2 and TrxR2 protein expression in H9c2 cells after 24 and 48 hours of treatment.	33
Figure 9. Effect of 10 μ M carvedilol treatment on TXNIP protein expression in CV-1 cells after 24 and 48 hours of treatment.	34
Figure 10. Time dependent effect of 10 μ M carvedilol on TXNIP protein in H9c2 cells for 2, 4, 12, 24, 48 and 72 hours.	35
Figure 11. Effect of propranolol, atenolol and metoprolol on TXNIP protein expression in H9c2 cells for 24 hours.....	36
Figure 12. Effect of 10 μ M carvedilol on TXNIP mRNA expression as measured by PCR. H9c2 cells were treated for 24 and 48 hours, before isolating mRNA.	37
Figure 13. Effect of protease inhibitor MG132 on carvedilol mediated degradation of TXNIP. H9c2 cells were treated for 24 hours.....	38

Figure 14. Effect of 10 μ M carvedilol on nuclear and cytoplasmic expression of TXNIP protein in H9c2 cells after 24 hours of treatment.....	39
Figure 15. Effect of 10 μ M carvedilol on mitochondrial expression of TXNIP protein in H9c2 cells after 24 and 48 hours of treatment.	40
Figure 16. Effect of 10 μ M carvedilol on expression of pERK in H9c2 cells after 24 hours of treatment.....	41
Figure 17. (A) Anti-TXNIP antibody immunoblots of untreated and 10 μ M carvedilol treated samples immunoprecipitated with anti-PARP antibody. (B) anti-Trx1 antibody immunoblots of untreated and 10 μ M carvedilol treated samples immunoprecipitated with anti-TXNIP antibody.	42
Figure 18. The effect of carvedilol treatment on Trx1 activity.....	43
Figure 19. Cell viability assay in H9c2 cells with no glucose, 25mM glucose and 50 mM glucose and growth medium for 3 days.....	55
Figure 20. Effect of no glucose medium on cytoplasmic TXNIP protein expression in H9c2 cells after 24 hours treatment.....	56
Figure 21. Effect of 50mM glucose medium on cytoplasmic TXNIP protein expression in H9c2 cells after 24 hours treatment.....	57
Figure 22. Effect of a single dose of 40 Gy of X-rays for 5 minutes on cytoplasmic TXNIP protein expression in H9c2 cells after 24 hours treatment.	58
Figure 23. Effect of hypoxia-reoxygenation procedure on cytoplasmic TXNIP protein expression in H9c2 cells after 6 hours hypoxia and 24 hours reoxygenation.....	59
Figure 24. Effect of 0.5 μ M doxorubicin treatment on cytoplasmic TXNIP protein expression in H9c2 cells after 24 hours treatment.	60

Figure 25. Cell viability assay in H9c2 cells treated with a combination of 10 μ M carvedilol and 0.5 μ M doxorubicin for 3 days.....	77
Figure 26. Cell viability assay in H9c2 cells treated with a combination of 10 μ M carvedilol and 0.5 μ M doxorubicin for 24 hours.	79
Figure 27. Cell viability assay in H9c2 cells treated with 10 μ M carvedilol pretreatment for 24 hours followed by treatment with carvedilol and 0.5 μ M doxorubicin for 24 hours.	81
Figure 28. Cell viability assay in H9c2 cells treated with a combination of 10 μ M propranolol and 0.5 μ M doxorubicin for 3 days.	83
Figure 29. Cell viability assay in H9c2 cells treated with 10 μ M propranolol pretreatment for 24 hours followed by treatment with propranolol and 0.5 μ M doxorubicin for 24 hours.	84
Figure 30. ROS production in H9c2 cells with pretreatment of carvedilol followed by treatment with carvedilol and doxorubicin for short time periods (30 minutes-4 hours)..	85
Figure 31. ROS production in H9c2 cells pretreatment with carvedilol followed by treatment with carvedilol and doxorubicin for 12 and 24 hours.	86
Figure 32. ROS production in H9c2 cells treated with a combination of carvedilol and doxorubicin for 12 and 24 hours.	87
Figure 33. Effect of 10 μ M carvedilol and 0.5 μ M doxorubicin treatments on cytoplasmic TXNIP expression in H9c2 cells after 24 hour treatment.....	88
Figure 34. Effect of 10 μ M carvedilol and 0.5 μ M doxorubicin treatments on nuclear TXNIP expression in H9c2 cells after 24 hour treatment.....	89

Figure 35. Effect of 10 μ M carvedilol and 0.5 μ M doxorubicin treatments on mitochondrial TXNIP expression in H9c2 cells after 24 hour treatment.....	90
Figure 36. Effect of 10 μ M carvedilol and 0.5 μ M doxorubicin treatments on Trx1 expression in H9c2 cells after 24 hour treatment.....	91
Figure 37. Effect of 10 μ M carvedilol and 0.5 μ M doxorubicin treatments on TrxR1 expression in H9c2 cells after 24 hour treatment.....	92
Figure 38. Effect of 10 μ M carvedilol and 0.5 μ M doxorubicin treatments on Trx2 expression in H9c2 cells after 24 hour treatment.....	93
Figure 39. Effect of 10 μ M carvedilol and 0.5 μ M doxorubicin treatments on TrxR2 expression in H9c2 cells after 24 hour treatment.....	94
Figure 40. Effect of 10 μ M carvedilol and 0.5 μ M doxorubicin treatments on PARP and cleaved PARP expression in H9c2 cells after 24 hour treatment.....	95
Figure 41. Effect of 10 μ M carvedilol and 0.5 μ M doxorubicin treatments on ASK1 expression in H9c2 cells after 24 hour treatment.....	96
Figure 42. Anti-ASK1 antibody immunoblots of 10 μ M carvedilol and 0.5 μ M doxorubicin treatments immunoprecipitated with anti-Trx2 antibody.....	97
Figure 43. Anti-TXNIP antibody immunoblots of 10 μ M carvedilol and 0.5 μ M doxorubicin treatments immunoprecipitated with anti-PARP antibody.....	98
Figure 44. Effect of carvedilol in TXNIP localization under normal conditions.	105

LIST OF TABLES

Table 1. H9c2 cells treated with a combination of 10 μ M carvedilol and 0.5 μ M doxorubicin for 3 days.....	78
Table 2. H9c2 cells treated with a combination of 10 μ M carvedilol and 0.5 μ M doxorubicin for 24 hours.	80
Table 3. H9c2 cells treated with 10 μ M carvedilol pretreatment for 24 hours followed by treatment with carvedilol and 0.5 μ M doxorubicin for 24 hours.....	82

ABSTRACT

EVALUATION OF THE EFFECT OF CARVEDILOL ON THE THIOREDOXIN
PATHWAY IN H9C2 RAT CARDIOMYOCYTES

METAB ALHARBI

2019

The thioredoxin (Trx) system is an endogenous antioxidant system that affects cell function and survival through controlling cellular redox status. Trx and TrxR are the main enzymes in this system while thioredoxin interacting protein (TXNIP) is a negative regulator. This study's goal was to better understand the Trx system's involvement in the cardiovascular disease and modulate the pathway through drug treatment.

Carvedilol is a non-selective β -blocker that also exhibits antioxidant properties, but the exact mechanism of the antioxidant effect is still unclear. H9c2 rat cardiomyocytes were used to examine the effect of carvedilol on the Trx system under normal conditions. Interestingly, carvedilol was able to decrease TXNIP not through its expression or proteasomal degradation but through increased TXNIP nuclear localization. Immunoprecipitation also showed an increase in TXNIP-PARP complexation in the nucleus and a decrease in Trx-TXNIP complexation in the cytosol. The results indicate that carvedilol may exhibit its antioxidant activity through altering TXNIP subcellular localization.

TXNIP is known to be important in both physiologic and pathophysiologic conditions. Western blot data showed that TXNIP in the cytosol will increase with increasing glucose concentration. Oxidative stress inducers such as doxorubicin, hypoxia-reoxygenation, and radiation were able to decrease cytosolic TXNIP.

Doxorubicin is a commonly utilized anticancer drug that induces oxidative stress and therefore causes cardiac toxicity. A study was conducted to determine if carvedilol could protect against doxorubicin-induced cardiotoxicity through TXNIP modulation. Carvedilol and doxorubicin alone reduced cytosolic TXNIP. Doxorubicin increased mitochondrial translocation of TXNIP accompanied by the induction of apoptosis. However, carvedilol was not able to prevent TXNIP mitochondrial translocation, but it did protect against doxorubicin-induced apoptosis. The complex of Trx2 and the pro-apoptotic ASK1 in the mitochondria was increased with carvedilol pretreatment followed by doxorubicin exposure. The increase in the ASK1-Trx2 complex can reduce apoptosis through decreased ASK1 activation. This was confirmed through Western blot of cleaved PARP. The findings are consistent with reports of TXNIP's response to mild oxidative stress conditions.

In conclusion, this study shows for the first time that carvedilol impacts TXNIP localization and complexation and that the Trx pathway may be involved in carvedilol's observed cardioprotective effect.

CHAPTER 1. INTRODUCTION AND BACKGROUND

1.1 Thiol Redox State

Thiol redox state (TRS) refers to the balance between reduced thiols and their corresponding disulfides. In living cells, TRS plays an important role in several biological processes including protein configuration, enzymatic function, and regulation of transcription factor action.¹

Thiols are organosulfur compounds characterized by a carbon-bonded sulfhydryl (-SH) functional group. Both protein thiols and non-protein thiols are present in cells. Protein thiols in the cell contain cysteine amino acid residues. Nonprotein thiols refer to low molecular weight thiols such as glutathione (GSH). Thiols have a very important antioxidant role in the biological system as a first line defense against free radicals and reactive oxygen species (ROS). Thiols can be oxidized to disulfides upon encountering free radicals or ROS. Some disulfide molecules are symmetric disulfides such as glutathione disulfide (GSSG) which is formed between two identical thiol-containing molecules. The mixed disulfides are formed between two different molecules, such as a protein thiol and GSH. Thiols can also act as reducing agents for certain protein disulfide bonds. The oxidized disulfides can be reduced back to their corresponding thiols by enzymes such as glutathione reductase (GR), glutaredoxin (Grx), and thioredoxin reductase (TrxR).²

The ratio between thiols and disulfides is used as an indicator of TRS. The normal ratio of GSH to GSSG in whole cell lysates is approximately 100:1. However, the ratio of thiols to disulfides varies by subcellular location; the GSH to GSSG ratio in the

endoplasmic reticulum can be as low as 1:1, for example. Thiol oxidative stress occurs when the ratio of thiols to disulfides is lower than normal. This can occur due to reductions in thiols and/or increases in the oxidized disulfides. Part of the cellular response to oxidative stress is to increase thiol antioxidant capacity; for example, induction of GSH synthesis occurs in response to oxidative stress.

1.2 Pathways Regulating Thiol Redox State

1.2.1 Thioredoxin

Thioredoxin (Trx) is an abundant antioxidant molecule that exists in multiple species including humans, plants, fungi, and some bacteria and archaea. In 1964, the initial Trx was found in *E. coli*, where it was acting as an electron donor for the ribonucleotide reductase enzyme. Later, it became obvious that thioredoxin plays essential roles in other cellular mechanisms.³ Trx can prevent or reduce ROS in the cell, regulate programmed cell death by maintaining apoptosis signal-regulating kinase 1 (ASK1) activity, act as a growth factor, and regulate DNA synthesis.^{4, 5}

Trx is a small molecular weight protein of ~12kDa.⁴ Human cells have three Trx isoforms: Trx1 in the cytosol, Trx2 in mitochondria, and Trx3 in testis. All Trx proteins have the same active catalytic motif of cysteine-glycine-proline-cysteine (Cys-Gly-Pro-Cys). The cysteine residues of this motif are used to reduce disulfide bonds in oxidized substrate proteins. This will result in a disulfide bond between the two cysteines which will be reduced back via the thioredoxin reductase enzyme (TrxR) with the help of nicotinamide adenine dinucleotide phosphate (NADPH) (Figure 1). The details of the Trx catalyzed reduction of protein disulfides are provided below.

The Trx catalytic reaction is a nucleophilic substitution reaction (SN2). The reaction starts with a nucleophilic attack of the N-terminal cysteine of the Cys-Gly-Pro-Cys motif on the disulfide. As a result of this step, there will be an intermediate disulfide complex between Trx and the substrate. This intermediate complex will be reduced by a nucleophilic attack by the C-terminal cysteine. This one catalytic reduction cycle will give a reduced protein and oxidized Trx. Trx in its disulfide form is more stable than reduced form. This alteration in stability between the disulfide and reduced forms of thioredoxin is an important driving force for the reaction to occur. There are multiple factors that affect the rate of the reduction reaction, such as the pKa of the cysteine, the geometry of a linear transition-state, the electrostatic atmosphere of the surrounding amino acids ^{6, 7}, the pH of the solvent ⁸ and entropy.⁹

The Trx-fold can be found in multiple proteins and is highly evolutionarily conserved. Trx catalyzed reduction of protein disulfides is critical for regulating of activity of multiple enzymes and therefore is important for maintenance of cellular homeostasis. Importantly, experiments with Trx knockout mice demonstrated that lack of this protein is embryonically lethal.¹⁰

1.2.2 Thioredoxin Reductase

Thioredoxin reductase (TrxR) is a member of the pyridine nucleotide disulfide oxidoreductase family, which is structurally different from other proteins as it includes a unique amino acid called selenocysteine (Sec).¹¹ Human TrxR is a 55kDa molecular weight protein. The catalytic domain of TrxR includes a selenothiol bond between the selenocysteine and the C-terminal cysteine.¹¹ TrxR has three major isoforms: TrxR1 is

cytosolic, TrxR2 is mitochondrial, and thioredoxin glutathione reductase (TGR) is testis specific. All three isoforms contain a Sec residue.¹² The main function of TrxR is to maintain thioredoxins in a reduced state. Other proteins, such as Glutaredoxin 2 (Grx2) and Protein Disulfide Isomerase (PDI), are also known to be reduced by TrxR.^{13, 14} It has also been associated with multiple cellular signaling mechanisms and acts like a direct antioxidant in the cell to maintain cellular redox homeostasis. Recently, inhibition of TrxR has been suggested as a target for cancer treatment.^{15, 16}

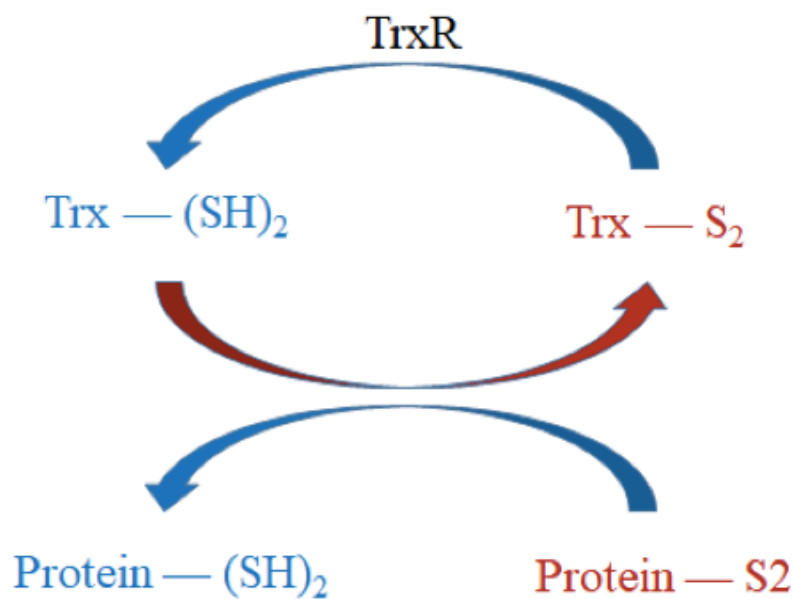


Figure 1. Redox cycle of thioredoxin

1.2.3 Thioredoxin-Interacting Protein

Thioredoxin-interacting protein (TXNIP), also known as vitamin D-upregulated protein (VDUP1) or thioredoxin-binding-protein-2 (TBP2), works as a biological

negative regulator for the Trx protein. TXNIP was initially cloned in the HL-60 leukemia cell line treated with 1,25-dihydroxyvitamin D3.¹⁷ Since its initial discovery, TXNIP has been identified as an important protein in both physiologic and pathophysiologic conditions. Literature reports indicate that TXNIP is able to block the function and activity of Trx. TXNIP can competitively bind to Trx and prevent it from binding to other proteins such as ASK1.¹⁸ TXNIP can inhibit Trx via formation of a mixed disulfide bond with the active site motif of reduced Trx (Figure 2). High expression of TXNIP can reduce Trx activity in cases leading to an increase in protein oxidation in the cell. TXNIP is a member of the α -arrestin superfamily of proteins and also exerts redox independent functions such as its ability to act as a cell growth regulator, a tumor suppressor gene, regulator of cell apoptosis, and modulator of the inflammatory response.¹⁰

TXNIP is a ubiquitously expressed redox protein and can localize between cellular compartments, mainly the cytosol, nucleus and mitochondria.^{3, 19, 20} Under normal conditions, TXNIP can be found in the cytosol and nucleus. Importin α is responsible for transport of TXNIP into the nucleus. TXNIP shuttles to the mitochondria under oxidative stress conditions. Beside TXNIP's ability to bind to Trx1 in the cytosol, it can also bind to poly (ADP-ribose) polymerase (PARP) in the nucleus. Under oxidative stress, TXNIP will bind to Trx2 in the mitochondria, leading to decreased Trx2 binding to ASK1. This will lead to ASK1 phosphorylation and activation, causing stimulation of the mitochondrial pathways of apoptosis by both cytochrome c release and caspase-3 cleavage.²¹

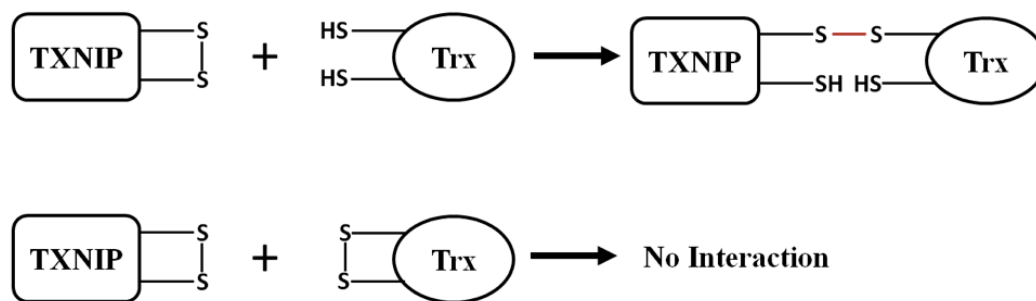


Figure 2. TXNIP-Trx Complexation

1.2.4 Glutathione

The tripeptide glutathione (GSH), γ -L-glutamyl-L-cysteinyl-glycine, is the most ubiquitous thiol in biological systems. The GSH concentration is high in most tissues (around 5 mM); however, the GSH concentration can vary in subcellular organelles. GSH is synthesized in the cytosol by the action of the enzymes γ -glutamylcysteine synthase (GCS) and glutathione synthase (GS). GSH serves a protective function in cells by acting as an antioxidant and nucleophile. The oxidized form GSSG is reduced back to GSH by the action of glutathione reductase (GR) (figure: 3).

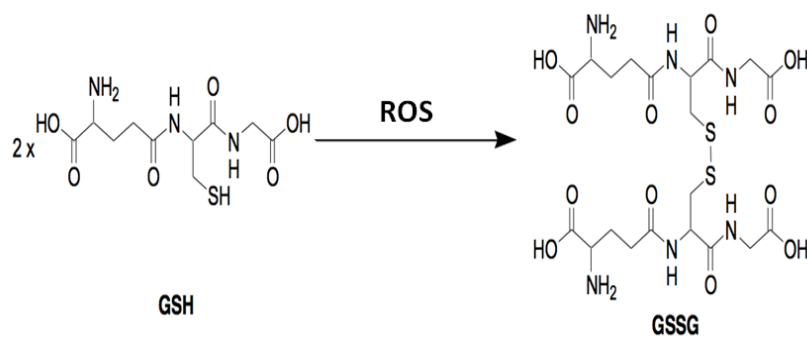


Figure 3. Reduced glutathione (GSH) and oxidized glutathione (GSSG)

1.3 Free Radicals and Oxidative Stress

Free radicals were discovered in the early 1900s by Moses Gomberg. It was thought that free radicals were not present in biological systems until the 1950s, when studies showed their existence and their role in disease pathogenesis and aging.²² Since then, understanding of the effect of free radicals on living organisms has expanded enormously. Free radicals were once thought to be only damaging species, but studies have proven that they play a major role in biological systems under normal conditions.

Free radicals are atoms or molecules which have unpaired electron or electrons in the outer orbital. Free radicals are unstable and highly reactive since they can attack other molecules to obtain electrons to be stable.²³ Molecules derived from oxygen are the most important free radicals. Oxygen free radicals include superoxide ($O_2^{\cdot-}$), hydroxyl (OH^{\cdot}), and peroxy radical (ROO^{\cdot}). The broader term reactive oxygen species (ROS) refers to both radical and nonradical reactive forms of oxygen. For example, peroxides are important nonradical ROS.

Normal cellular metabolism in living cells produces free radicals.²⁴ Studies have shown that most of the ROS are produced by the mitochondria respiratory chain and subsequently produce toxic metabolic byproducts.²⁵ Mitochondria produce ATP in which oxygen (O_2) is reduced to water. While mitochondrial respiration is occurring, the electron transport chain will release electrons from the incompletely reduced O_2 to form superoxide. Manganese superoxide dismutase (Mn-SOD) will convert that to H_2O_2 in the mitochondrial matrix.²⁶ ROS generated in mitochondria can migrate to the cytoplasm leading to oxidative damage to other cellular structures.²⁷ NADPH oxidase and cytochrome P450 contribute to ROS production for redox signaling and cell proliferation.

A small amount of ROS is produced at the endoplasmic reticulum and nuclear membrane which are mainly connected with the action of cytochrome P450 family enzymes.^{28,29}

Elimination of ROS is important to maintenance of cellular homeostasis.

Antioxidants are molecules that can quench damaging free radicals and ROS.

Antioxidants are divided into endogenous antioxidant systems and exogenously administered antioxidants. The thiol redox state systems described above are major endogenous antioxidant systems. Glutathione can directly quench ROS, or it can indirectly act as an antioxidant by acting as a cofactor for detoxifying enzymes such as glutathione peroxidase (GPX). The thioredoxin system acts as an antioxidant by regulating the protein thiol-disulfide ratio. Other endogenous antioxidant systems include superoxide dismutase (SOD) and catalase. Exogenous antioxidants primarily come from food or supplement sources such as ascorbic acid (vitamins C), α -tocopherol (Vitamin E), carotenoids, anthocyanins, and polyphenols.

The balance between the oxidation and elimination of ROS will result in a steady state redox balance in living cells. This balance can be disrupted for multiple reasons such as increased ROS production from endogenous or exogenous sources, decreased production or intake of antioxidants, or inactivation of major antioxidant enzymes. When one or more of these reasons occur, an imbalance occurs between ROS production and elimination. This will result in oxidative stress where damage to the cell and disruption of cellular functions can take place leading to several pathologies such as cardiovascular disease, cancer, diabetes mellitus, and autoimmune disorders.³⁰⁻³²

1.4 Oxidative Stress and Cardiovascular Disease

According to the World Health Organization's (WHO) global status report, cardiovascular disorders (CVD) are the leading causes of death worldwide. CVD causes 17.9 million deaths per year, 31% of deaths globally. CVD costs hundreds of billions of dollars globally, with expected costs of \$1044 billion by 2030.³³ CVD includes a variety of cardiovascular conditions including heart failure, myocardial infarction, stroke, arrhythmias, and heart valve diseases. There are well-known risk factors for CVD, for instance diabetes, aging, obesity, tobacco smoking, family history, and oxidative stress.

Although CVD are multifactorial diseases, oxidative stress has been found in several cardiovascular conditions. A direct cause and effect relationship between oxidative stress and CVD has not been clearly elucidated. Some literature has demonstrated specific damage to the cardiovascular system from oxidative stress leading to disease development. On the other hand, it can be claimed that oxidative stress may be a consequence of cardiovascular disease. Therefore, it may be associated with some secondary effects of the disease process. This is still an unsettled question based on data in the literature. A description of the effects of oxidative stress and thiol abnormalities in specific cardiovascular disorders can be found below.

1.4.1 Heart Failure (HF)

Heart failure is a complicated clinical disorder that can result from any structural or functional cardiac change that weakens the ability of the ventricle to work normally. HF is a leading cause of morbidity and mortality and causes multiple complications such as fluid retention, which also causes pulmonary congestion and peripheral edema, and

low cardiac output.³⁴ Extensive clinical and experimental studies over the past several years have shown significant evidence that oxidative stress is enhanced and might be a major player in HF.³⁵ The increased production of ROS, mainly ($O_2^{\cdot-}$), was observed in patients with congestive heart failure. The same study also showed a significant decrease in thiols such as GSH and SOD, as well as a decrease in vitamin C in those patients.³⁶ Those findings have been correlated with increased severity of heart failure.

Numerous reports have shown that Trx1 prevents apoptosis, which has a crucial role in the development of heart failure. Trx binds to the N-terminal region of ASK1 leading to decreased activation of ASK1 and inhibition of the ASK1-JNK-p38 apoptosis pathway.^{21,37} Furthermore, an in vivo study showed that overexpression of Trx1 prevented mitochondrial dysfunction and protected septic mice against heart failure.³⁸ Serum Trx also has been used as a biomarker for heart failure severity. TrxR2 plays an essential role in heart development and function. A study in TrxR2 knockout mice showed morphological changes in the development of the cardiac cells leading to death in a short time after birth.³⁹ TrxR2 inactivation in aging mice lead to increased ROS production and HIF-1 activation which led to mitochondrial damage and later cardiac failure.⁴⁰

1.4.2 Atherosclerosis

Oxidized low-density lipoprotein (LDL) uptake was shown to be one of the initial causes of atherosclerosis.⁴¹ Oxidized LDL is more easily taken up by macrophages to form foam cells, the initial step in fatty streak formation in atherosclerotic blood vessels. Lipid lowering agents, such as lovastatin, can reduce LDL oxidation.⁴² Iron catalyzed

free radical reactions may also be linked to development of atherosclerosis; an in vivo study found that atherosclerotic lesions formed in an animal model has a significant increase in iron content.⁴³

1.4.3 Hypertension

Increased levels of ($O_2^{\cdot-}$) and H_2O_2 have been reported with hypertension patients.⁴⁴ On the other hand, the levels of some antioxidants like GSH, vitamin D, and SOD have been reported to be decreased in hypertensive patients.^{45, 46} Vitamin C improved endothelial function by restoring the nitric oxide mediated vasodilation in hypertensive patients.¹⁹ The renin-angiotensin system (RAAS) has been associated with stimulating oxidative stress in vascular and endothelial smooth muscle cells, which might be a significant mechanism for the etiology of hypertension.⁴⁷

It should be noted that oxidative stress is not limited to hypertension, heart failure, or atherosclerosis as the presence of ROS has also been documented in other cardiovascular conditions such as diabetic cardiomyopathy and mitral regurgitation. Since ROS are known to reduce heart function, it appears that cardiovascular malfunctions seen in patients with different types of heart disease may be in part due to oxidative stress.

Because of the role identified for oxidative stress in CVD, use of antioxidants in treatment and prevention of CVD has been explored. Preclinical evidence suggested that exogenous antioxidants could be effective in CVD treatment. However, clinical trial data has been disappointing. To date, antioxidants have not shown beneficial effect in human trials for CVD treatment. In fact, some trials have shown that antioxidant treatment

contributed to negative outcomes. For example, vitamin E use in heart failure was not only ineffective, but it also increased heart failure hospitalizations. Possible reasons for this lack of clinical effect include pro-oxidant effects of small molecule antioxidants, the multifactorial nature of CVD, and the contribution of nonradical oxidative modifications.

1.5 TXNIP in Cardiovascular Disease

TXNIP has a crucial role in cardiovascular and non-cardiovascular disorder development due to its extensive physiological significance. The first study to examine TXNIP's effect on cardiomyocytes showed a significant decrease in the TXNIP gene expression in response to exposing NRVM cells, a rat neonatal ventricular cell line, to mechanical strain. In the same study, TXNIP was induced in the presence of ROS in a dose-dependent manner leading to cardiomyocyte apoptosis.⁴⁸ Another study showed that TXNIP knockout mice were less susceptible to cardiac hypertrophy after a month of pressure overload. However, this effect was lost after two months, and cardiac remodeling was detected in those mice.⁴⁹ This beneficial effect of TXNIP knockout was observed due to metabolic changes as the mice showed higher glucose uptake in the cardiomyocytes. In a different study, TXNIP was found to mediate Trx1 localization to the nucleus leading to regulation of multiple transcription factors such as histone deacetylase 4 (HDAC4), a negative regulator of cardiac hypertrophy.⁵⁰ In vivo, knockout of TXNIP improved cardiac function in a diabetic mouse model.¹⁰ In aging mice, TXNIP mRNA expression and protein level were higher than normal in the aorta, while decreasing TXNIP reduced mortality.⁵¹

TXNIP was found to be upregulated in an in vivo model of myocardial ischemia leading to apoptosis via ASK1 activation. TXNIP was also found to be involved in the cardiac remodeling occurrence after cardiac ischemia. TXNIP reduction was found to inhibit collagen synthesis and decrease myocardial scar tissue creation.¹⁸

TXNIP is connected very closely to lipid metabolism. Abnormalities in TXNIP can lead to atherosclerosis and increase the chance of developing coronary artery disease. HcB-19 mice, which have a mutation in the TXNIP gene leading to reduced expression, exhibit increased insulin secretion, hypoglycemia, and hypertriglyceridemia in the fasting state. It was hypothesized that this is due to abnormal cellular redox status caused by TXNIP downregulation.⁴⁰ On the other hand, TXNIP can cause atherosclerosis via decreased thioredoxin activity and subsequently TNF-induced inflammation leading to enhanced endothelial inflammation.¹⁸

1.6 TXNIP and Glucose Regulation

Numerous studies have demonstrated that TXNIP has a crucial role in hepatic glucose production. TXNIP expression increases under hyperglycemic conditions, and it has a critical role in the pathogenesis of diabetes. TXNIP has multiple metabolic effects which cause or aggravate diabetes, such as controlling insulin sensitivity, inhibiting glucose uptake in tissues, increasing production of glucose in the liver, and causing β -cell dysfunction.

Intracellular abnormalities in HcB-19 mice and TXNIP knockout mouse models have been well characterized.^{40, 49} TXNIP deficient mice undergo fasting hypoglycemia and loss of glucagon activity. Compared to normal mice, the livers of TXNIP knockout

mice produced significantly less glucose.⁴⁹ These hepatocytes were not affected by circulating hormones and other substrates. There was no effect in glycogen metabolism and the activity of glucose-6-phosphatase (G6-P) which is the main enzyme in gluconeogenesis. A different study showed that phosphoenolpyruvate carboxykinase (PEPCK), which is also the main enzyme in the metabolic pathway of gluconeogenesis, was unaffected in TXNIP knockout mice compared to normal mice.⁵² It's very well known that one of the main functions of TXNIP is controlling the redox status in the cellular system by influencing different molecules such as Trx and NADP/NADPH. This observation connects to the impact of TXNIP expression on glucose level since cellular redox status is documented to affect gluconeogenesis.⁵³

In an *in vivo* study, TXNIP reduction improved insulin function and decreased glucose level in diabetic mice.⁵⁴ Another study showed that TXNIP knockout increased insulin function and insulin receptor signaling in obese mice.⁵⁵ These data strongly support the redox and non-redox functions of TXNIP in glucose regulation and the need to control this protein in order to treat diabetes.

1.7 Current Approaches to Modulate TXNIP

Theoretically, TXNIP's physiological and pathophysiological effects can be modulated by altering its synthesis, elimination, expression level, activity, binding to ASK1 or PARP, or its localization and shuttling in the cell. Certain of these approaches have been previously reported in the literature.

In vitro, TXNIP overexpression induces apoptosis and also interferes with glucose metabolism.^{56, 57} There are several reports on the ability of insulin to suppress TXNIP.^{58,}

⁵⁹ A study on human adipocyte cells showed that insulin was able to reduce mRNA expression of TXNIP within four hours. In this same study, the authors examined the effect of insulin receptor knock-out on TXNIP expression. The study found that in insulin receptor KO mice treated with streptozotocin (STZ), insulin treatment failed to reduce TXNIP expression, indicating that the effect of insulin on TXNIP level is mediated through the insulin receptor.⁶⁰ Other studies have shown the ability of insulin to increase TXNIP ubiquitination and proteasomal degradation.⁶¹ cAMP activation by forskolin was also seen to escalate TXNIP ubiquitination and proteasomal degradation.⁶² Metformin activation of AMPK signaling, which has a crucial role in cellular metabolic homeostasis, can also inhibit TXNIP expression in pancreatic β -cells.⁶³

Verapamil and diltiazem, calcium channel blocking agents, have been shown to suppress TXNIP expression. An in vitro study showed that TXNIP mRNA expression and protein level were reduced with verapamil and diltiazem treatment. The same group showed that pancreatic β -cell survival rate increased in STZ-diabetic mice with those medications.⁵⁴ Verapamil is currently undergoing a randomized controlled trial for the reduction of TXNIP expression in β cells in type 1 diabetic patients.⁵⁸ Another study has shown that ramipril, an angiotensin-converting enzyme inhibitor, is able to suppress TXNIP expression leading to restoration of cardiovascular homeostasis.⁶⁴

1.8 Carvedilol

Carvedilol is a non-selective β -adrenoceptor blocker which also can cause peripheral vasodilation mainly by α 1-adrenergic blockade (Figure 4). Carvedilol is used in the treatment of heart failure and hypertension. The action of carvedilol in heart failure

is believed to be related to the β -adrenoceptor blockade. The sympathetic nervous system is activated in heart failure leading to tachycardia and reduced ventricular filling time. The β -adrenoceptor blockade reduces heart rate, increases filling time, and improves cardiac output. Multiple studies suggested that, in addition to carvedilol blockade of adrenergic receptors, it also possesses antioxidant activity.^{65, 66} Since oxidative stress has been observed in heart failure, it is possible that this antioxidant activity also contributes to carvedilol's therapeutic effectiveness in heart failure.

This antioxidant activity of carvedilol differentiates it from other β -adrenoceptor blockers. The mechanism of the antioxidant activity is not well understood yet, although some studies suggest that carvedilol acts as a free radical scavenger. Some other studies showed that carvedilol is able to suppress the enzymatic generation of ROS. There is some evidence that the additional mechanism for carvedilol may translate to improved therapeutic outcomes. A randomized controlled trial found that compared to metoprolol, a selective β_1 receptor blocker without antioxidant activity, carvedilol treatment in diabetic patients with hypertension resulted in a significant reduction of the inflammation marker microalbuminuria.⁶⁷ Furthermore, the COMET Trial showed a significant reduction in mortality with carvedilol treatment compared with metoprolol treatment in heart failure patients.⁶⁸ However, there is a need for more studies to fully understand the antioxidant mechanism of carvedilol and its effect in cardioprotectivity.

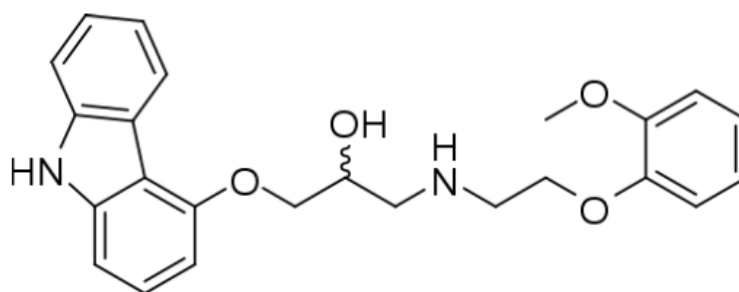


Figure 4. Carvedilol structure

1.9 Doxorubicin

Doxorubicin is an anthracycline compound that was first extracted from the pigment-producing *Streptomyces peucetius* (Figure 5). Doxorubicin is widely used in the treatment of a variety of cancers such as lung, thyroid, non-Hodgkin's and Hodgkin's lymphoma, prostate and sarcoma cancers. Doxorubicin is toxic to cardiomyocytes, where it can cause heart failure after multiple doses.⁶⁹ There is strong evidence suggesting that the mechanisms of anticancer activity are different than the mechanism of cardiotoxicity.

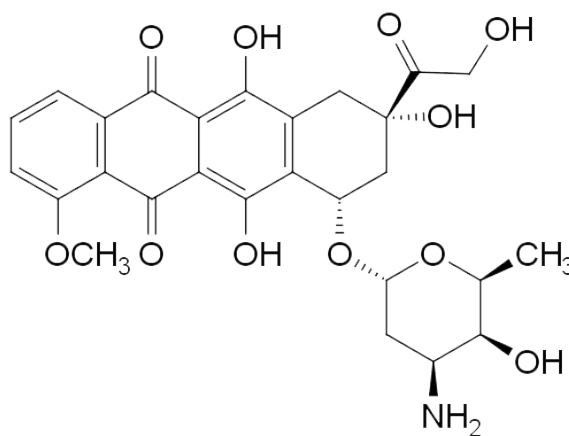


Figure 5. Doxorubicin structure

Doxorubicin can act as an intercalating agent with the cancer cells' DNA leading to blockade of macromolecular biosynthesis. It is also an inhibitor of topoisomerase II-mediated DNA repair which will interfere with the DNA replication step. Doxorubicin has also been shown to increase production of oxygen free radicals which can induce destruction of other cellular structures due to lipid peroxidation, DNA breaks, and activation of apoptotic pathways.⁷⁰

Doxorubicin toxicity can be acute (approximately 11%) where it happens within 72 hours after its administration; the most common acute cardiotoxicity is arrhythmia development. While the occurrence of chronic doxorubicin cardiotoxicity (occurring after a month of administration) is significantly lower (about 1.7%), it presents major clinical treatment challenges as the chronic toxicity limits the cumulative dose of doxorubicin that can be administered. Chronic doxorubicin toxicity has been associated with the development of cardiomyopathy and congestive heart failure. Several studies have suggested that doxorubicin cardiac toxicity is due to oxidative stress.⁷¹⁻⁷³ The major proposed mechanisms of doxorubicin cardiotoxicity are increased ROS and lipid peroxidation. Doxorubicin also decreases antioxidants in cardiac muscle including GSH and reduces activity of antioxidant enzymes such as TrxR and GPx.

It is likely that multiple mechanisms in addition to oxidative stress are contributing to doxorubicin cardiotoxicity.⁷⁰ For example, studies also showed doxorubicin is able to inhibit nucleic acid and protein synthesis, change adrenergic function, and reduce expression of cardiac-specific genes. Long-term administration of

doxorubicin in vivo stimulated an early reduction in ejection fraction and decreased sarcoplasmic reticular function.⁷⁴

1.10 Research Objectives

Oxidative stress and thiol oxidative stress have been shown to be important components in the pathogenesis of cardiovascular diseases. Therefore, finding an effective approach to mitigating these processes is required. Since direct antioxidants have not shown benefit in cardiovascular disease in clinical trials, alternative approaches are needed. One such approach is to modulate the activity of endogenous antioxidant systems such as the thioredoxin pathway.

Carvedilol is unique among other beta-blockers in that it exhibits antioxidant activity. Studies have shown efficacy of carvedilol in diseases such as heart failure that include a thiol oxidative stress component. The mechanism of carvedilol's antioxidant activity is still not fully understood. It is also unclear how this antioxidant activity contributes to carvedilol's efficacy in conditions where thiol oxidative stress occurs. Previous studies in this laboratory indicated that carvedilol's protection may involve modulation of the thioredoxin pathway. Therefore, the objective of this study was to measure the effect of carvedilol on the thioredoxin system, especially TXNIP, and its related pathways in cardiomyocytes. The specific aims of this research were:

1. To examine the effect of carvedilol on the thioredoxin system in H9c2 rat cardiomyocytes.
2. To evaluate the effect of glucose concentration and different oxidative stress inducers on H9c2 cell viability and TXNIP expression.

3. To explore the cardioprotective effects of carvedilol and its mechanisms in rat cardiomyocytes against doxorubicin toxicity.

CHAPTER 2: THE EFFECT OF CARVEDILOL ON THE THIOREDOXIN PATHWAY IN H9C2 CELLS

2.1 Introduction

Thioredoxin (Trx), thioredoxin reductase (TrxR), and thioredoxin-interacting protein (TXNIP) are the major proteins in the thioredoxin system, a thiol oxidoreductase system involved in maintenance of cellular redox status. The Trx active site includes a Cys-Gly-Pro-Cys motif which reduces disulfide bonds in other proteins, creating a disulfide bond in the Trx active site in the process which is then reduced by TrxR. The two isoforms of these proteins are localized in different places within the cell; Trx1 and TrxR1 are mainly found in the cytoplasm, while Trx2 and TrxR2 are found in the mitochondria. TXNIP, also known as thioredoxin binding protein-2 (TBP-2) and vitamin D3 upregulated protein (VDUP1), was originally identified as a negative regulator of Trx1; TXNIP forms a mixed disulfide with reduced Trx, therefore inhibiting its interaction with other proteins.³ In addition to regulation of redox status, the thioredoxin system regulates other pathways including apoptosis, cell cycle regulation, and glucose metabolism.^{21, 75, 76}

Redox state imbalances have been implicated in a number of disease states, including cardiovascular disorders such heart failure, diabetic cardiomyopathy, and ischemia-reperfusion injury.⁷⁷⁻⁷⁹ Since the thioredoxin system is an important regulator of cellular redox state and apoptosis, involvement of this pathway in cardiovascular disorders is an area of research interest. Previous research has shown upregulation of Trx1 or Trx2 is beneficial in protecting the heart from oxidative damage and inhibiting cardiomyocyte apoptosis.^{80, 81} On the other hand, TXNIP has been associated with the

development of cardiovascular disorders. Overexpression of TXNIP has been reported to induce oxidative stress through inhibition of Trx activity and apoptotic cell death through activation of ASK1, while knockdown of TXNIP in cardiomyocytes inhibits apoptosis and improves cell survival.⁸²⁻⁸⁵ Because of this role of the thioredoxin-related proteins in cardiovascular disorders, the pathway is a potential target for drug development.

Carvedilol, a non-selective α/β -blocker, is used clinically in the management of cardiovascular disorders such as heart failure. In addition to the adrenergic receptor blockade, carvedilol has also demonstrated antioxidant and antiapoptotic activities.⁸⁶ Previous literature reports have also shown that carvedilol can impact endogenous antioxidant pathways. Carvedilol induced a reduction in the ratio of reduced to oxidized glutathione and increased the activity of the enzyme glutathione peroxidase.⁸⁷⁻⁹¹ Two previous studies have examined the effect of carvedilol on Trx1 expression. The first study showed upregulation of thioredoxin expression in vascular smooth muscle cells treated with the active enantiomer of carvedilol.⁹² A recent article reported an increase in Trx1 expression following carvedilol treatment in spontaneously hypertensive rats.⁹³ The objective of this study was to conduct a comprehensive evaluation of carvedilol's impact on proteins in the thioredoxin system.

2.2 Materials and Methods

2.2.1 Reagents and Antibodies

Carvedilol (Sigma, C3993) was dissolved in DMSO; the final concentration of DMSO in cell culture studies was 0.2%. Propranolol (Sigma, P0884), atenolol (Sigma, A7655) and metoprolol (Sigma, M5391) were dissolved in water. MG132 (Santa Cruz, sc351846) and verapamil (Sigma, V-4629) were dissolved in ethanol. For RNA extraction, TRIzol reagent was purchased from Invitrogen (15596-026) and AccessQuick RT-PCR system from Promega (A1701).

Trx1 and PARP antibodies were purchased from Cell Signaling Technology (2298S and 9542); TrxR1 and TXNIP antibodies were obtained from Novus Biologicals, Inc (NBP2-27095 and NBP2-20619); antibodies to Trx2, TrxR2, Lamin A/C, actin, pERK, and secondary antibody goat anti-rabbit were purchased from Santa Cruz Biotechnology (sc-133201, sc-376868, sc-376248, sc-2004 and sc-7210); and the goat anti-mouse secondary antibody was obtained from Bio-Rad (170-6516).

2.2.3 Cell Culture

H9c2 rat embryonic cardiac myoblasts were purchased from the American Type Culture Collection (ATCC, Manassas, VA, USA) and maintained in Dulbecco's modified Eagle's medium (DMEM, ATCC). The CV-1 monkey kidney cell line was obtained from ATCC and maintained in Roswell Park Memorial Institute medium (RPMI 1640, HyClone, SH3002701). All medium contained 10% (v/v) fetal bovine serum and 1%

(v/v) penicillin/streptomycin, and cells were maintained at 37°C with 5% CO₂. Only cells with passage number below 20 were utilized.

2.2.4 Evaluation of Proteins in the Thioredoxin Pathway by Western Blot

Western blot was used to determine the protein level of TXNIP, Trx1, and TrxR1. Two million H9c2 cells were seeded to 75 cm² flasks and allowed to attach overnight. The cells were then treated with carvedilol 10 µM for 24 or 48 hours. Control cells were incubated with medium containing vehicle. Verapamil (50 and 100 µM) was used as a positive control in TXNIP analysis. TXNIP level was evaluated with other beta-blockers (propranolol, atenolol, and metoprolol; 10 µM) for comparison. TXNIP Western blot was also conducted in an additional cell line; in this study, two million CV-1 cells were treated with carvedilol 10 µM for 24 or 48 hours. Cells were collected by trypsinization and centrifuged at 1000 x g for 5 minutes. The cells were lysed in lysis buffer containing 20 mM HEPES (pH 7.4), 1% Triton X-100, 150 mM NaCl, 1 mM EDTA, 1 mM EGTA, and 1× broad-spectrum protease inhibitors (Thermo Fisher Scientific, 88665). Total protein concentrations were determined using the Bradford protein assay, and samples containing between 25-50 µg of protein were separated by 8% or 12% SDS-PAGE followed by transfer onto PVDF membranes. The membranes were blocked using 0.5% bovine serum albumin (BSA; Sigma, A3294) for 3 hours followed by incubation with primary antibody (1:10,000) for 12 hours. HRP-conjugated secondary antibody was then added for 1 hour at room temperature. Visualization was conducted using a kit from GE Biosciences and quantified using a Bio-Rad imaging system. Actin was used as the housekeeping protein. In addition, a Western blot for phosphorylated ERK was conducted following the same procedure.

2.2.5 Rt-PCR

Rt-PCR was performed according to the manufacturer's instructions (Promega). mRNA extracted from H9c2 cells was reverse transcribed (45 minutes at 45 °C) to cDNA using AMV reverse transcriptase followed by amplification of the cDNA product using PCR. The cDNA template was denatured at 94°C for 2 minutes followed by the 20/30/40 cycles, with each cycle having denaturation (94°C for 30 second, annealing (60°C for 60 seconds) and extension (60°C for 120 seconds), except for the last extension which was performed at 68°C for 5 minutes and held at 4°C. 1.2 % agarose gel containing ethidium bromide was used to run the PCR products. Primers used for PCR genotyping were:

TXNIP-FORWARD, 5'-TCAACGCTTTCTGCCTCTCT-3'

TXNIP-REVERSE, 5'-ACACCTTGGAAAGACCATGC-3'

GAPDH-FORWARD, 5'-CAACTCCCTCAAGATTGTCAGCAA-3'

GAPDH-REVERSE, 5'-GGCATGGACTGTGGTCATGA-3'

2.2.6 Proteasomal Inhibition

In order to investigate the impact on proteasomal degradation of TXNIP, two million H9c2 cells were placed in a 75 cm² flask and allowed to attach overnight. Cells were exposed to the proteasomal inhibitor MG-132 for 2 hours followed by treatment with carvedilol 10 µM or vehicle for 24 hours. The cells were collected by trypsinization and centrifuged at 1000 x g for 5 minutes. Cells were lysed in lysis buffer and Western blot was conducted as described above.

2.2.7 Isolation of Mitochondrial Fractions from H9c2 Cells

Ten million H9c2 cells were seeded in petri dishes (100 mm) and allowed to attach overnight. The cells were then treated with carvedilol 10 µM for 24 hours. Control

cells were incubated with medium containing vehicle. Mitochondrial fractions were isolated using a mitochondria isolation kit for cultured cells (Thermo Fisher Scientific, 89874), as per manufacturer's instructions. Western blot was conducted for Trx2, TrxR2 and TXNIP as described above. Cytochrome c was used as the housekeeping protein.

2.2.8 Cell Fractionation and Nuclear Isolation

The cytoplasmic and nuclear fractions were isolated as previously described.⁹⁴ H9c2 cells were seeded in 100-mm petri dishes overnight and then treated with carvedilol 10 μ M for 24 hours. Then cells were washed twice with cold phosphate buffered saline (PBS) and collected by scraping with 5 mL of hypotonic buffer [10 mM KCl, 1.5 mM MgCl₂, 1 mM sodium orthovanadate, 1 M Tris and 1x protease inhibitors (Thermo science #88665)]. The cells were centrifuged at 1000 x g for 10 minutes at 4°C. The pellet was resuspended in 600 μ L of cold hypotonic buffer. A loose fitting Dounce homogenizer over ice was used to gently separate the cytoplasmic and nuclear fractions followed by centrifugation (1000 x g for 7 minutes at 4°C). The nuclear fraction contained in the pellet was extracted with cold high salt buffer (10 mM Tris-Cl, pH 7.4, 400 mM NaCl, 25% glycerol and 1x protease inhibitors) for 30 minutes at 4°C and then centrifuged at 20817 x g at 4°C for 10 min. The supernatant was used for Western blot analysis as described above. Actin was used as the housekeeping protein.

2.2.9 Immunoprecipitation

H9c2 cells were treated with carvedilol 10 μ M for 24 hours. Following treatment, the cells were washed with PBS and scraped using lysis buffer. Protein concentrations were determined using the Bradford protein assay. 300 μ g total protein was immunoprecipitated with agarose-conjugated anti-PARP or anti-TXNIP antibody in 1 mL

of lysis buffer overnight at 4°C. The immunocomplexes were captured by adding 55 µL of protein G agarose and incubated for 3 hours at 4°C. Then the immunocomplexes were spun down at 300 RPM for 10 minutes and the pellet was washed three times with lysis buffer. The pellet was collected and suspended in SDS-sample buffer, boiled for 10 minutes, and then Western blot was conducted using anti-TXNIP or anti-Trx1 antibody.

2.2.10 Thioredoxin Activity Assay

H9c2 cells were harvested and lysed with lysis buffer (20mM HEPES at pH 7.4, 1% Triton X-100, 150mM NaCl, 1mM EDTA, 1mM EGTA, and 1× protease arrest). Trx activity was measured using a fluorescence assay kit (Cayman IMCO Corp., #FkTRX-02-V2), following the manufacturer's protocol. Briefly, the assay is based on the reduction of a disulfide bond in insulin by Trx. The insulin in the assay is labeled with eosin allowing for detection of Trx activity by fluorescence as the reduced insulin exhibits higher fluorescence compared to oxidized insulin. Around 10 µg of protein extract was used in the assay. Fluorescence was detected using an excitation wavelength of 520 nm and an emission wavelength of 545 nm. The increase in fluorescence was observed for 60 minutes. A standard curve was constructed using human recombinant Trx1.

2.2.11 Statistical Analysis

Data are expressed as means ± standard deviation (SD) from three independent experiments. Statistical analysis was done using ANOVA followed by Tukey's post hoc test. A p value of <0.05 was considered to be statistically significant.

2.3 Results

2.3.1 Carvedilol's Impact on Major Thioredoxin Proteins: Trx1, TrxR1, Trx2, TrxR2 and TXNIP

The protein level of TXNIP, Trx1, and TrxR1 was determined in the cytosol following 10 μ M carvedilol treatment for 24 and 48 hours. The mitochondrial isoforms Trx2 and TrxR2 were evaluated in the mitochondria after a 24 hour treatment. The cytosolic level of TXNIP decreased significantly with carvedilol treatment for 24 hours compared to control; this decrease was sustained at 48 hours. The positive control verapamil also reduced cytosolic TXNIP expression by 40% (Figure 6). Protein expression for Trx1, TrxR1, Trx2, and TrxR2 was not statistically significantly different from control at either time point (Figures 7 & 8).

In order to investigate if the reduction in TXNIP was cell line specific, TXNIP Western blots were conducted in CV-1 cells. A similar decrease in TXNIP in the cytosol was observed in the CV-1 cell line (Figure 9).

The time dependence of the effect of carvedilol on TXNIP expression was evaluated using Western blot. H9c2 cells were treated with carvedilol for 2, 4, 12, 24, 48, and 72 hours. No changes in TXNIP were observed through 12 hours; the decrease in cytosolic TXNIP was observed starting at 24 hours and was sustained through 48 and 72 hours (Figure 10).

2.3.2 Comparison with Other Beta-Blockers

To determine if the reduction in TXNIP is a class effect, three other beta-blockers were selected to represent the pharmacologic class. Propranolol is a nonselective beta-blocker like carvedilol while atenolol and metoprolol represent the beta-1 selective

agents. No decrease in TXNIP was observed with any of the other beta-blockers indicating that this may be a unique feature of carvedilol (Figure. 11).

2.3.3 Investigation of the mechanism of TXNIP Reduction

Since the protein level of TXNIP was reduced, rt-PCR was conducted to determine if gene expression was also changed. No change in TXNIP mRNA was found at either time point (24 and 48 hours) indicating that a change in gene expression was not responsible for the change in TXNIP protein level (Figure 12).

Proteasomal degradation of TXNIP was investigated using MG132, a non-specific proteasome inhibitor. If enhanced proteasomal degradation was responsible for the decrease in TXNIP observed with carvedilol exposure, proteasomal inhibition should reverse the effects. However, the reduction in TXNIP was still observed in the presence of MG132 (Figure 13).

2.3.4 Impact of Carvedilol on TXNIP Localization in Nucleus and Mitochondria

TXNIP is known to traffic between the nucleus, cytosol, and mitochondria. Therefore, TXNIP levels in subcellular fractions were determined. A statistically significant increase in TXNIP was found in the nuclear fraction (Figure 14). However, no change in TXNIP in the mitochondria was observed (Figure 15). This indicates that the reduction of TXNIP in the cytosol occurred due to enhanced sequestration of TXNIP in the nucleus. Lamin A/C protein was used for subcellular fractions verifying that the nuclear fractions were successfully separated from the cytosol. Similarly, cytochrome c was used to verify the mitochondrial isolation.

Because ERK signaling has been reported to be connected to importin-alpha nuclear transport, Western blot was conducted in H9c2 cells to measure the effect of 10

μ M carvedilol treatment for 24 hours on pERK expression. We observed a significant increase in pERK expression from carvedilol treatment (Figure 16).

2.3.5 Effect of carvedilol on TXNIP-PARP and TXNIP-Trx1 Protein Complexation

TXNIP is known to be complexed with PARP in the nucleus.⁹⁵ To verify the increase of TXNIP in the nuclear fraction, immunoprecipitation was performed for the PARP-TXNIP complex. Following immunoprecipitation with anti-PARP antibody, Western blot of untreated cells showed the presence of TXNIP indicating that the complex between TXNIP and PARP was present under normal conditions. The carvedilol treated samples showed an increase in the PARP-TXNIP complex providing further confirmation of increased TXNIP localization in the nucleus (Figure 17A).

Immunoprecipitation was also performed to determine the effect of carvedilol on the TXNIP-Trx1 complex in the cytosol. Carvedilol significantly decreased the TXNIP-Trx1 complex after 24 hours of treatment (Figure 17B).

2.3.6 Effect of Carvedilol on Trx1 activity

To illustrate the effect of carvedilol treatment on Trx1 activity, cells were treated with 10 μ M of carvedilol for 24 hours; then Trx1 activity in lysed cells was compared with a standard curve. The activity of Trx1 did not change between the control and treatment (Figure 18).

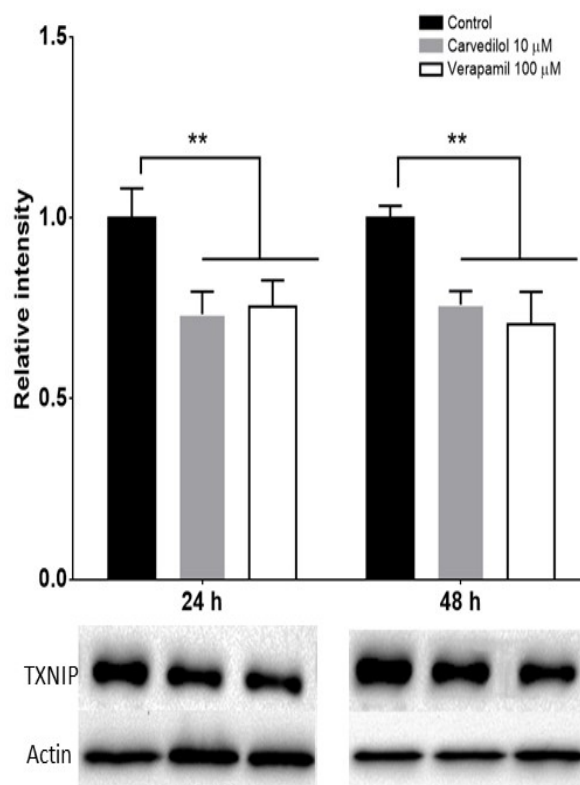


Figure 6. Effect of 10 μ M carvedilol treatment on TXNIP in H9c2 cells after 24 and 48 hours of treatment. 100 μ M Verapamil was used as a positive control.

The data are presented as relative intensity (protein/actin) and expressed as the means \pm SD of three independent experiments. Two-way ANOVA and Tukey's post hoc test were performed to analyze data at each time point. ** $p < 0.01$ compared with control group.

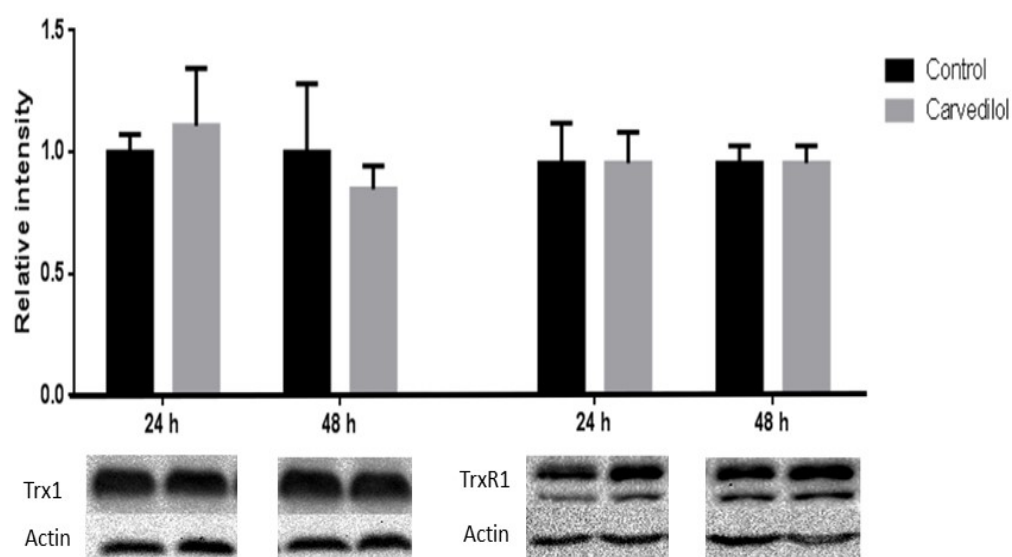


Figure 7. Effect of 10 μ M carvedilol treatment on Trx1 and TrxR1 in H9c2 cells after 24 and 48 hours of treatment.

The data are presented as relative intensity (protein/actin) and expressed as the means \pm SD of three independent experiments. Two-way ANOVA and Tukey's post hoc test were performed to analyze data at each time point. ** $p < 0.01$ compared with control group.

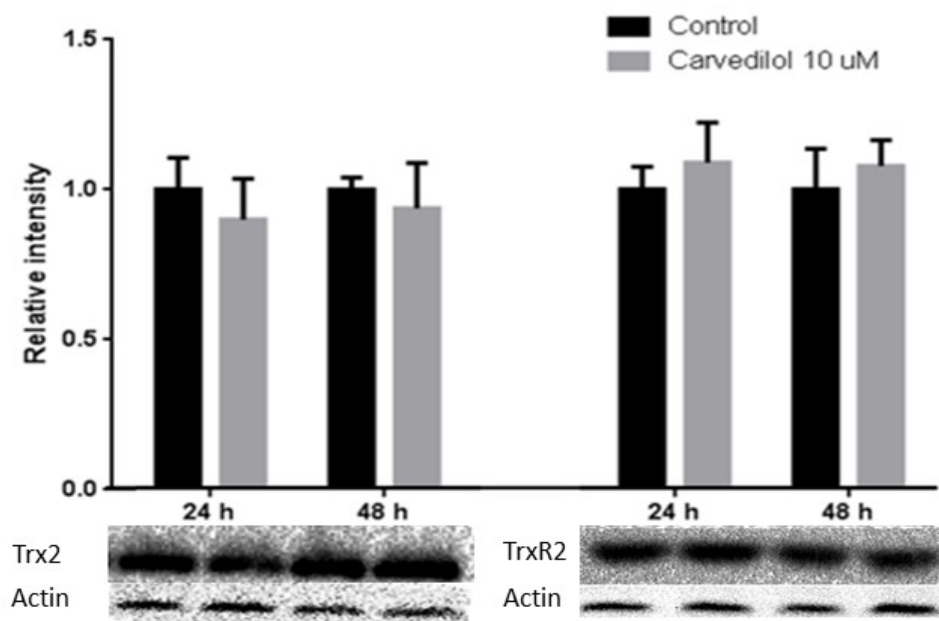


Figure 8. Effect of 10 μ M carvedilol treatment on Trx2 and TrxR2 protein expression in H9c2 cells after 24 and 48 hours of treatment.

The data are presented as relative intensity (protein/actin) and expressed as the means \pm SD of three independent experiments. Two-way ANOVA and Tukey's post hoc test were performed to analyze data at each time point. ** $p < 0.01$ compared with control group.

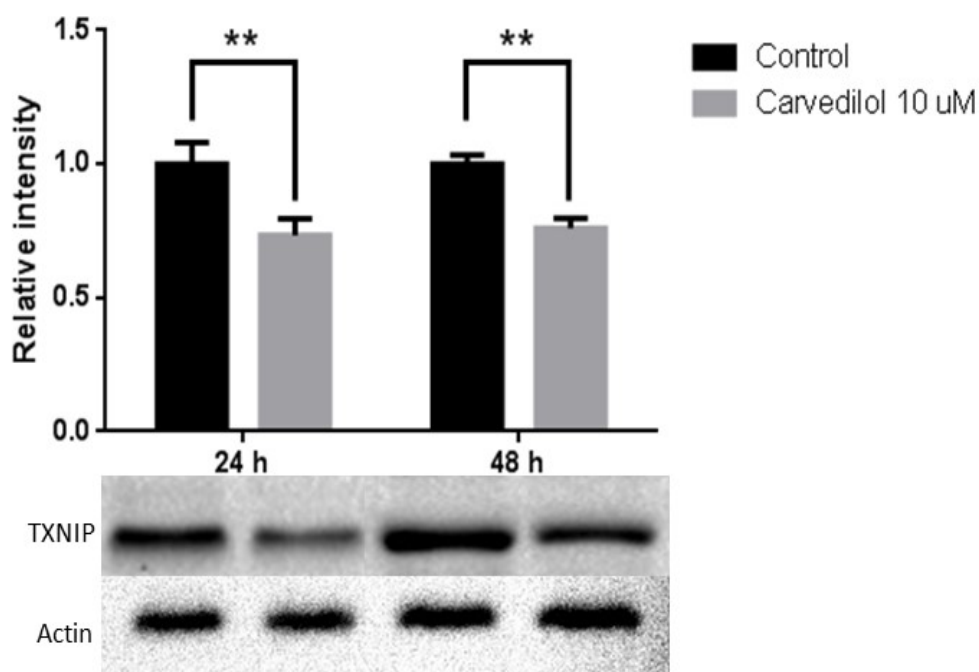


Figure 9. Effect of 10 μ M carvedilol treatment on TXNIP protein expression in CV-1 cells after 24 and 48 hours of treatment.

The data are presented as relative intensity (protein/actin) and expressed as the means \pm SD of three independent experiments. Two-way ANOVA and Tukey's post hoc test were performed to analyze data at each time point. ** $p < 0.01$ compared with control group.

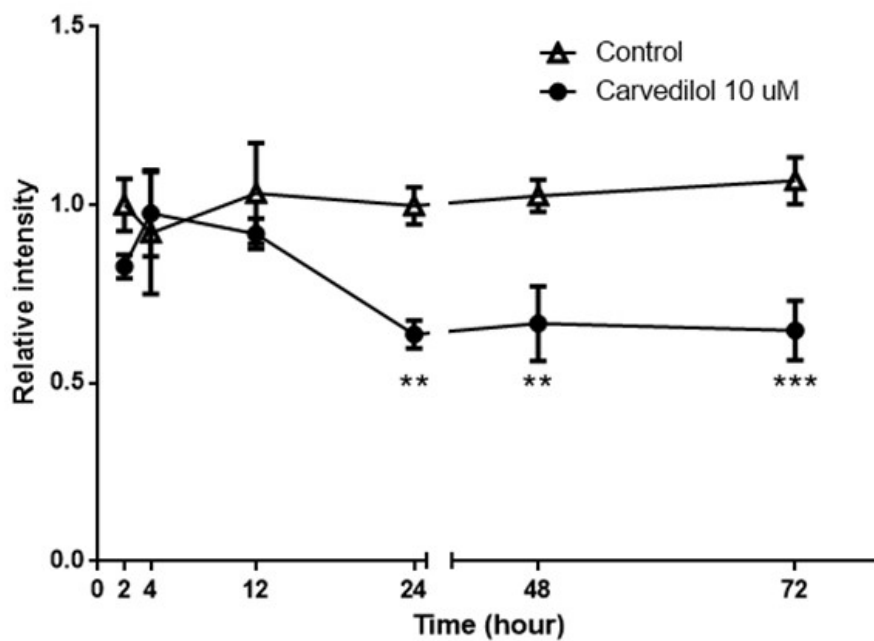


Figure 10. Time dependent effect of 10 μ M carvedilol on TXNIP protein in H9c2 cells for 2, 4, 12, 24, 48 and 72 hours.

The data are presented as relative intensity (protein/actin) and expressed as the means \pm SD of three independent experiments. Two-way ANOVA and Tukey's post hoc test were performed to analyze data at each time point.

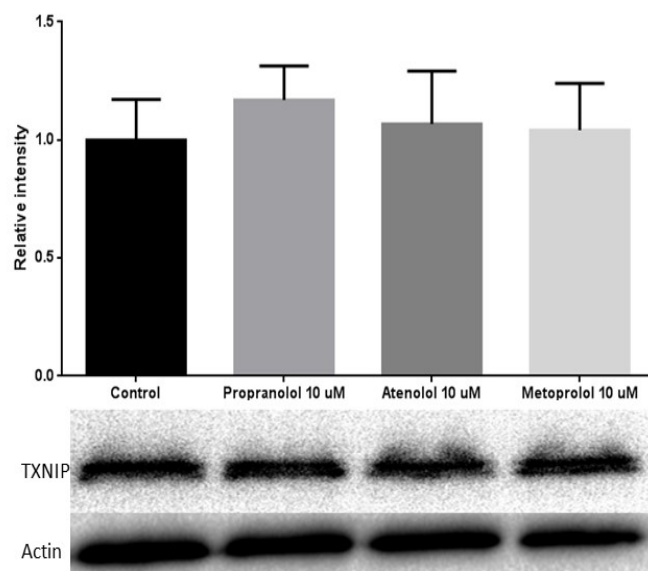


Figure 11. Effect of propranolol, atenolol and metoprolol on TXNIP protein expression in H9c2 cells for 24 hours.

The data are presented as relative intensity (protein/actin) and expressed as the means \pm SD of three independent experiments. One-way ANOVA and Tukey's post hoc test were performed to analyze data.

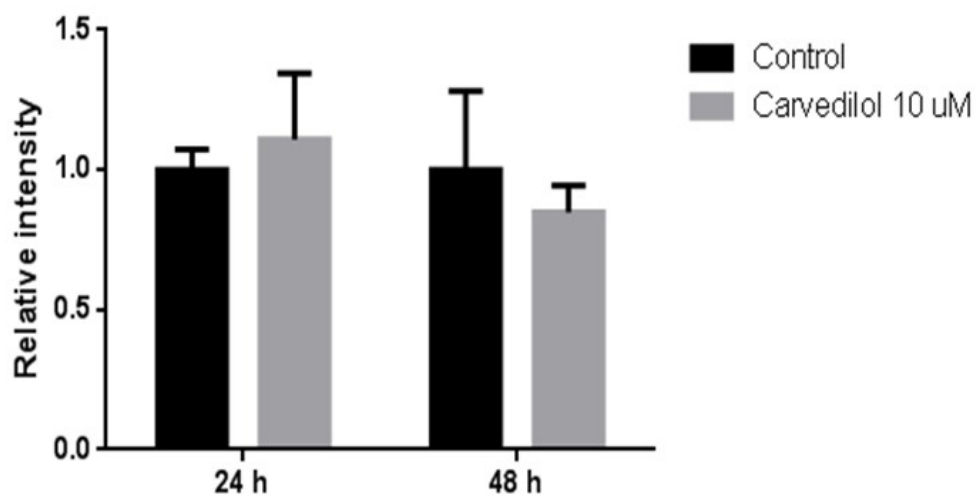


Figure 12. Effect of 10 μ M carvedilol on TXNIP mRNA expression as measured by PCR. H9c2 cells were treated for 24 and 48 hours, before isolating mRNA.

The data are presented as relative intensity (protein/actin) and expressed as the means \pm SD of three independent experiments. Two-way ANOVA and Tukey's post hoc test were performed to analyze data at each time point.

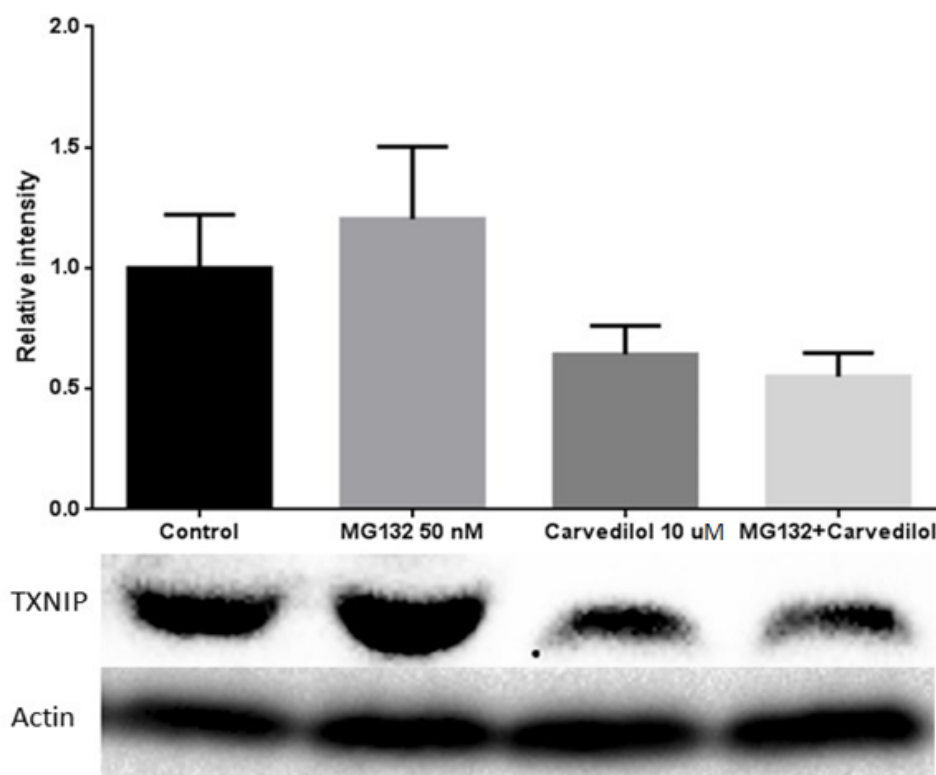


Figure 13. Effect of protease inhibitor MG132 on carvedilol mediated degradation of TXNIP. H9c2 cells were treated for 24 hours.

The data are presented as relative intensity (protein/actin) and expressed as the means \pm SD of three independent experiments. Two-way ANOVA and Tukey's post hoc test were performed to analyze data at each time point.

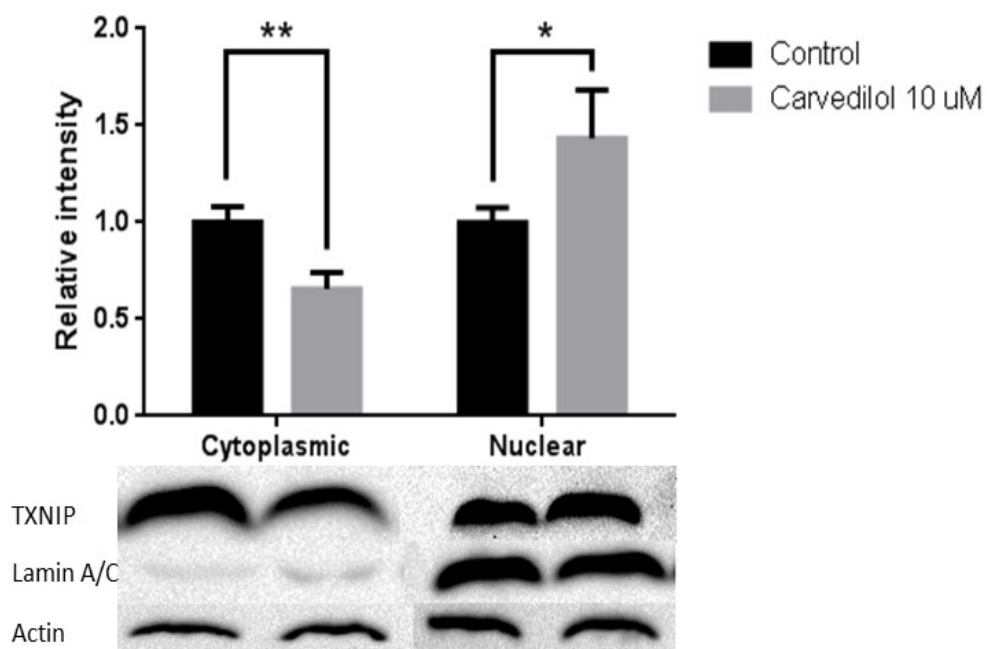


Figure 14. Effect of 10 μ M carvedilol on nuclear and cytoplasmic expression of TXNIP protein in H9c2 cells after 24 hours of treatment.

Lamin A/C was used to examine the purity of nuclear separation. The data are presented as relative intensity (protein/actin) and expressed as the means \pm SD of three independent experiments. Two-way ANOVA and Tukey's post hoc test were performed to analyze data at each time point. * $p < 0.05$ and ** $p < 0.01$ compared with control group.

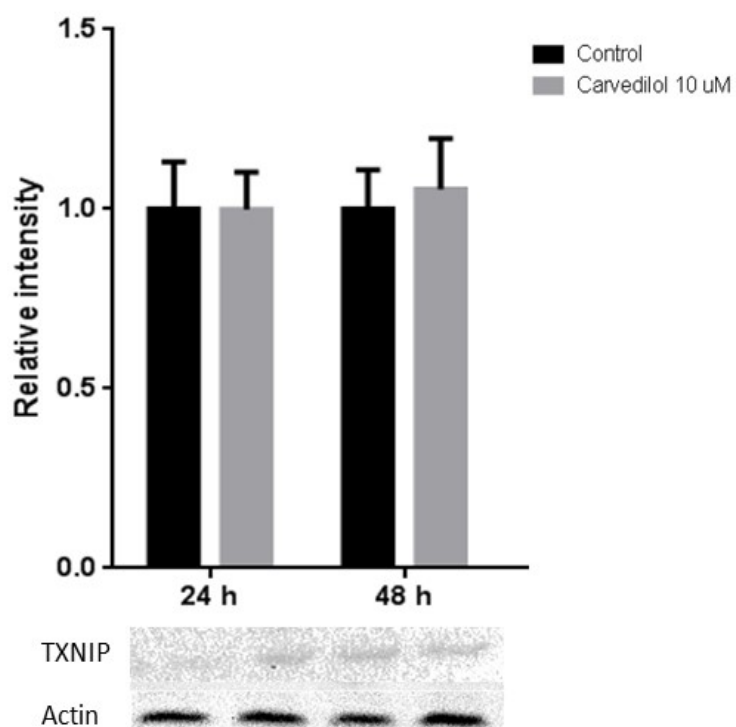


Figure 15. Effect of 10 μ M carvedilol on mitochondrial expression of TXNIP protein in H9c2 cells after 24 and 48 hours of treatment.

The data are presented as relative intensity (protein/actin) and expressed as the means \pm SD of three independent experiments. Two-way ANOVA and Tukey's post hoc test were performed to analyze data at each time point.

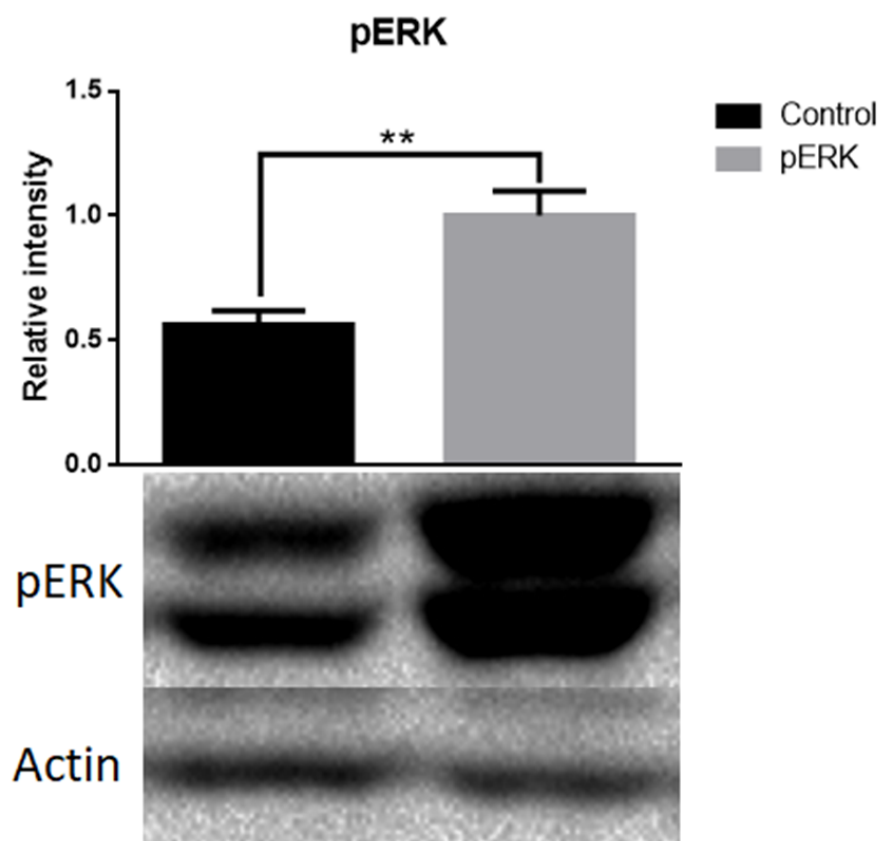


Figure 16. Effect of 10 μ M carvedilol on expression of pERK in H9c2 cells after 24 hours of treatment.

The data are presented as relative intensity (protein/actin) and expressed as the means \pm SD of three independent experiments. One-way ANOVA and Tukey's post hoc test were performed to analyze data at each time point. ** $p < 0.01$ compared with control group.

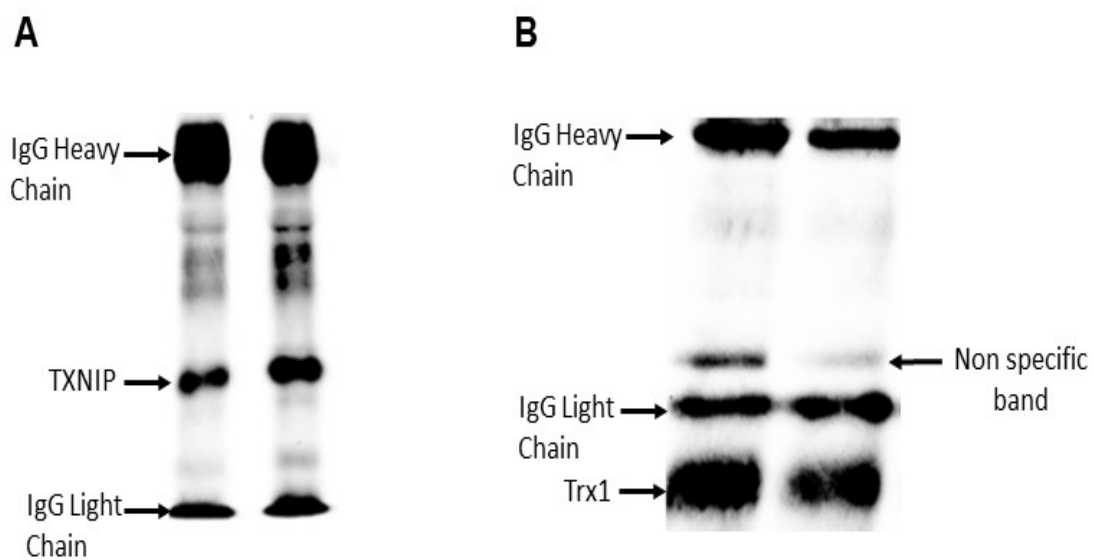


Figure 17. (A) Anti-TXNIP antibody immunoblots of untreated and 10 μ M carvedilol treated samples immunoprecipitated with anti-PARP antibody. (B) anti-Trx1 antibody immunoblots of untreated and 10 μ M carvedilol treated samples immunoprecipitated with anti-TXNIP antibody.

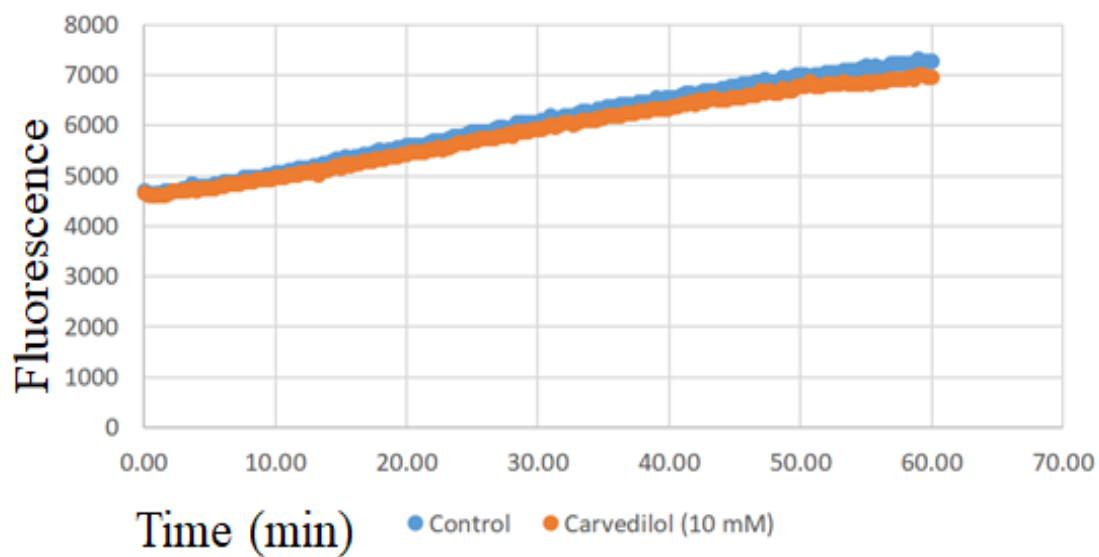


Figure 18. The effect of carvedilol treatment on Trx1 activity.

The data are presented as fluorescence intensity as the means \pm SD of three independent experiments. One-way ANOVA and Tukey's post hoc test were performed to analyze data at each time point.

2.4 Discussion

The present study was designed to explore the effect of carvedilol on the thioredoxin system in H9c2 cells. It was found that carvedilol treatment induced a statistically significant reduction in TXNIP in the cytosol. Further mechanistic studies showed that this reduction was not caused by decreased gene expression or increased protein degradation; instead, an increase in TXNIP in the nucleus was observed. Furthermore, carvedilol was also found to increase TXNIP-PARP complexation in the nuclear fraction and decrease TXNIP-Trx1 complexation in the cytosol.

Verapamil, a calcium channel blocker, has been reported to reduce TXNIP expression in vitro and in vivo.^{53, 54} In fact, verapamil is currently in clinical trials for TXNIP reduction in type 1 diabetes.⁹⁶ Therefore, verapamil was utilized as a positive control in this study. A similar reduction of TXNIP in the cytosol was observed between verapamil and carvedilol; however, the mechanism of reduction appears to be different between the two drugs. In response to verapamil treatment in mice, quantitative real-time rt-PCR showed a significant decrease in the gene expression of TXNIP.⁵³ No change in TXNIP mRNA was observed with carvedilol in this study indicating that a reduction in gene expression is not responsible for the decrease in TXNIP. Another study has shown that insulin was able to reduce the TXNIP level by degradation via the proteasomal pathway in pancreatic INS-1 cells.²⁷ The decrease in TXNIP by carvedilol was not reversed by proteasomal inhibition by MG132 indicating that this is also not the mechanism for carvedilol's reduction in TXNIP.

Endogenous TXNIP is known to shuttle between subcellular compartments. In the cytosol, TXNIP is found complexed with Trx under normal conditions.⁹⁷ Importin α was

found to move TXNIP between the cytosol and nucleus.^{76, 98} PARP is a nuclear protein activated by DNA damage associated with oxidative stress.⁹⁹ Studies have shown that under basal conditions PARP complexes with TXNIP, preventing it from migration to the mitochondria. In this study, carvedilol treatment showed a significant increase in TXNIP in the nucleus with an accompanying increase in TXNIP-PARP complexation. The reduction of cytosolic TXNIP with carvedilol treatment was accompanied by a decrease in TXNIP-Trx1 complexation in the cytosol. Because the total amount of Trx1 in the cytosol remained unchanged with carvedilol treatment, the reduction in the complex indicates that there would either be an increase in free Trx or an increase in Trx1 complexation with other proteins such as the pro-apoptotic ASK1. This indicates that carvedilol may be reducing oxidative stress and/or protecting cells against apoptosis via modulation of the thioredoxin pathway. The mechanism by which carvedilol increases TXNIP accumulation in the nucleus is not known and will require further study.

TXNIP has also been shown to translocate to the mitochondria in response to oxidative stress.^{98, 100, 101} Under oxidative stress, TXNIP shuttles to the mitochondria and binds to Trx2, which will lead to ASK1 release mediating cell apoptosis.⁶⁴ Since these studies were not conducted in cells undergoing oxidative stress, no change in Trx2, TrxR2, and TXNIP in the mitochondria was expected. The results confirmed that there was no change in Trx2 or TrxR2 with carvedilol treatment, and TXNIP was not detected in the mitochondria.

Our hypothesis was that Trx activity would increase with carvedilol treatment due to the decrease in the cytosolic TXNIP. Unexpectedly, no change in Trx activity was observed. A literature search revealed another study where Trx activity did not change

with a decrease in TXNIP. This study found that TXNIP knockout produced cardioprotection independent of Trx activity.¹⁰⁶ This indicates that a change in Trx activity would not be required for carvedilol to have a positive impact on cardiac function through TXNIP modulation. On other hand, the literature indicates that ERK signaling may be involved in nuclear translocation.¹⁰² Another study showed that TXNIP knockout was associated with a significant increase in phosphorylation of ERK. That is consistent with our findings as pERK significantly increased with the reduction of TXNIP in the cytosol and its increase in the nucleus.

In conclusion, carvedilol treatment in H9c2 cells produced an increase in TXNIP in the nucleus paired with increased PARP-TXNIP complexation. This potentially could impact oxidative stress and apoptosis in cardiomyocytes treated with carvedilol. Further studies will reveal the impact of increased nuclear TXNIP on oxidative stress and apoptosis.

CHAPTER 3. THE EFFECT OF GLUCOSE CONCENTRATION AND OXIDATIVE STRESS ON TXNIP LEVEL IN H9C2 CELLS.

3.1 Introduction

Thioredoxin-interacting protein (TXNIP), also known as vitamin D-upregulated protein (VDUP1) or thioredoxin-binding-protein-2 (TBP2), acts as a biological negative regulator for the thioredoxin (Trx) protein. TXNIP has been identified as an important protein in both physiologic and pathophysiologic conditions. The main physiological effect TXNIP has is its ability to regulate the cellular redox state by binding and preventing Trx in a redox dependent manner. TXNIP is also a member of the α -arrestin superfamily of proteins and can utilize redox independent mechanisms such as acting like a cell growth regulator, a tumor suppressor gene, regulator of cell apoptosis, and modulator of the inflammatory response.¹⁰

Numerous studies have shown that TXNIP plays a significant role in the pathogenesis of diabetes. TXNIP expression was found to be induced in pancreatic β -cells under high glucose conditions. TXNIP reduction in a diabetes mouse model improved insulin function and decreased glucose level.⁵⁴ Knocking out TXNIP in obese mice increased insulin function and signaling of the insulin receptor.⁵⁵ Verapamil, a calcium channel blocker, is currently undergoing randomized controlled trials for its ability to decrease TXNIP expression in β cells in type 1 diabetic patients.⁵⁸ These data strongly support the important role of TXNIP redox and non-redox functions in glucose regulation and the need to better regulate this protein in order to treat diabetes and related conditions such as diabetic cardiomyopathy.

Literature reports have shown the significant role of TXNIP in cardiovascular disease development. In neonatal rat ventricular myocytes cells (NRVM), TXNIP expression was significantly increased in response to ROS induction in concentration-dependent manner.⁴⁹ Diabetic cardiomyopathy is a cardiac dysfunction associated with diabetic patients where hyperglycemia in the heart leads to ventricular dysfunction and heart failure. A study diabetic mouse hearts showed that deletion of the TXNIP gene will enhance cardiac inotropy leading to enhanced cardiac function in those mice.⁶⁰

Under oxidative stress, TXNIP is able to block the function and activity of Trx by competitively binding to Trx and preventing it from binding to other proteins such as ASK1. TXNIP can inhibit Trx via formation of a mixed disulfide bond with the active site motif of reduced Trx. High expression of TXNIP under oxidative stress can reduce Trx activity leading to an increase in protein oxidation in the cell.

In the previous chapter, we have seen that carvedilol, an antioxidant beta blocker, has the ability to decrease TXNIP expression in H9c2 cells under normal conditions. Carvedilol was able to move TXNIP to the nucleus and increased its complexation with the PARP protein. However, much is still unknown about the effect of glucose concentration and reactive oxygen species inducers in TXNIP expression in normal cardiac cells. Therefore, our objectives in this study were:

1. To evaluate the cell viability of H9c2 cells under different concentrations of glucose

2. To determine the effect of glucose concentration on TXNIP expression in H9c2 cells
3. To measure TXNIP expression under different oxidative stress induction conditions in H9c2 cells

3.2 Materials and Methods

3.2.1 Reagents and Antibodies

Doxorubicin (SIGMA, D1515) was dissolved in DMSO to make a 0.5 mM stock solution and was filtered using a Medical Millex-GP filter (0.22 μm , sterilized; Millipore). The final concentration of DMSO in cell culture studies was less than 0.2%. Stock solutions were saved at -80°C and were diluted in growth medium to the desired concentrations for cell culture treatment. TXNIP antibody was obtained from Novus Biologicals, Inc (NBP2-20619). Actin antibody and secondary antibody goat anti-rabbit were purchased from Santa Cruz Biotechnology (sc-2004 and sc-7210).

3.2.2 Cell Culture

In this study, rat embryonic cardiac myoblasts, H9c2 cells, were purchased from the American Type Culture Collection (ATCC, Manassas, VA, USA) and maintained in Dulbecco's modified Eagle's medium (DMEM, ATCC). Growth medium contained 10% (v/v) fetal bovine serum and 1% (v/v) penicillin/streptomycin, and cells were maintained at 37°C with 5% CO_2 . All experiments were performed in a passage number below 20.

3.2.3 Cell Viability

H9c2 cells were seeded and treated in a 96-well plate, and cell viability was measured by colorimetric assay containing MTT (3-(4, 5)-dimethylthiazol-2, 5-diphenyltetrazolium bromide). H9c2 cells with density of 1,000 cells/well were seeded and allowed to attach overnight. Growth medium was then removed, and medium with no glucose, 25mM glucose, or 50 mM glucose was added to the cells for 3 days. Then MTT assay was conducted by replacing the medium with medium containing 0.5 mg/ml MTT solution (50 μl /well) and incubated in the dark at 37°C for 4 hours. DMSO was used to

dissolve the formed purple formazan product (150 μ l/well for one hour). A SpectraMax M2 microplate reader (Molecular Devices, Sunnyvale, CA, USA) was used to measure the absorbance of each well by using a test wavelength of 570 nm and a reference wavelength of 650 nm.

3.2.4 Glucose Effect on TXNIP Protein Expression in H9c2 Cells

Two million H9c2 cells were seeded in 75 cm² flasks and allowed to attach overnight. Medium with no glucose, 25 mM glucose, or 50 mM glucose was added for 24 hours. Then cells were detached using trypsin and centrifuged at 1000 x g for 5 minutes. The cells were separately lysed in lysis buffer containing 20 mM HEPES (pH 7.4), 1% Triton X-100, 150 mM NaCl, 1 mM EDTA, 1 mM EGTA, and 1 \times broad-spectrum protease inhibitors (Thermo Fisher Scientific, 88665). Bradford protein assay was used to determine the total protein concentration, and samples containing 50 μ g of protein were separated by 8% SDS-PAGE followed by transfer onto PVDF membranes. 0.5% bovine serum albumin (BSA; Sigma, A3294) was used to block the membranes for 3 hours followed by incubation with primary antibody (1:10,000) overnight. HRP-conjugated secondary antibody was then added for 1 hour at room temperature. Visualization of the bands was performed using a kit from GE Biosciences and quantified using a Bio-Rad imaging system. For this experiment, actin was used as a housekeeping protein.

3.2.5 Doxorubicin Treatment

Two million H9c2 cells were seeded in 75 cm² flasks and allowed to attach overnight. The cells were then treated with doxorubicin 0.5 μ M. Control flasks were incubated with medium containing vehicle during the treatment period. Sample collection and western blot was performed as described above.

3.2.6 Hypoxia and Reoxygenation

Hypoxia and reoxygenation were conducted using a method reported by Liao et al, with minor modification.¹⁰⁴ Two million H9c2 cells were seeded in 75 cm² flasks and allowed to attach overnight in 25 mM glucose DMEM. Cells then were washed with PBS buffer twice, and new medium was added. The flask then was placed for 6 hours in a hypoxia chamber, saturated with 5% CO₂/95% N₂. After that, cells were incubated for reoxygenation in an incubator containing 5% CO₂ at 37°C for another 24 hours.

3.2.7 Radiation Procedure

Two million H9c2 cells were seeded in 75 cm² flasks and allowed to attach overnight in DMEM. A single dose of 40 Gy of X-rays for 5 minutes was directed to the cells using a 160-kVp X-ray high energy linear accelerator using Faxitron cabinet irradiator (Faxitron Bioptics, Lincolnshire, IL).

3.2.8 Statistical Analysis

Data are expressed as means \pm standard deviation (SD) from three independent experiments. Statistical analysis was done using ANOVA followed by Tukey's post hoc test. A p value of <0.05 was considered to be statistically significant.

3.3 Results

3.3.1 Glucose Concentration Effect on Cell Viability

The regular growth medium (DMEM) for H9c2 cell growth contains 25 mM glucose. Since different glucose concentrations would be utilized for the study of TXNIP expression, a cell viability assay was conducted to determine the effect of glucose concentration on H9c2 cell viability. An MTT assay was conducted to determine cell viability in cells incubated with 50 mM glucose, 25 mM glucose, or no glucose for 72 hours. No significant change in cell viability with the different glucose concentrations was observed (Figure 19).

3.3.2 Impact of Glucose Concentration on TXNIP Expression

H9c2 cells were treated with different concentrations of glucose and TXNIP expression was measured. TXNIP level was increased significantly with increasing glucose concentration. When incubated with glucose free DMEM compared to 25 mM glucose DMEM, H9c2 cell expression of cytosolic TXNIP was significantly reduced to less than 50% of the normal level (Figure 20). When the glucose concentration was doubled to 50 mM, the cells exhibited a 1.5-fold increase in TXNIP expression (Figure 21).

3.3.3 Impact of Doxorubicin Treatment on TXNIP Expression

H9c2 cells were treated with 0.5 μ M doxorubicin, and TXNIP expression was measured by western blot. The expression of TXNIP was decreased around 50% with doxorubicin exposure (Figure 24).

3.3.4 Effect of Hypoxia Reoxygenation on TXNIP Expression

H9c2 cells were reoxygenated for 24 hours after 6 hours of hypoxia, and TXNIP expression was measured by western blot. TXNIP expression decreased around 60% with this hypoxia-reoxygenation procedure (Figure 23).

3.3.5 Effect of Radiation on TXNIP Expression

H9c2 cells were exposed to a single dose of 40 Gy of X-rays for 5 minutes, and TXNIP expression was measured by western blot. This dose slightly decreased TXNIP expression, but this did not reach statistical significance (Figure 22).

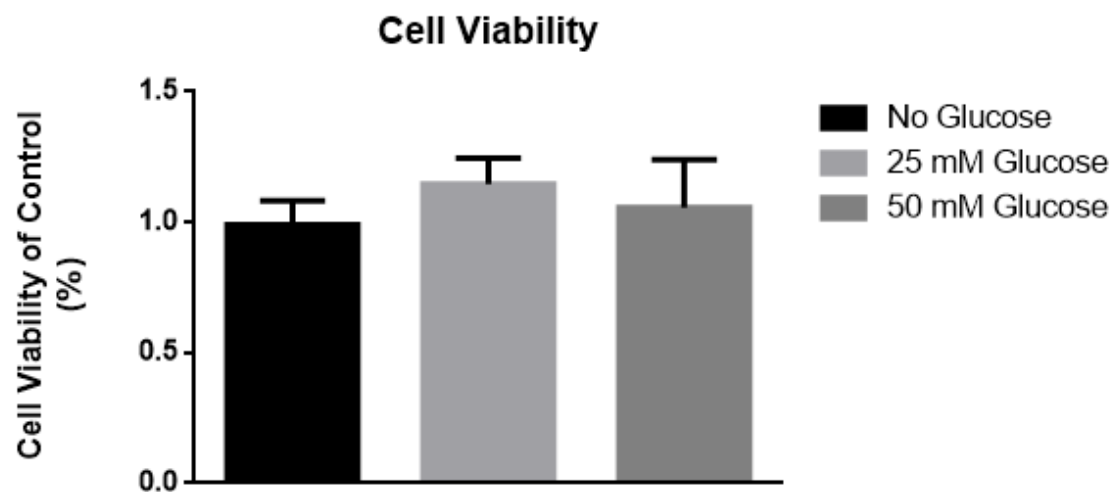


Figure 19. Cell viability assay in H9c2 cells with no glucose, 25mM glucose and 50 mM glucose and growth medium for 3 days.

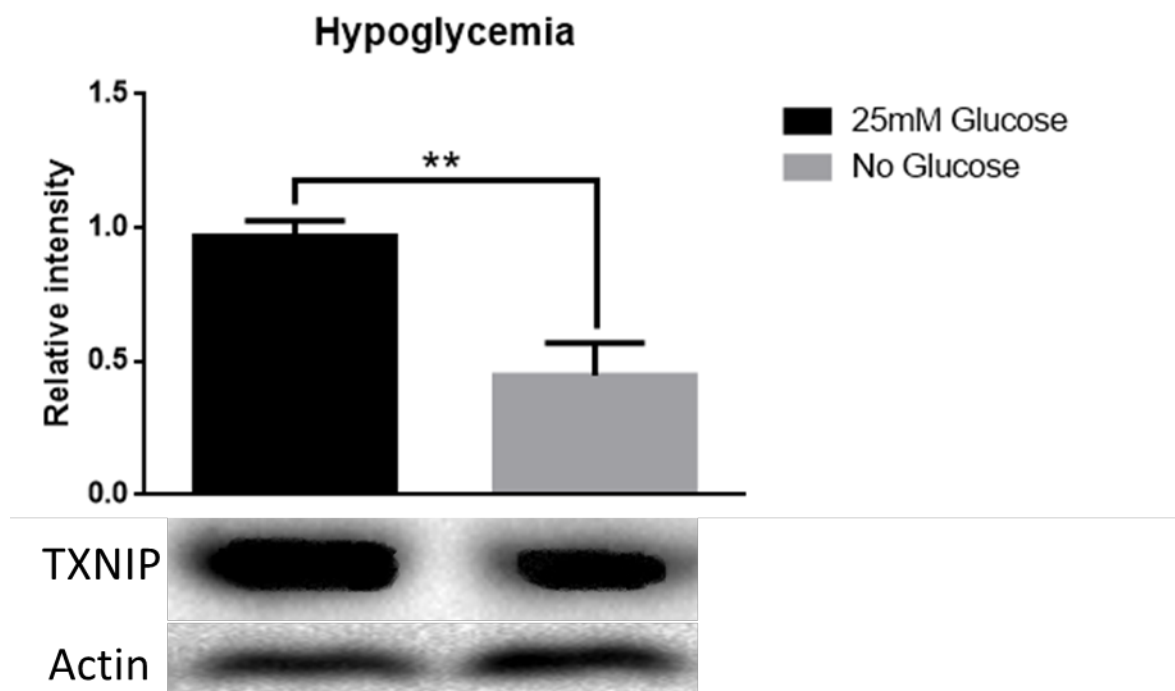


Figure 20. Effect of no glucose medium on cytoplasmic TXNIP protein expression in H9c2 cells after 24 hours treatment.

The data are presented as relative intensity (protein/actin) and expressed as the means \pm SD of three independent experiments. One-way ANOVA and Tukey's post hoc test were performed to analyze data at each time point. ** $p < 0.01$ compared with control group.

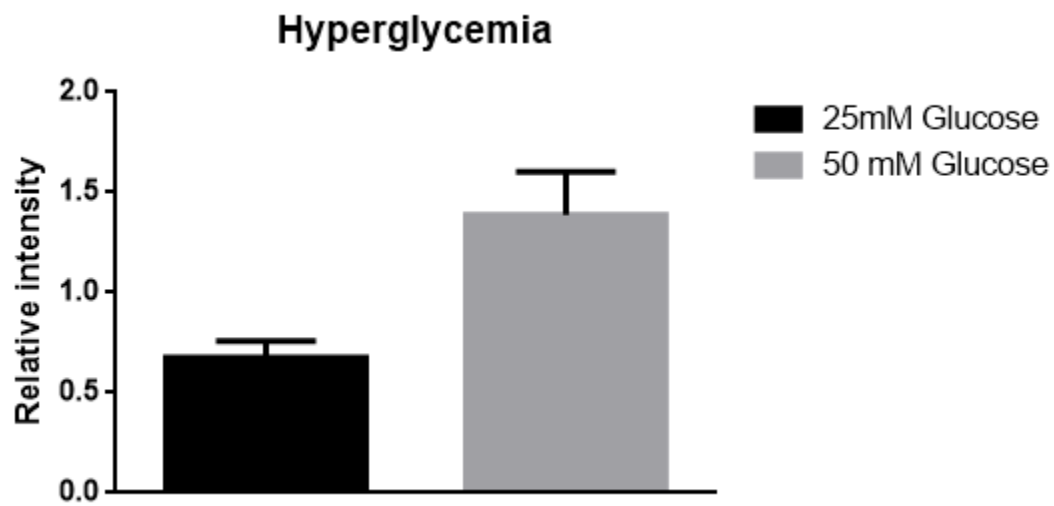


Figure 21. Effect of 50mM glucose medium on cytoplasmic TXNIP protein expression in H9c2 cells after 24 hours treatment.

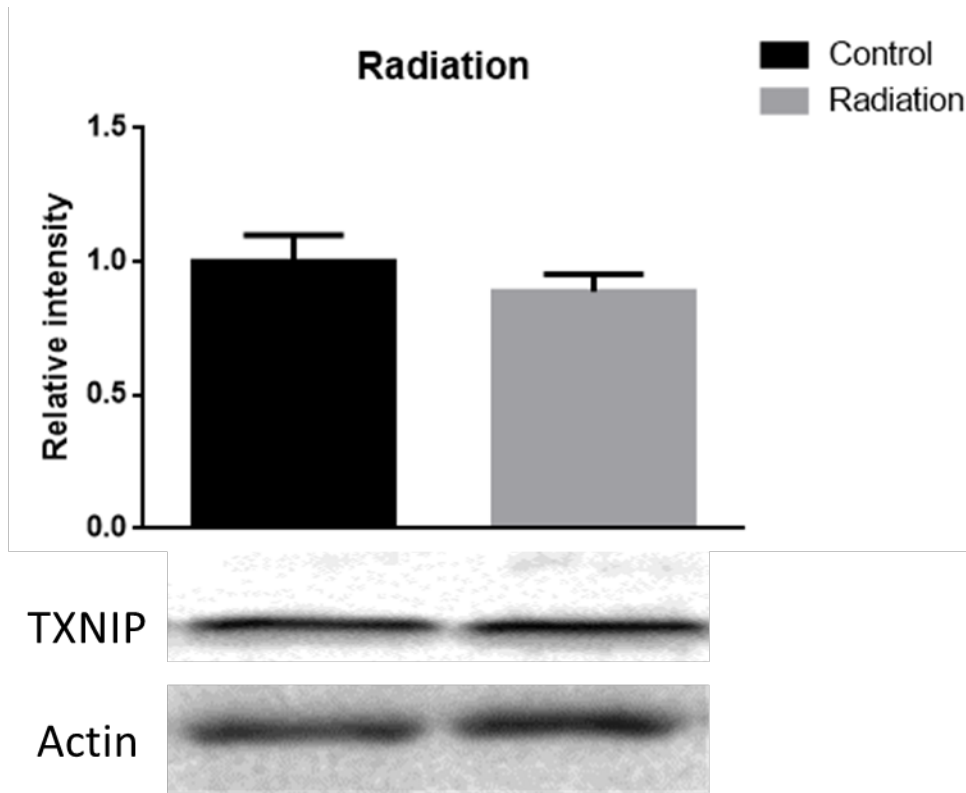


Figure 22. Effect of a single dose of 40 Gy of X-rays for 5 minutes on cytoplasmic TXNIP protein expression in H9c2 cells after 24 hours treatment.

The data are presented as relative intensity (protein/actin) and expressed as the means \pm SD of three independent experiments. One-way ANOVA and Tukey's post hoc test were performed to analyze data at each time point.

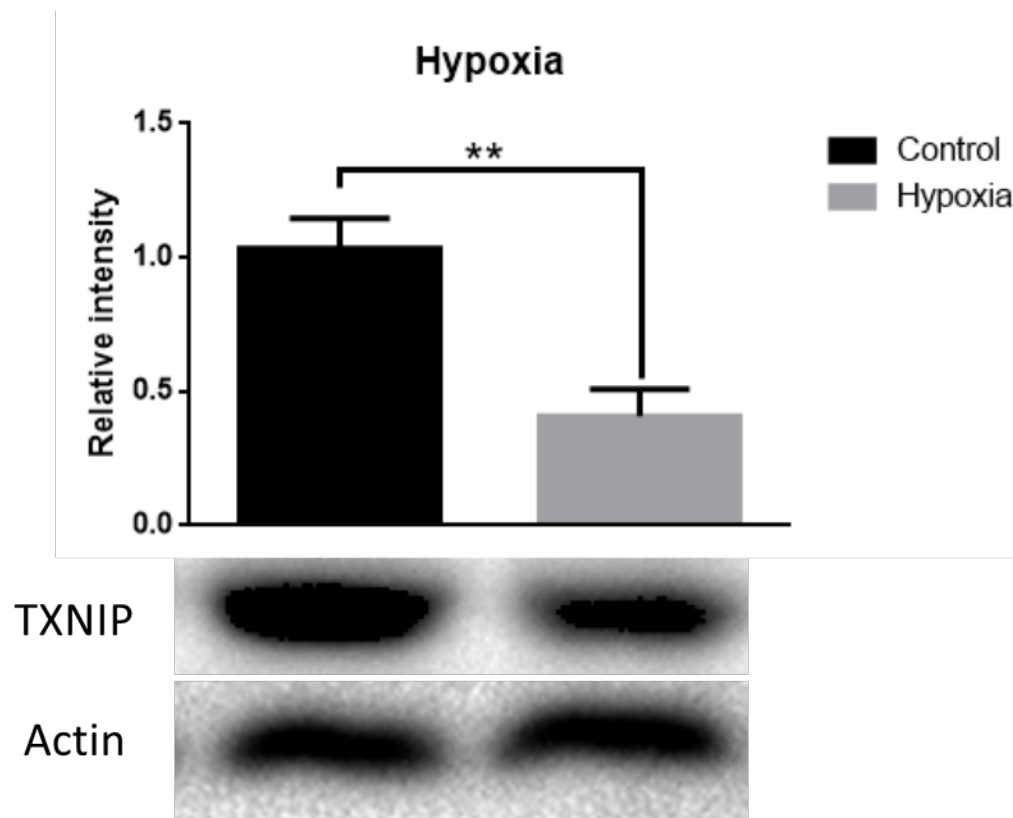


Figure 23. Effect of hypoxia-reoxygenation procedure on cytoplasmic TXNIP protein expression in H9c2 cells after 6 hours hypoxia and 24 hours reoxygenation.

The data are presented as relative intensity (protein/actin) and expressed as the means \pm SD of three independent experiments. One-way ANOVA and Tukey's post hoc test were performed to analyze data at each time point.

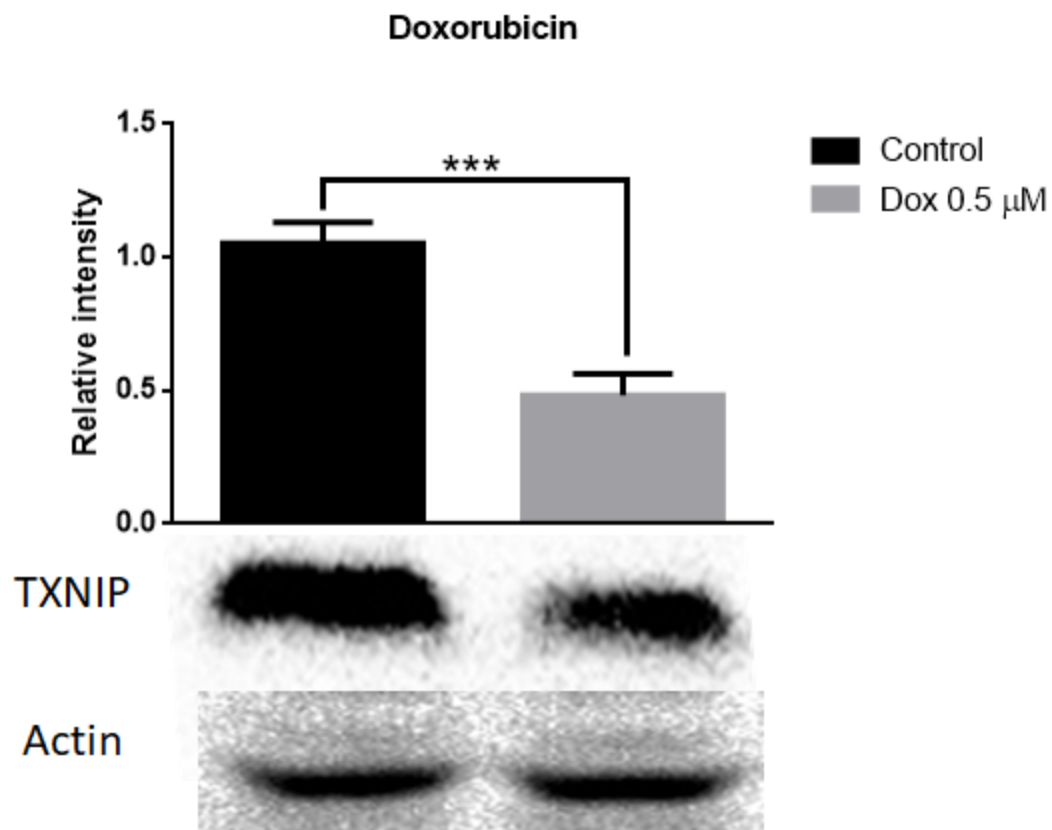


Figure 24. Effect of 0.5 μ M doxorubicin treatment on cytoplasmic TXNIP protein expression in H9c2 cells after 24 hours treatment.

The data are presented as relative intensity (protein/actin) and expressed as the means \pm SD of three independent experiments. One-way ANOVA and Tukey's post hoc test were performed to analyze data at each time point. *** $p < 0.001$ compared with control group.

3.4 Discussion

This present study was designed to examine the effect of glucose concentration on cytosolic TXNIP expression in H9c2 cells. It also showed the effect of different oxidative stress inducers on cytosolic TXNIP. It was found that TXNIP expression significantly increased with higher concentrations of glucose. Furthermore, 0.5 μ M doxorubicin significantly decreased TXNIP expression. Similar to doxorubicin, reoxygenation of cells after hypoxia conditions led to TXNIP reduction. Exposing cells to 40 Gy of X-rays for 5 minutes did not significantly affect TXNIP expression.

TXNIP has an important role in the pathogenesis of diabetes.^{52, 54, 55} It has been shown that TXNIP has multiple metabolic effects which cause or augment diabetes, such as increasing production of glucose in the liver and causing β -cell dysfunction.⁷⁹ Clinical trials are ongoing for the therapeutic application of reducing TXNIP expression in diabetes. H9c2 cells regularly grow in 25 mM glucose. Consistent with observations made in other cell types, cytosolic TXNIP was significantly increased with increased glucose concentration in the growth medium and significantly reduced in glucose free medium.

As previously described, TXNIP has been shown to have a variety of negative effects on glucose regulation. Since an increase in cytosolic TXNIP was observed with hyperglycemia in the cardiac cells, modifying TXNIP expression under hyperglycemic conditions might be a good therapeutic target for diabetic cardiomyopathy. Diabetic cardiomyopathy is a form of heart failure that occurs in diabetic patients but is not related to a specific cardiovascular abnormality such as hypertension. The exact cause of diabetic cardiomyopathy is not known, but several abnormalities have been associated with the

development of this condition. One of those abnormalities is increased production of free radicals and reactive oxygen species. Cai, et al found that diabetic mice induced by STZ exhibited higher levels of lipid peroxidation. Thiol oxidative stress was also observed in this study with an imbalance in mitochondrial reduced versus oxidized glutathione.¹⁰⁵ The thioredoxin pathway has also been implicated in the development of diabetic cardiomyopathy. Decreased expression of mitochondrial Trx2 was found in H9c2 cells grown in high glucose growth medium. The same study found reduced expression of Trx2 in STZ diabetic rats.¹⁰ A recent study examined the effect of glucose concentration on expression of TXNIP in H9c2 cells. The authors found that increasing concentrations of glucose up to 25 mM significantly increased TXNIP.¹⁰⁶ Our results further extend this up to 50 mM glucose, and additional increases in cytosolic TXNIP were observed. The same study found that TXNIP knockout mice exhibited improved cardiac function following induction of diabetes by STZ compared to wild type mice.¹⁰ This important finding demonstrates the potential of TXNIP modulation in therapy of diabetic cardiomyopathy.

Doxorubicin is an anthracycline agent used to treat several types of cancer. It has a high toxicity especially in cardiac cells because of its ability to increase ROS production which can lead to heart failure.⁶⁹ Impact on the thioredoxin pathway by doxorubicin has been previously observed as doxorubicin is known to inhibit TrxR.¹⁰⁷ However, no reports on doxorubicin's impact on TXNIP are available. In this study, cytosolic TXNIP expression was decreased significantly with doxorubicin treatment. This is likely because of increased ROS production which is known to move TXNIP to the mitochondria.

Ischemia-reperfusion injury is another important oxidative stress-mediated insult to the heart. Ischemia-reperfusion injury occurs after heart cells that were previously deprived of oxygen (for example, in a myocardial infarction) are reperfused. Reactive oxygen species are produced quickly after the reintroduction of oxygen to the cells. The source of these reactive oxygen species is not clear but may include leakage of radicals from the mitochondria or activation of immune system cells.¹⁰³ In this study, ischemia-reperfusion injury was modeled using a hypoxia chamber followed by reintroduction to the regular oxygen environment of a normal incubator.¹⁰⁸ Similar to doxorubicin, we saw a significant decrease in cytosolic TXNIP expression with the hypoxia-reoxygenation process. These results show that TXNIP expression is affected by cellular redox status and the presence of ROS in the system.

Radiation is a well known source of oxidative stress in cells by causing generation of ROS leading to apoptosis.¹⁰⁹ According to previous work in this laboratory, 40 Gy of radiation from X-rays will cause stress to H9c2 cells but with little mortality (data not published). In this study, exposing cells to 40 Gy of X-ray radiation showed a trend toward decreasing TXNIP expression, but it did not reach a statistically significant level. With increasing radiation doses, it is possible that the reduction may be more significant with increasing levels of oxidative stress.

In conclusion, both glucose level and oxidative stress impact the cytosolic concentration of TXNIP in H9c2 cardiomyocytes. The impact of hyperglycemia on TXNIP is consistent with other literature reports. The reduction in cytosolic TXNIP is consistent with the movement of TXNIP to the mitochondria. Because of the clear reduction of TXNIP from doxorubicin treatment and the clinical relevance of doxorubicin

cardiotoxicity, doxorubicin was selected to move forward for a more detailed study of the effect on TXNIP and related proteins.

CHAPTER 4. THIOREDOXIN PATHWAY MODULATION BY CARVEDILOL AND DOXORUBICIN TOXICITY IN H9C2 CELLS

4.1 Introduction

Doxorubicin is an antitumor antibiotic belonging to the anthracycline family. It is an important antineoplastic agent with topoisomerase-inhibiting and DNA intercalating activity.⁷² It is often used alone or combined with other agents to treat a variety of cancers such as lymphoma, breast cancer, bladder cancer, ovarian cancer and prostate cancer. Cardiac toxicity is the major dose dependent side effect. Both acute and chronic cardiotoxicity can occur. The chronic toxicity manifests primarily as a dilated cardiomyopathy. Multiple mechanisms are thought to be responsible for this myocardial damage, such as ROS production, apoptosis and mitochondrial dysfunction. Free radical generation remains the central focus in doxorubicin induced cardiotoxicity.⁷³ Cardiomyocytes are known to not have as effective of an antioxidant protection system compared to other cell types, and it is well known that ROS production can extremely alter many organelles in the cell. In vivo studies have shown that enhanced antioxidant expression greatly reduced doxorubicin induced cardiac toxicity. Another in vivo study showed that treating mice with doxorubicin led to reduced glutathione peroxidase and glutathione reductase activity as well as a decrease in GSH level. Doxorubicin also increased the GSSG level in those mice cardiomyocytes.⁷¹

Numerous studies have indicated that antioxidants should be able to block or at least decrease the cardiotoxicity of doxorubicin without major effect on the antitumor effect of this drug. The most prominent of the antioxidant protections to date is dexrazoxane, an iron chelating antioxidant that is FDA approved for prevention of

doxorubicin-induced cardiotoxicity. Although there are multiple antioxidant agents with a selective ROS blocking mechanism showing promising results, all of the antioxidant options have limitations such as toxicity and inconsistency. An *in vivo* study found that overexpression of Trx1 in mice protected the heart from damaging reactive oxygen species.¹¹⁰ Although no studies have been conducted on TXNIP in doxorubicin cardiac injury, Gao et al found that downregulation of TXNIP protected cells against doxorubicin kidney injury.¹⁰³ This indicates that decreasing TXNIP has potential in protection against doxorubicin-induced toxicity.

Carvedilol is a non-selective antagonist at beta and alpha 1-adrenoceptors. It also has been observed to possess antioxidant and antiapoptotic effects. Carvedilol is FDA approved for treatment of hypertension and mild to severe congestive heart failure (CHF). Multiple studies have shown that carvedilol has effect in prevention of doxorubicin cardiac toxicity. Carvedilol has been recently used as a prophylactic agent in patients receiving anthracycline medications. The exact mechanism of carvedilol effect on doxorubicin-induced cardiotoxicity is not clear.

Previously, we have seen that carvedilol increased the nuclear localization of TXNIP, the negative regulator of the thioredoxin protein. It concomitantly decreased cytosolic TXNIP. It was also observed that doxorubicin treatment decreased the level of TXNIP in the cytosol while increasing its movement into the mitochondria. Because effects on TXNIP were observed with both agents, we hypothesized that carvedilol may be able to protect against doxorubicin-induced cardiotoxicity through modulation of TXNIP localization. Therefore, in the present study, we investigated the potential effect

of carvedilol on the thioredoxin pathway in cardiomyocyte cells treated with doxorubicin.

In this study, our objectives were:

1. To evaluate the impact of carvedilol on H9c2 cells apoptosis and viability after exposure to doxorubicin
2. To determine the effect of carvedilol on TXNIP and thioredoxin related proteins in H9c2 cardiomyocytes treated with doxorubicin
3. To study the effect of doxorubicin on TXNIP complexation with other proteins

4.2 Materials and Methods

4.2.1 Reagents and Antibodies

Carvedilol and propranolol (Sigma, C3993 and P0884) were dissolved in DMSO to make 5 mM carvedilol and propranolol stock solutions and were filtered by using a Medical Millex-GP filter (0.22 μ m, sterilized; Millipore). Doxorubicin (Sigma, D1515) was dissolved in DMSO to make a 0.5 mM stock solution and was filtered using a Medical Millex-GP filter (0.22 μ m, sterilized; Millipore). All stock solutions were stored at -80°C and were diluted in DMEM medium to the needed concentrations for cell culture treatment. The final concentration of DMSO in cell culture studies was less than 0.2%.

Trx1 and PARP antibodies were purchased from Cell Signaling Technology (2298S and 9542); TrxR1 and TXNIP antibodies were obtained from Novus Biologicals, Inc (NBP2-27095 and NBP2-20619); antibodies to Trx2, TrxR2, Lamin A/C, cytochrome c, actin, and secondary antibody goat anti-rabbit were purchased from Santa Cruz Biotechnology (sc-133201, sc-376868, sc-376248, sc-2004 and sc-7210); and the goat anti-mouse secondary antibody was obtained from Bio-Rad (170-6516).

4.2.2 Cell Culture

H9c2 cells (rat embryonic cardiac myoblasts) were obtained from the American Type Culture Collection (ATCC, Manassas, VA, USA) and maintained in Dulbecco's modified Eagle's medium (DMEM, ATCC). DMEM contained 10% (v/v) fetal bovine serum and 1% (v/v) penicillin/streptomycin, and cells were maintained at 37°C with 5% CO₂. Cells with passage number below 20 were used.

4.2.3 Cell Viability

H9c2 cells were seeded and treated in 96-well plates, and cell viability was measured by colorimetric assay containing MTT (3-(4, 5)-dimethylthiazol-2, 5-diphenyltetrazolium bromide). H9c2 cells with density of 1,000 cells/well were seeded and allowed to attach overnight. The cells were treated with doxorubicin (0.01, 0.1, 0.5 and 1.0 μM) and carvedilol (10 μM) or propranolol (10 μM). Cells were treated in different orders to determine the best protective effect of carvedilol against doxorubicin. First, a combination of doxorubicin and carvedilol was attempted; cells were treated with the combination for 24 or 72 hours. Second, cells were pre-treated with carvedilol for 24 hours followed by a treatment with a combination of carvedilol and doxorubicin for an additional 24 hours. Following drug treatment, the treatment medium was replaced with regular growth medium, and the cells were allowed to grow for a total of 5 days. MTT assay was conducted by replacing the medium with medium containing 0.5 mg/ml MTT solution (50 μl /well) and incubated in the dark at 37°C for at least 4 hours. DMSO (150 μl /well) was added for one hour to dissolve the formed purple formazan product. SpectraMax M2 microplate reader (Molecular Devices, Sunnyvale, CA, USA) was used to measure the absorbance of each well by using a test wavelength of 570 nm and a reference wavelength of 650 nm.

At the end of the MTT assay, we calculated the doxorubicin and carvedilol combination effect by comparing observed viability to predicted viability. MTT assay results provided observed cell viability, while the predicted cell viability was calculated by multiplying the individual treatment effects. Then we subtracted observed viability from the predicted to decide if the carvedilol and doxorubicin combination treatment was

additive, antagonistic, or synergistic. This combination will be additive if the net effect is equal to the product of the individual compounds. It will be antagonistic if the net effect is less than the individual effects while this combination effect will be synergistic if carvedilol added to the toxicity of doxorubicin.

4.2.4 Reactive Oxygen Species (ROS) Production

Carboxy-H₂DCFDA or C400 (Invitrogen, Life Technologies) was used to measure ROS production. C400 is a cell-permeable probe, and it will be cleaved by cellular esterase and oxidized by ROS upon its entry into the cytoplasm which will produce fluorescence. Briefly, H9c2 cells were seeded in 96 well plates at a density of 20,000 cells/well and allowed to attach overnight. Cells were pretreated with carvedilol 10 μ M for 24 hours. The cells then were treated with carboxy-H₂DCFDA for 40 minutes followed by a combination of carvedilol 10 μ M and doxorubicin 0.5 μ M or 1 μ M. SpectraMax M2 fluorescence microplate reader (Molecular Devices, Sunnyvale, California) was used to measure the fluorescence intensity at 492 nm excitation and 527 nm emission at different time points ranging from 30 minutes to 4 hours.

4.2.5 Examination of TXNIP, Trx1, TrxR1 and c-PARP Proteins in H9c2 Cells by Western Blot

TXNIP, Trx1, TrxR1 and c-PARP was determined by using western blot. Two million H9c2 cells were seeded in 75 cm² flasks and allowed to attach overnight. The cells were then pretreated with carvedilol 10 μ M for 24 hours followed by a combination of carvedilol 10 μ M and doxorubicin 0.5 μ M. Control and doxorubicin flasks were incubated with medium containing vehicle during the pretreatment period. Then cells were detached using trypsin and centrifuged at 1000 x g for 5 minutes. The cells were

separately lysed in lysis buffer containing 20 mM HEPES (pH 7.4), 1% Triton X-100, 150 mM NaCl, 1 mM EDTA, 1 mM EGTA, and 1× broad-spectrum protease inhibitors (Thermo Fisher Scientific, 88665). Bradford protein assay was used to determine the total protein concentration, and samples containing 50 µg of protein were separated by 8% or 12% SDS-PAGE followed by transfer onto PVDF membranes. 0.5% bovine serum albumin (BSA; Sigma, A3294) was used to block the membranes for 3 hours followed by incubation with primary antibody (1:10,000) overnight. HRP-conjugated secondary antibody was then added for 1 hour at room temperature. Visualization of the bands was performed using a kit from GE Biosciences and quantified using a Bio-Rad imaging system. For this experiment, actin was used as a housekeeping protein.

4.2.6 Isolation of Mitochondrial Fractions from H9c2 Cells

Five million H9c2 cells were seeded in 175 cm² flasks and allowed to attach overnight. The cells were then pretreated with carvedilol 10 µM for 24 followed by a combination of carvedilol 10 µM and 0.5 µM doxorubicin. Control and doxorubicin flasks were incubated with medium containing vehicle. Then cells were detached by trypsin and centrifuged at 1000 x g for 5 minutes. A mitochondria isolation kit for cultured cells (Thermo Fisher Scientific, 89874) was used to isolate the mitochondria. Western blot was conducted for Trx2, TrxR2, TXNIP, and ASK1 as described above. Cytochrome c was used to measure the mitochondrial fraction purity. Actin was used as a housekeeping protein

4.2.7 Cell Fractionation and Nuclear Isolation

Ten million H9c2 cells were seeded in 100-mm petri dishes and allowed to attach overnight. The cells were then pretreated with carvedilol 10 µM for 24 hours followed

with a combination of carvedilol 10 μ M and doxorubicin 0.5 μ M. Control and doxorubicin flasks were incubated with medium containing vehicle. Then cells were washed twice with cold phosphate buffered saline (PBS), scraped, and collected with 5 mL of hypotonic buffer [10 mM KCl, 1.5 mM MgCl₂, 1 mM sodium orthovanadate, 1 M Tris and 1x protease inhibitors (Thermo science #88665)]. The cells were centrifuged at 1000 x g for 10 minutes at 4°C. Then 600 μ L of cold hypotonic buffer was used to re-suspend the pellet. Exactly 23 strikes on the suspension by a loose fitting Dounce homogenizer over ice was used to gently separate the cytoplasmic and nuclear fractions. Then the suspension was centrifuged at 1000 x g for 7 minutes at 4°C. The supernatant contained the cytoplasmic fraction while the pellet contained the nuclear fraction. The pellet was extracted with cold high salt buffer (10 mM Tris-Cl, pH 7.4, 400 mM NaCl, 25% glycerol and 1x protease inhibitors) for 30 minutes at 4°C and then centrifuged at 20817 x g at 4°C for 10 min. The supernatant was used for Western blot analysis as described above. Lamin A/C was used to measure the nuclear fraction purity, and actin was used as the housekeeping protein.

4.2.8 Immunoprecipitation

Five million H9c2 cells were seeded in 100-mm petri dishes and allowed to attach overnight. The cells were pretreated with carvedilol 10 μ M for 24 hours followed by a combination of carvedilol 10 μ M and doxorubicin 0.5 μ M. Control and doxorubicin flasks were incubated with medium containing vehicle during the pretreatment. Then the cells were washed with PBS and scraped using lysis buffer. Bradford assay was used for measuring protein concentrations. 300 μ g total protein was immunoprecipitated with agarose-conjugated anti-Trx2 or anti-PARP antibody in 1 ml of lysis buffer overnight at

4°C. Then 55 µL of protein G agarose was used to capture the immunocomplexes followed by incubation for 3 hours at 4°C. The immunocomplexes were centrifuged at 3000 RPM for 10 minutes, and the pellet was washed three times with lysis buffer. Then the pellets were collected and suspended in SDS-sample buffer and heated for 10 minutes. Western blot then was performed using anti-TXNIP or anti-ASK1 antibody.

4.2.9 Statistical Analysis

Data are expressed as means \pm standard deviation (SD) from three independent experiments. Statistical analysis was done using ANOVA followed by Tukey's post hoc test. A p value of <0.05 was considered to be statistically significant.

4.3 Results

4.3.1 Cell viability

An MTT assay was conducted to determine cell viability in cells treated with doxorubicin plus carvedilol. H9c2 cells were treated at the same time with both 10 μ M carvedilol and 0.5 μ M doxorubicin for 1 and 3 days. Doxorubicin produced a dose dependent decrease in cell viability. However, the combination treatment did not yield any change in cell viability between carvedilol and doxorubicin concentrations at all concentrations (Figure 25 & Figure 26).

The 24 hour pretreatment of 10 μ M carvedilol followed by 0.01, 0.1, 0.5 and 1 μ M doxorubicin showed significant viability differences between doxorubicin alone and the cells with carvedilol treatment. The most significant protection was between 1 μ M doxorubicin treatment and carvedilol ($p < 0.001$) (Figure 27). The antagonistic effect was calculated to be 48%. Carvedilol pretreatment with 0.1 and 0.5 μ M doxorubicin also showed a statistically significant increase in viability compared to doxorubicin alone. No statistically significant difference was observed with 0.01 μ M doxorubicin (Table 1).

Propranolol, another nonselective beta-blocker, was used as a comparison. Propranolol did not exhibit any protection against doxorubicin toxicity in H9c2 cells with combination and with pretreatment respectively (Figure 28 & Figure 29).

4.3.2 Effect of Carvedilol Pretreatment on Doxorubicin-Induced ROS Production

Studies have shown that doxorubicin is able to produce ROS in a dose and time dependent manner. To determine whether carvedilol pretreatment can reduce ROS production or not, cells were pretreated with carvedilol for 24 hours followed with combination treatment. Doxorubicin 0.5 μ M did not induce a statistically significant

increase in ROS. However, doxorubicin 1 μM showed a statistically significant increase in ROS which was reduced by treatment with carvedilol (Figure 30). ROS production was detected in 0.5 μM in 12 and 24 hours and carvedilol was able to reverse it (Figure 31). While with no carvedilol pretreatment in 12 and 24 hours the carvedilol was not able to reverse doxorubicin ROS production (Figure 32).

4.3.3 Carvedilol and Doxorubicin Combination Impact on Major Thioredoxin

Proteins: Trx1, TrxR1, Trx2, TrxR2 and TXNIP

The protein level of TXNIP, Trx1, and TrxR1 was determined in the cytosol following pretreatment with carvedilol 10 μM for 24 hours followed by combination of 10 μM carvedilol and 0.5 μM doxorubicin. The mitochondrial isoforms Trx2 and TrxR2 were evaluated in the mitochondria after the same treatment. The cytosolic level of TXNIP decreased significantly with carvedilol (40%) and doxorubicin (50%) individually. TXNIP decreased even further with a combination treatment of carvedilol and doxorubicin compared to control (70%) (Figure 33). Protein expression for Trx1 (Figure 36), TrxR1 (Figure 37), Trx2 (Figure 38), and TrxR2 (Figure 39) was not statistically significantly different from control at 24 hours for any treatments.

4.3.4 Impact of Carvedilol on TXNIP Localization in Nucleus and Mitochondria

TXNIP is known to shuttle between the nucleus, cytosol, and mitochondria. Here, we determined the TXNIP levels in subcellular fractions in cells treated with a combination of carvedilol and doxorubicin. Carvedilol increased TXNIP localization in the nucleus as expected. However, there was no statistically significant difference in TXNIP level for doxorubicin or the combination treatment compared to control in the nuclear fraction (Figure 34). Doxorubicin alone significantly increased TXNIP in the

mitochondria. Carvedilol treatment did not change the accumulation of TXNIP in the mitochondria caused by doxorubicin (Figure 35).

4.3.5 Carvedilol and Doxorubicin Combination Impact on PARP, cleaved PARP and ASK1 Level

The protein levels of PARP, cleaved PARP, and ASK1 were determined after pretreatment with carvedilol 10 μ M for 24 hours followed with a combination of carvedilol 10 μ M and doxorubicin 0.5 μ M. Carvedilol had no effect on PARP or cleaved PARP. Doxorubicin exhibited a significant increase in cleaved PARP, which is consistent with induction of apoptosis. Carvedilol partially blocked the increase in cleaved PARP indicating that carvedilol exhibited protection against doxorubicin-induced apoptosis (Figure 40) The ASK1 expression did not change with this treatment (Figure 41)

4.3.6 Effect of carvedilol on Trx1-ASK1 and TXNIP-PARP Protein Complexation

TXNIP is known to shuttle to the mitochondria under oxidative stress conditions and bind to Trx2, releasing ASK1 protein leading to apoptosis.¹¹¹ We performed immunoprecipitation in mitochondrial extracts to measure the Trx2-ASK1 complexation after carvedilol and doxorubicin treatment. Following immunoprecipitation with anti-Trx2 antibody, Western blot was performed with ASK1 antibody. This complex expression was slightly higher in carvedilol compared to control, and as expected doxorubicin decreased this complexation while the pretreatment with carvedilol reversed doxorubicin's effect (Figure 42). As described in chapter 2, carvedilol was able to increase the TXNIP-PARP complexation in the nucleus. The same observation was seen with carvedilol, while doxorubicin and the combination treatment showed the same level as control (Figure 43)

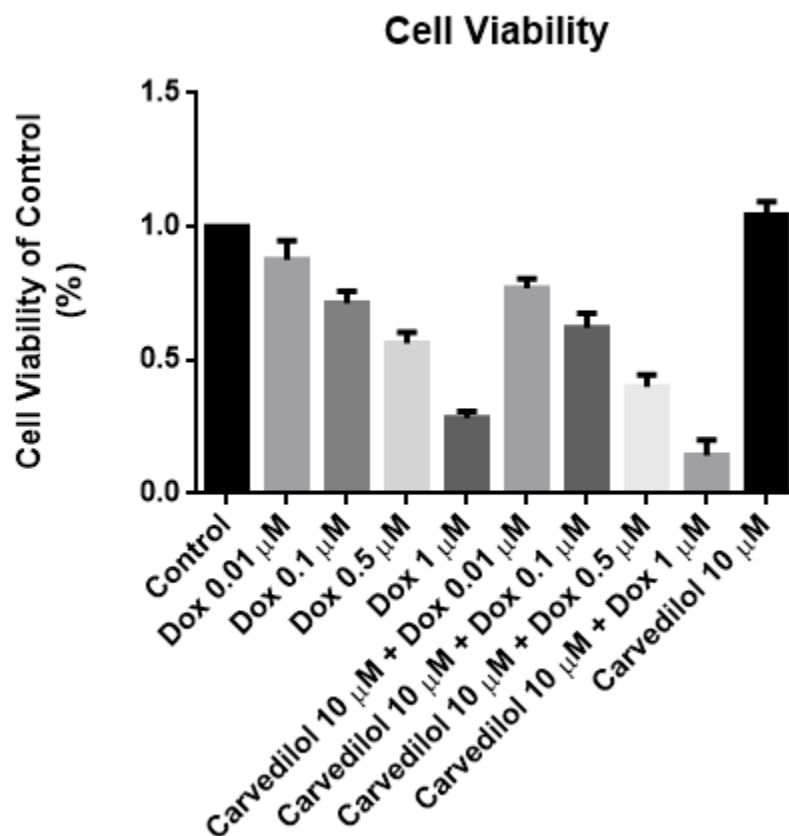


Figure 25. Cell viability assay in H9c2 cells treated with a combination of 10 μM carvedilol and 0.5 μM doxorubicin for 3 days.

This assay statistics are shown as percentage of control and expressed as the means \pm SD of 3 different experiments. One-way ANOVA followed by Tukey's post hoc test were performed to analyze data.

Table 1. H9c2 cells treated with a combination of 10 μ M carvedilol and 0.5 μ M doxorubicin for 3 days.

Treatment	Predicted Cell Viability (%)	Observed Cell Viability (%)	Effect (%)
0.01 μ M Dox + 10 μ M Carvedilol	80	77	3
0.1 μ M Dox + 10 μ M Carvedilol	70	62	8
0.5 μ M Dox + 10 μ M Carvedilol	52	48	4
1.0 μ M Dox + 10 μ M Carvedilol	26	21	5

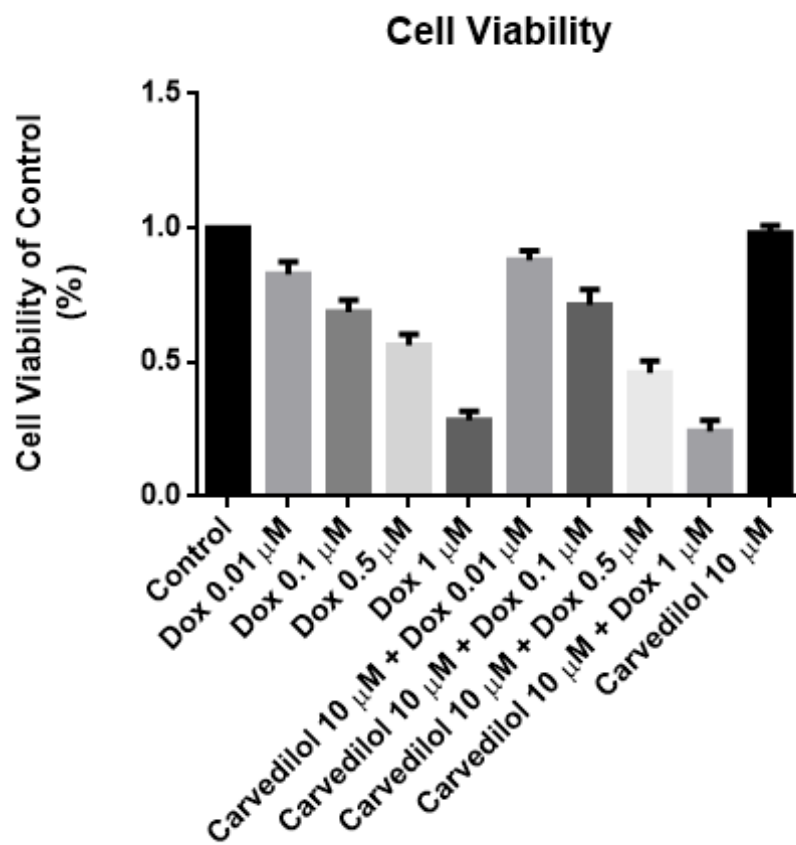


Figure 26. Cell viability assay in H9c2 cells treated with a combination of 10 μM carvedilol and 0.5 μM doxorubicin for 24 hours.

This assay statistics are shown as percentage of control and expressed as the means \pm SD of 3 different experiments. One-way ANOVA followed by Tukey's post hoc test were performed to analyze data.

Table 2. H9c2 cells treated with a combination of 10 μ M carvedilol and 0.5 μ M doxorubicin for 24 hours.

Treatment	Predicted Cell Viability (%)	Observed Cell Viability (%)	Effect (%)
0.01 μ M Dox + 10 μ M Carvedilol	89	87	2
0.1 μ M Dox + 10 μ M Carvedilol	78	73	5
0.5 μ M Dox + 10 μ M Carvedilol	52	49	2
1.0 μ M Dox + 10 μ M Carvedilol	31	28	3

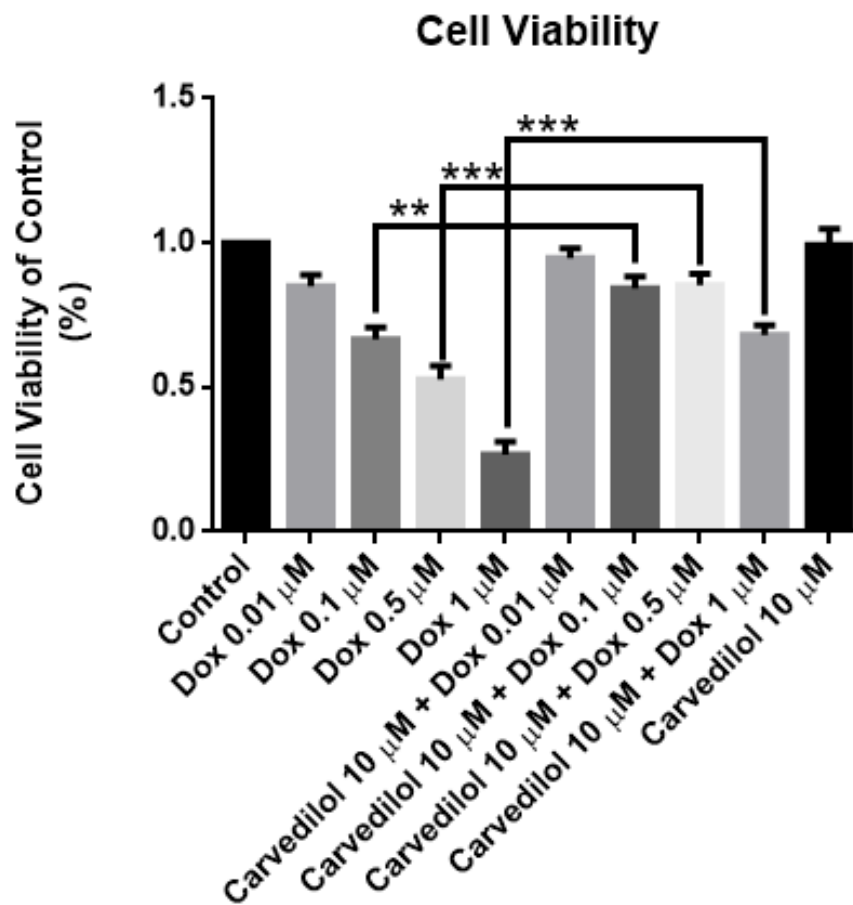


Figure 27. Cell viability assay in H9c2 cells treated with 10 μM carvedilol pretreatment for 24 hours followed by treatment with carvedilol and 0.5 μM doxorubicin for 24 hours.

This assay statistics are shown as percentage of control and expressed as the means \pm SD of 3 different experiments. One-way ANOVA followed by Tukey's post hoc test were performed to analyze data. ** $p < 0.01$ and *** $p < 0.001$ compared with control group.

Table 3. H9c2 cells treated with 10 μ M carvedilol pretreatment for 24 hours followed by treatment with carvedilol and 0.5 μ M doxorubicin for 24 hours.

Treatment	Predicted Cell Viability (%)	Observed Cell Viability (%)	Effect (%)
10 μ M Carvedilol /0.01 μ M Dox + 10 μ M Carvedilol	84	94	10
10 μ M Carvedilol /0.1 μ M Dox + 10 μ M Carvedilol	71	92	21
10 μ M Carvedilol /0.5 μ M Dox + 10 μ M Carvedilol	56	87	31
10 μ M Carvedilol 1.0 μ M Dox + 10 μ M Carvedilol	27	75	48

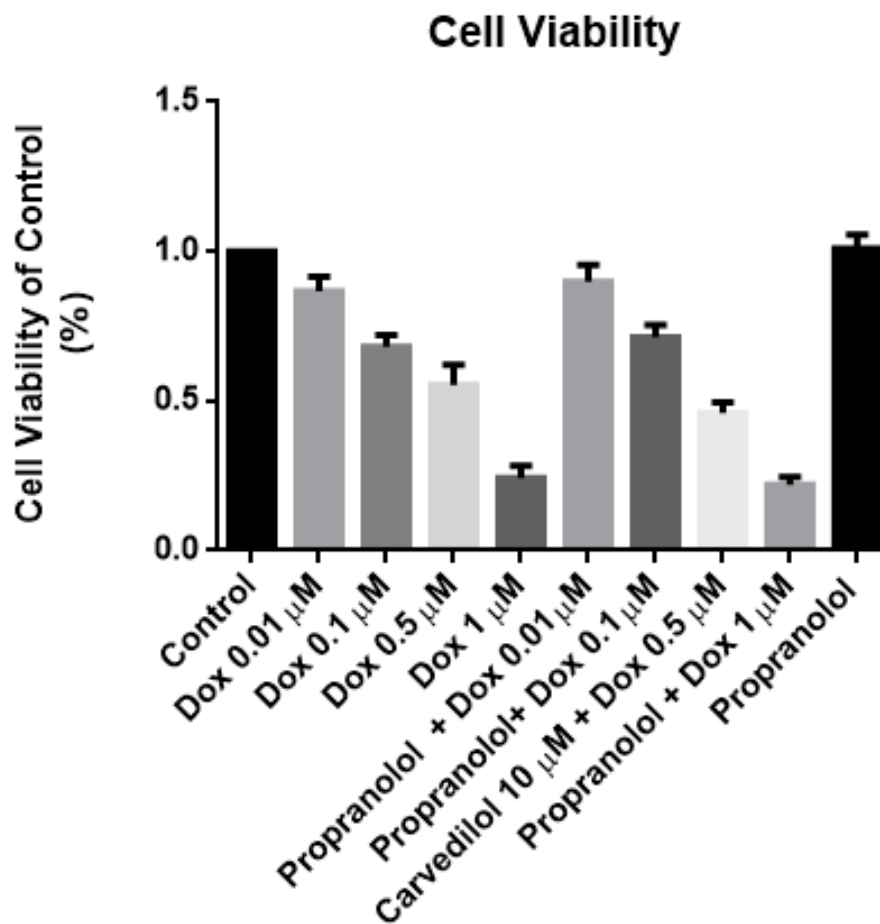


Figure 28. Cell viability assay in H9c2 cells treated with a combination of 10 μM propranolol and 0.5 μM doxorubicin for 3 days.

This assay statistics are shown as percentage of control and expressed as the means \pm SD of 3 different experiments. One-way ANOVA followed by Tukey's post hoc test were performed to analyze data.

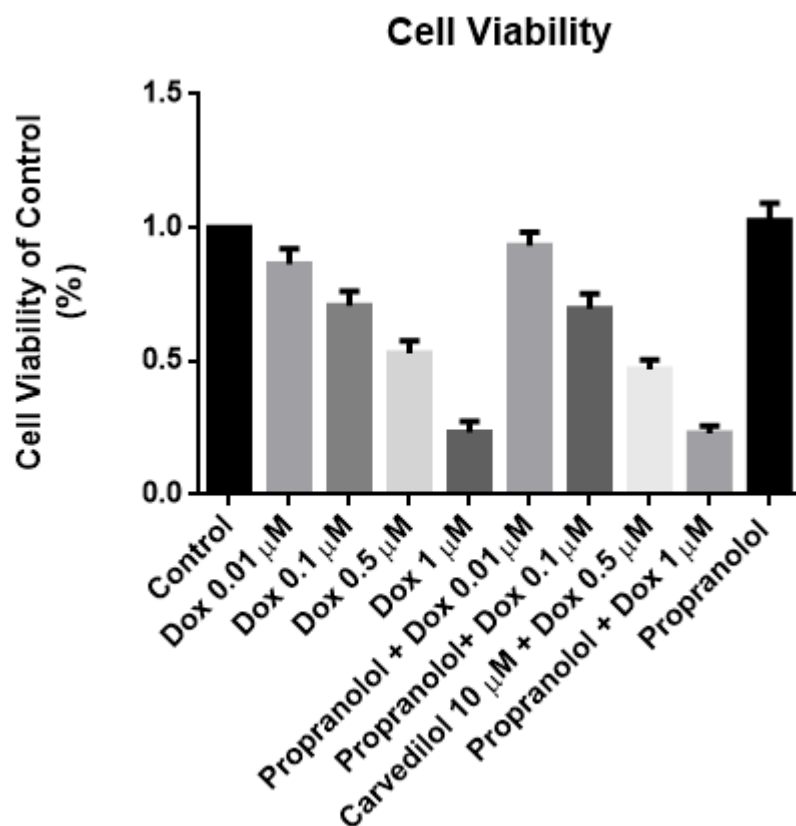


Figure 29. Cell viability assay in H9c2 cells treated with 10 μM propranolol pretreatment for 24 hours followed by treatment with propranolol and 0.5 μM doxorubicin for 24 hours.

This assay statistics are shown as percentage of control and expressed as the means \pm SD of 3 different experiments. One-way ANOVA followed by Tukey's post hoc test were performed to analyze data.

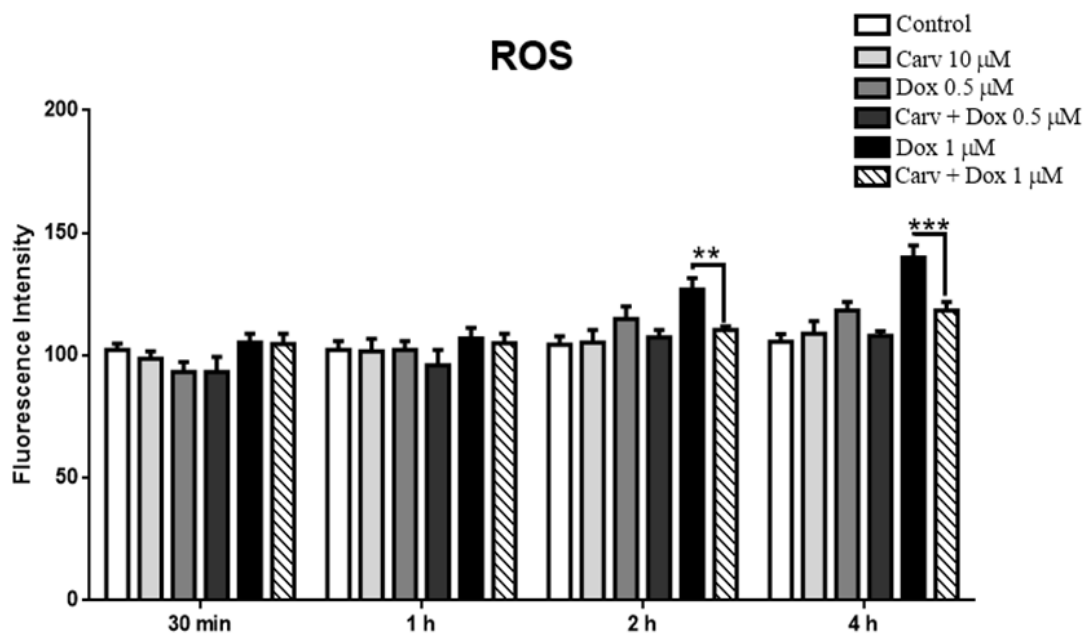


Figure 30. ROS production in H9c2 cells with pretreatment of carvedilol followed by treatment with carvedilol and doxorubicin for short time periods (30 minutes-4 hours). The data are presented as fluorescence intensity and expressed as the means \pm SD of three independent experiments. One-way ANOVA and Tukey's post hoc test were performed to analyze data at each time point. ** $p < 0.01$ and *** $p < 0.001$

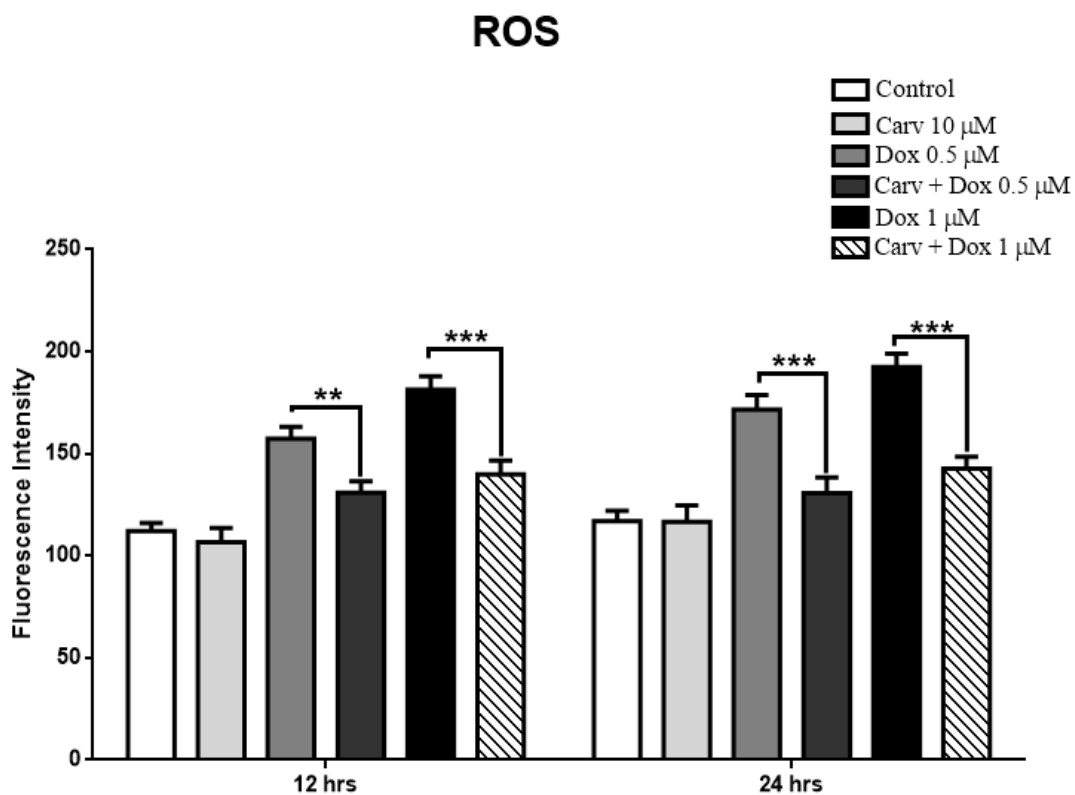


Figure 31. ROS production in H9c2 cells pretreatment with carvedilol followed by treatment with carvedilol and doxorubicin for 12 and 24 hours.

The data are presented as fluorescence intensity and expressed as the means \pm SD of three independent experiments. One-way ANOVA and Tukey's post hoc test were performed to analyze data at each time point. ** $p < 0.01$ and *** $p < 0.001$

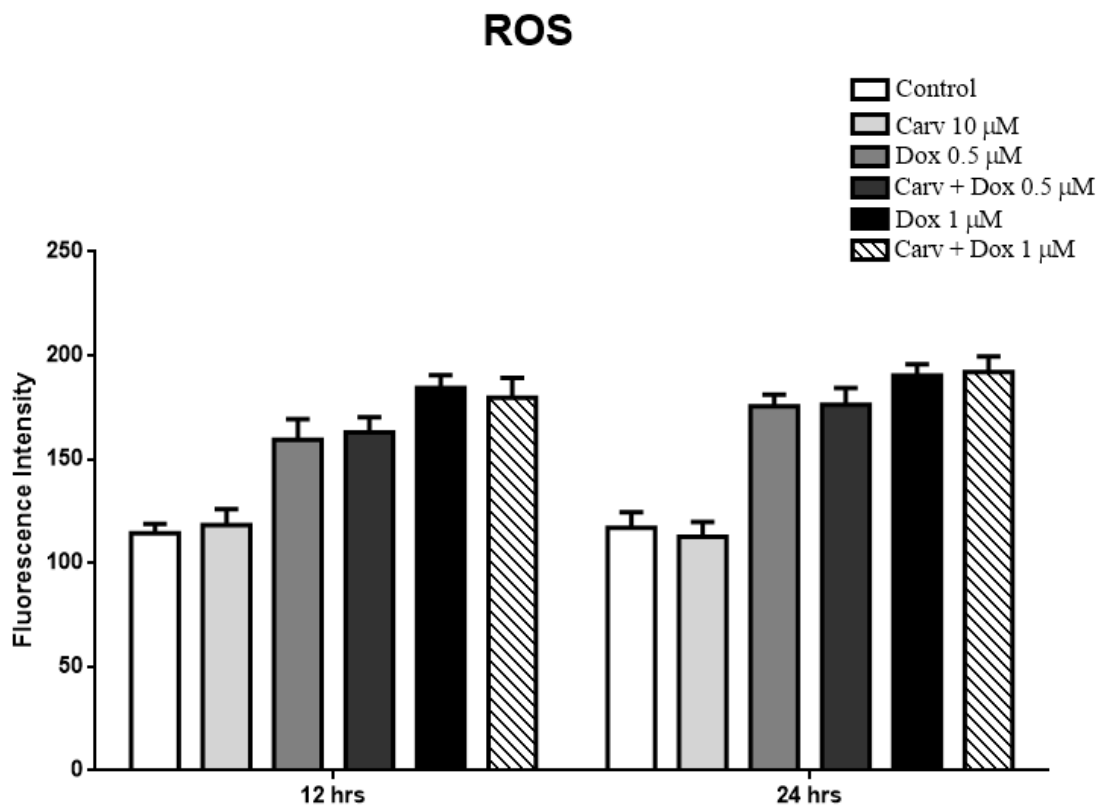


Figure 32. ROS production in H9c2 cells treated with a combination of carvedilol and doxorubicin for 12 and 24 hours.

The data are presented as fluorescence intensity and expressed as the means \pm SD of three independent experiments. One-way ANOVA and Tukey's post hoc test were performed to analyze data at each time point.

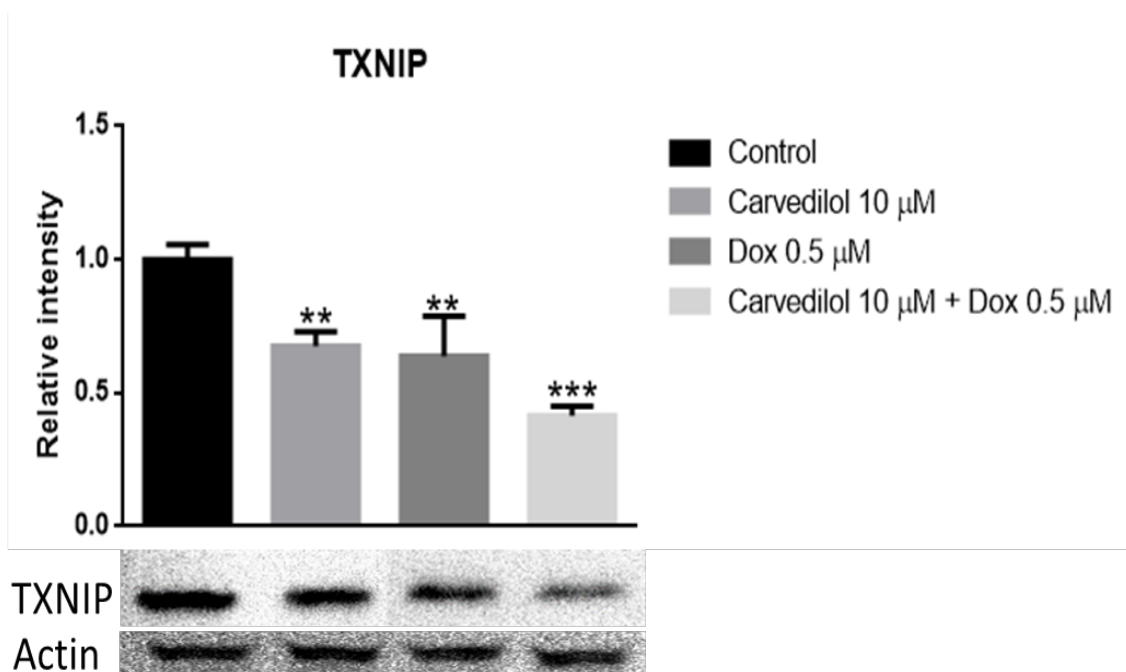


Figure 33. Effect of 10 μ M carvedilol and 0.5 μ M doxorubicin treatments on cytoplasmic TXNIP expression in H9c2 cells after 24 hour treatment.

The data are presented as relative intensity (protein/actin) and expressed as the means \pm SD of three independent experiments. One-way ANOVA and Tukey's post hoc test were performed to analyze data at each time point. ** $p < 0.01$ and *** $p < 0.001$ compared with control group.

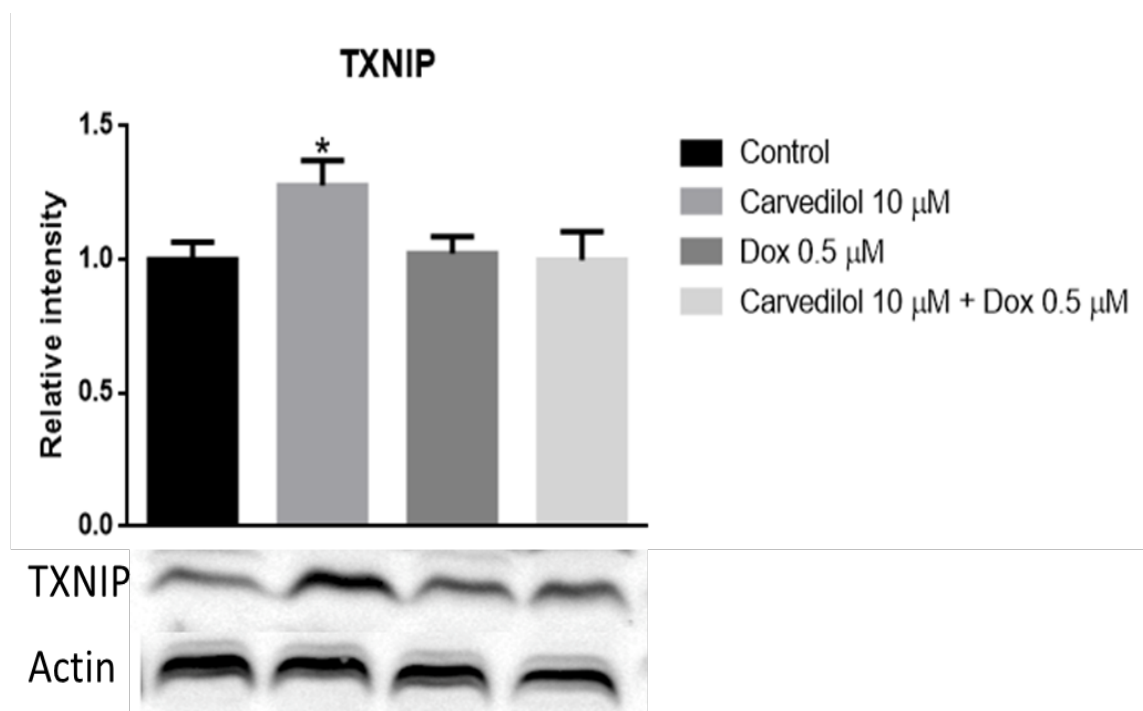


Figure 34. Effect of 10 μ M carvedilol and 0.5 μ M doxorubicin treatments on nuclear TXNIP expression in H9c2 cells after 24 hour treatment.

The data are presented as relative intensity (protein/actin) and expressed as the means \pm SD of three independent experiments. One-way ANOVA and Tukey's post hoc test were performed to analyze data at each time point. * $p < 0.05$ compared with control group.

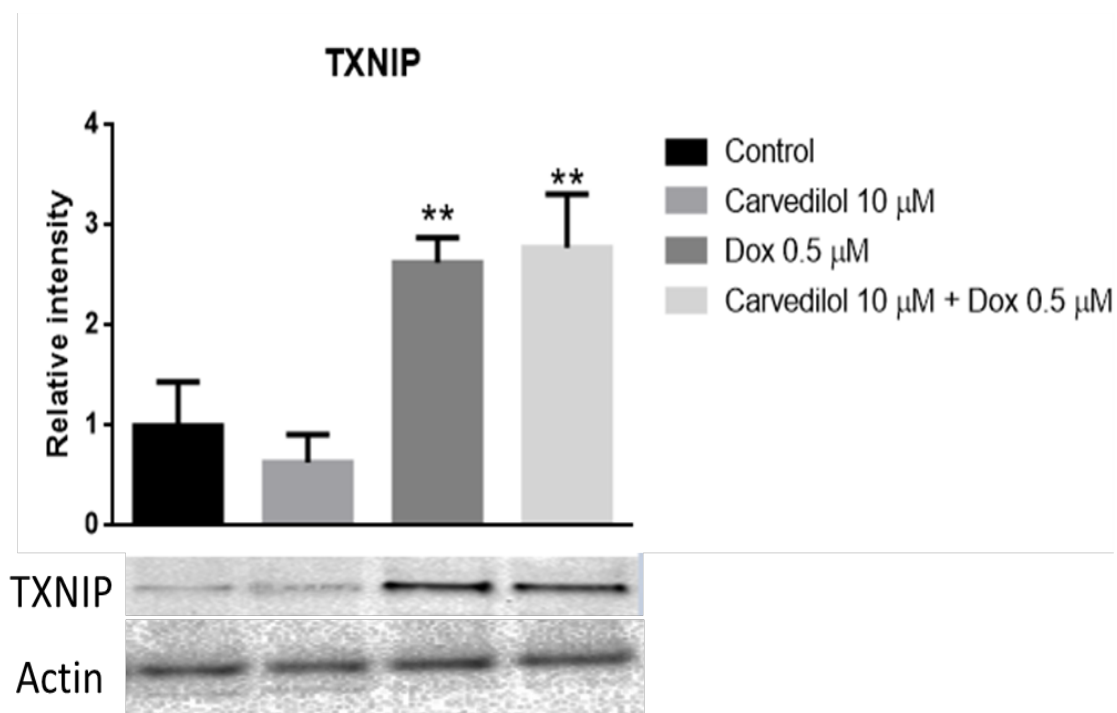


Figure 35. Effect of 10 μ M carvedilol and 0.5 μ M doxorubicin treatments on mitochondrial TXNIP expression in H9c2 cells after 24 hour treatment.

The data are presented as relative intensity (protein/actin) and expressed as the means \pm SD of three independent experiments. One-way ANOVA and Tukey's post hoc test were performed to analyze data at each time point. ** $p < 0.01$ and compared with control group.

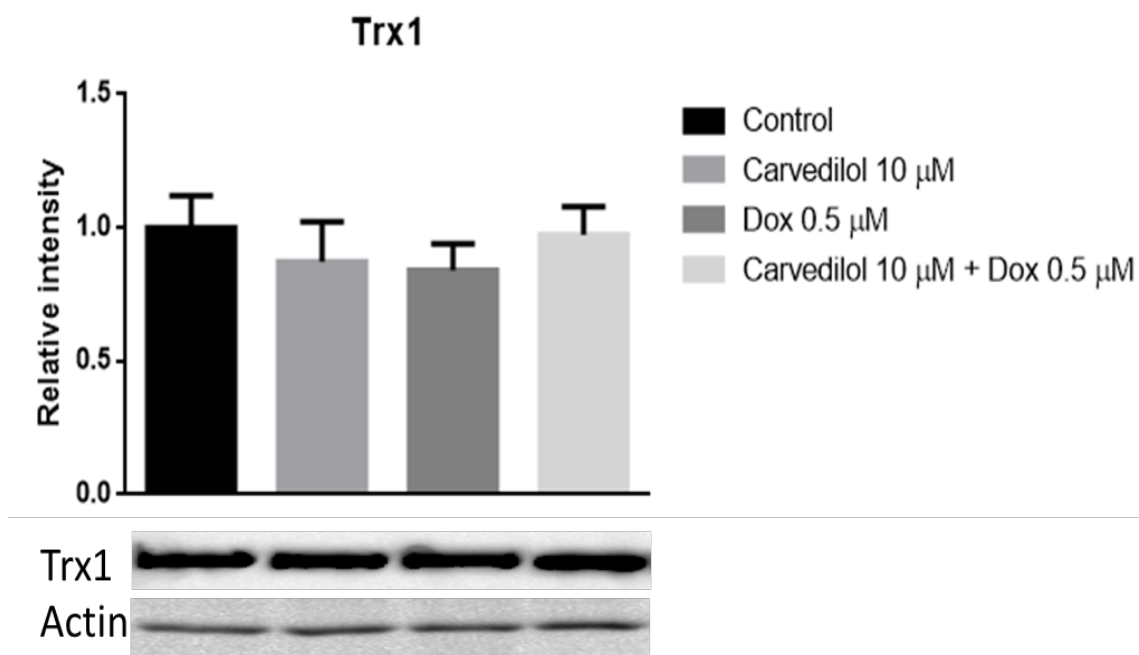


Figure 36. Effect of 10 μ M carvedilol and 0.5 μ M doxorubicin treatments on Trx1 expression in H9c2 cells after 24 hour treatment.

The data are presented as relative intensity (protein/actin) and expressed as the means \pm SD of three independent experiments. One-way ANOVA and Tukey's post hoc test were performed to analyze data at each time point.

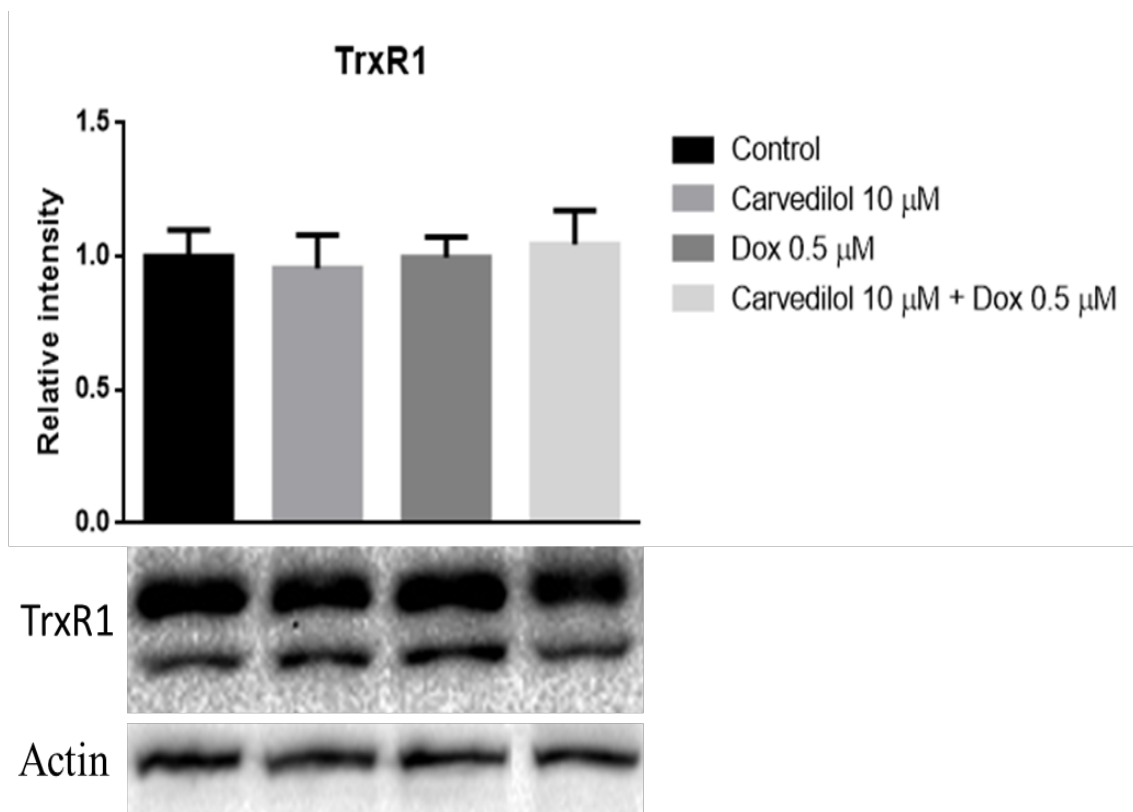


Figure 37. Effect of 10 μM carvedilol and 0.5 μM doxorubicin treatments on TrxR1 expression in H9c2 cells after 24 hour treatment.

The data are presented as relative intensity (protein/actin) and expressed as the means \pm SD of three independent experiments. One-way ANOVA and Tukey's post hoc test were performed to analyze data at each time point.

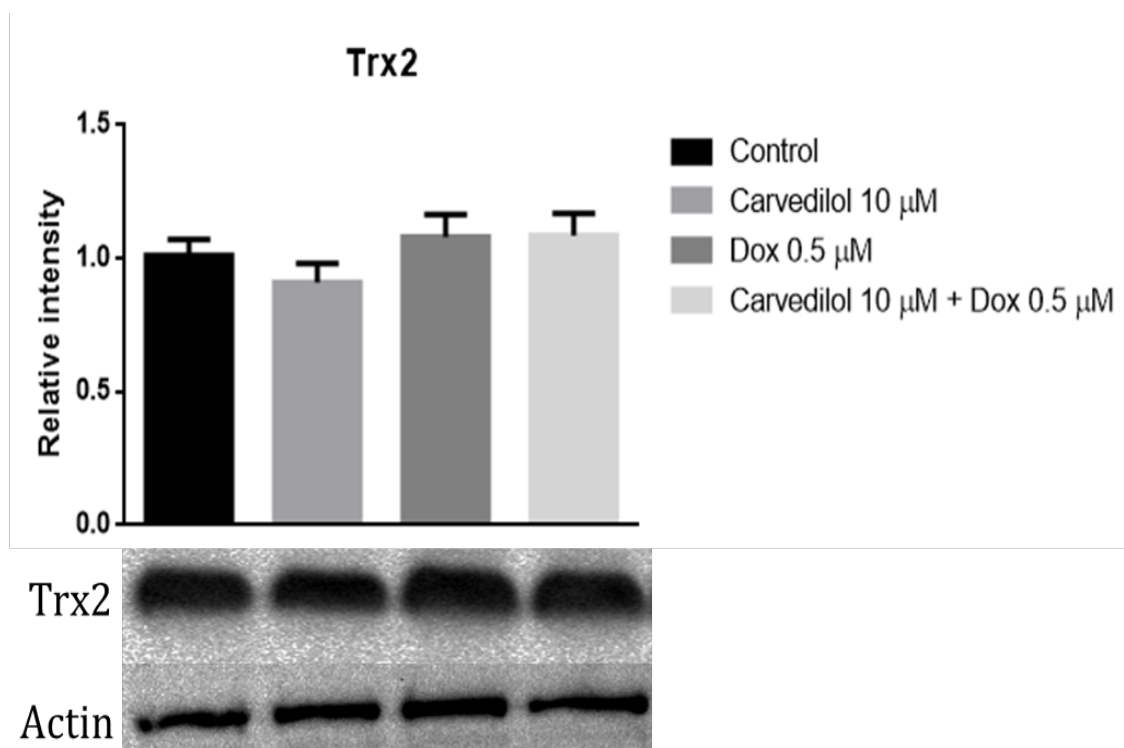


Figure 38. Effect of 10 μM carvedilol and 0.5 μM doxorubicin treatments on Trx2 expression in H9c2 cells after 24 hour treatment.

The data are presented as relative intensity (protein/actin) and expressed as the means \pm SD of three independent experiments. One-way ANOVA and Tukey's post hoc test were performed to analyze data at each time point.

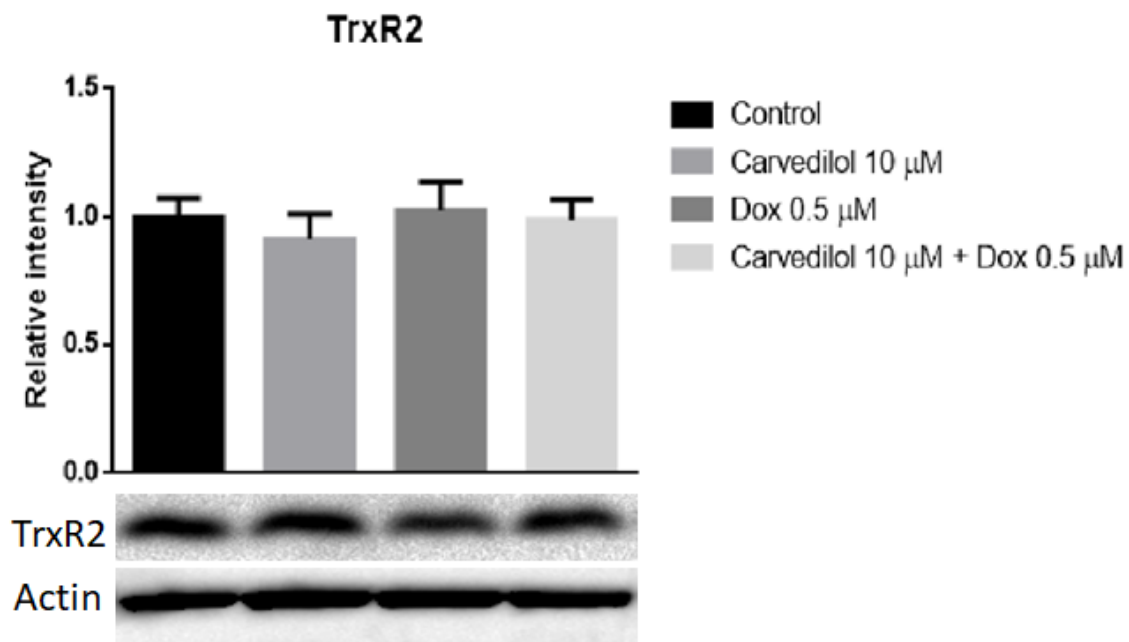


Figure 39. Effect of 10 μ M carvedilol and 0.5 μ M doxorubicin treatments on TrxR2 expression in H9c2 cells after 24 hour treatment.

The data are presented as relative intensity (protein/actin) and expressed as the means \pm SD of three independent experiments. One-way ANOVA and Tukey's post hoc test were performed to analyze data at each time point.

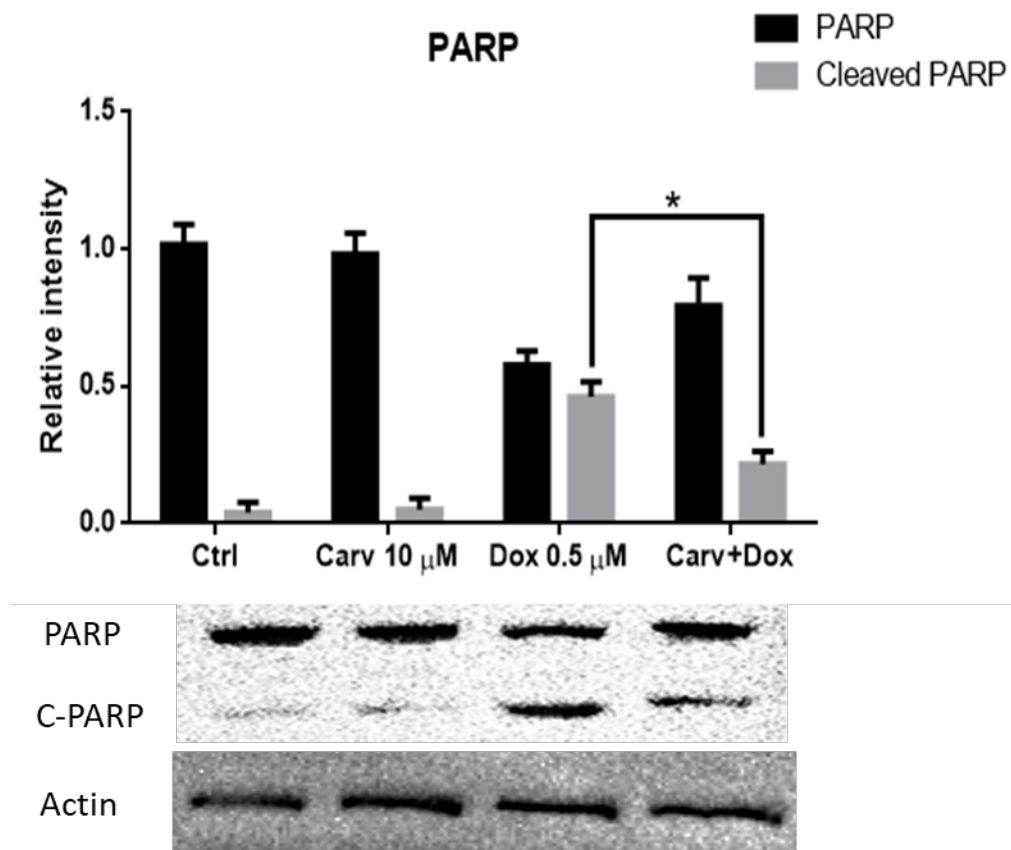


Figure 40. Effect of 10 μ M carvedilol and 0.5 μ M doxorubicin treatments on PARP and cleaved PARP expression in H9c2 cells after 24 hour treatment.

The data are presented as relative intensity (protein/actin) and expressed as the means \pm SD of three independent experiments. One-way ANOVA and Tukey's post hoc test were performed to analyze data at each time point. * $p < 0.05$

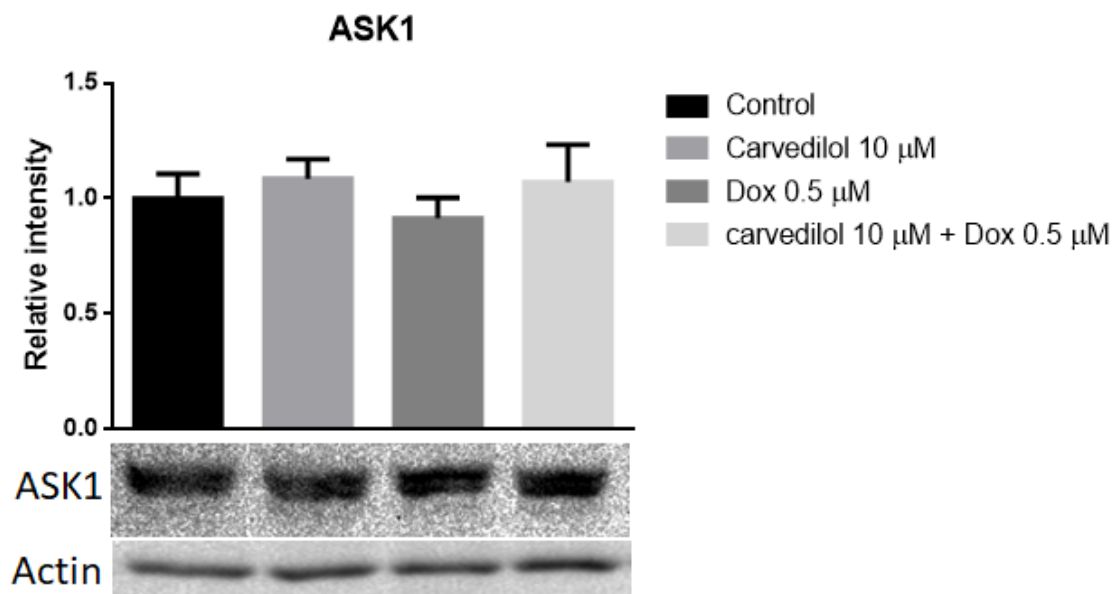


Figure 41. Effect of 10 μ M carvedilol and 0.5 μ M doxorubicin treatments on ASK1 expression in H9c2 cells after 24 hour treatment.

The data are presented as relative intensity (protein/actin) and expressed as the means \pm SD of three independent experiments. One-way ANOVA and Tukey's post hoc test were performed to analyze data at each time point

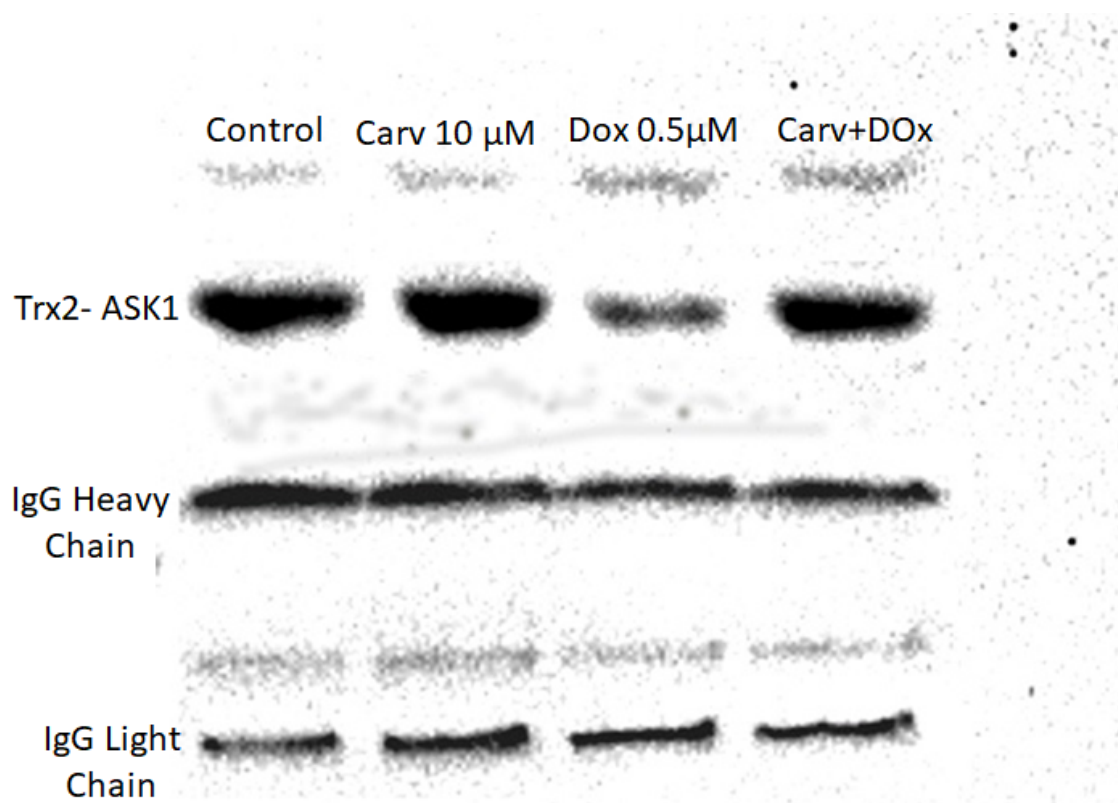


Figure 42. Anti-ASK1 antibody immunoblots of 10 μ M carvedilol and 0.5 μ M doxorubicin treatments immunoprecipitated with anti-Trx2 antibody.

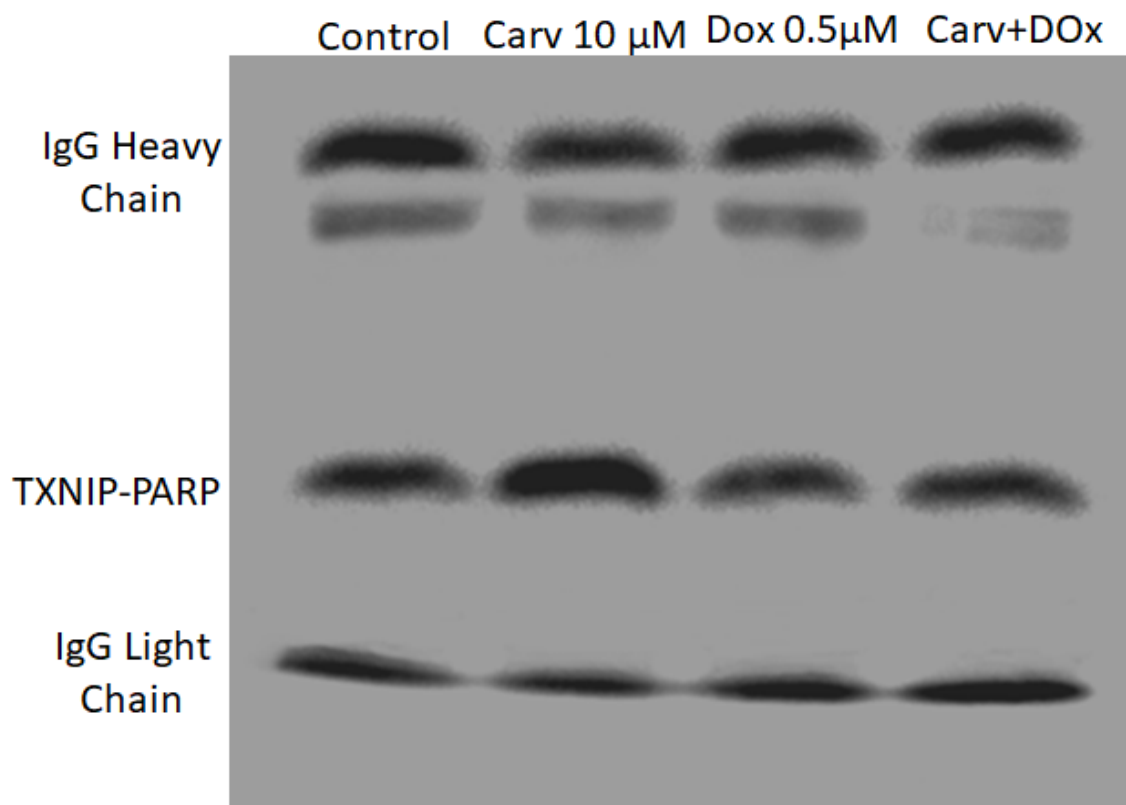


Figure 43. Anti-TXNIP antibody immunoblots of 10 μM carvedilol and 0.5 μM doxorubicin treatments immunoprecipitated with anti-PARP antibody.

4.4 Discussion

Doxorubicin-induced cardiotoxicity is believed to be mediated through the induction of oxidative stress. Carvedilol is unique among the beta-blockers as it has been shown to protect cardiomyocytes against oxidative stress. Multiple mechanisms have been suggested for carvedilol's protection such as free radical scavenging, suppressing the enzymatic generation of reactive oxygen species, and reduction of apoptotic and inflammation markers. However, there is limited information in the literature about the role of the thioredoxin pathway in carvedilol's antioxidant activity. In chapter 2, it was demonstrated that carvedilol was able to reduce TXNIP expression in the cytosol while increasing localization in the nucleus. This was accompanied by a change in TXNIP complexation with major proteins such as Trx1 and PARP. Chapter 3 showed the ability of doxorubicin to reduce cytoplasmic TXNIP expression. A previous literature report indicated that TXNIP downregulation was effective in reducing kidney injury induced by doxorubicin. Therefore, we investigated in this chapter the effect of carvedilol and doxorubicin treatment on TXNIP and related proteins in H9c2 rat cardiomyocytes. Our focus was to understand the involvement of the thioredoxin system in carvedilol cardioprotection and its impact on doxorubicin induced cardiotoxicity.

MTT assays were initially performed to test the possible cardioprotective effects of carvedilol. H9c2 cardiomyocyte cells were treated with carvedilol and doxorubicin at different times, orders, and concentrations. The best protective effect was shown when H9c2 cells were pretreated with carvedilol for 24 hours followed by treatment with carvedilol and doxorubicin for another 24 hours. Carvedilol exhibited significant antagonistic effects against doxorubicin with this regimen, and the greatest protection

was detected with the highest dose of doxorubicin (1 μ M). Other treatment regimens did not demonstrate any carvedilol protection against doxorubicin cardiac toxicity. Significantly, this indicates that pretreatment with carvedilol was required for the cardioprotection.

Carvedilol is well known in the literature for its antioxidant activity and its ability to bind and scavenge ROS in the body. On the other hand, increasing levels of mitochondrial reactive oxygen species are required for doxorubicin cardiac toxicity.¹¹² Our observation of increasing TXNIP in the mitochondria with doxorubicin treatment lines up with the literature. As a result, ROS production in H9c2 cells treated with carvedilol and doxorubicin was also determined. The results showed that 0.5 μ M doxorubicin treatment showed a significant increase in ROS production with 12 and 24 hour treatments. Shorter treatment times did not show significant ROS production with 0.5 μ M doxorubicin. However, 1 μ M doxorubicin did induce ROS production at short time points. This indicates that doxorubicin ROS production is time and dose dependent. As expected, 10 μ M carvedilol pretreatment was able to reduce the production of ROS induced by doxorubicin. However, this effect was only observed with carvedilol pretreatment. No benefit was found with combination treatment. This again confirms the necessity of carvedilol pretreatment and indicates that intracellular changes occurring within the 24 hour pretreatment are required for carvedilol's protection.

Next, the combination effect of carvedilol and doxorubicin on the thioredoxin system in H9c2 cells was evaluated to understand the role of this system in carvedilol cardiac protection against oxidative stress. We have already observed that doxorubicin

alone decreased TXNIP in the cytoplasm. Instead, TXNIP was found to be translocated to the mitochondria; this is consistent with induction of oxidative stress. Carvedilol alone initiated translocation of TXNIP to the nucleus. However, combination treatment of carvedilol and doxorubicin did not show accumulation of TXNIP in the nuclear fraction. Opposite to what we expected, carvedilol did not reverse TXNIP accumulation in the mitochondria with doxorubicin treatment as we observed the same level of TXNIP in the mitochondria with the combination treatment as doxorubicin alone. Furthermore, this combination treatment did not affect any other related proteins in this system.

TXNIP in the mitochondria can form a complex with Trx2. Formation of this complex is believed to release ASK1 leading to induction of apoptosis. Based on this, the TXNIP accumulation in the mitochondria would be expected to lead to reduced formation of the Trx2-ASK1 complex. This expected result was observed with doxorubicin treatment alone. However, carvedilol pretreatment did not exhibit decreased Trx2-ASK1 complexation compared to control. TXNIP complexation with PARP in the nucleus was also investigated. The TXNIP-PARP complexes seen with carvedilol alone were decreased in the combination treatment. This also support the translocation of TXNIP out of the nucleus to the mitochondria. On other hand, doxorubicin was able to increase cleaved PARP, a proapoptotic protein, indicating that doxorubicin is causing apoptosis in H9c2 cells. Carvedilol pretreatment was able to significantly reverse this effect. This observation is consistent with the increase in Trx2-ASK1 complex in the mitochondria indicating antiapoptotic effect.

The interaction between Trx and ASK1 involves a redox sensitive disulfide bond. The complex formation has been studied in detail between the cytosolic Trx1 and ASK1. The disulfide bond forms between cysteine-32 of Trx1 and cysteine-250 of ASK1. Upon oxidative stress, an intramolecular disulfide bond between cysteine-32 and cysteine-35 of Trx1 forms thereby releasing ASK1 from the complex. Then, ASK1 undergoes intramolecular disulfide bond formation leading to its activation and induction of apoptosis.¹¹¹ Under oxidative stress, TXNIP can translocate to the mitochondria where it can also form a disulfide bond with Trx. Under conditions of mild oxidative stress, a disulfide bond between cysteine-32 of Trx and cysteine-247 of TXNIP forms. This is often associated with increased activity of ASK1 leading to apoptosis. However, there is also evidence that the formation of the Trx-TXNIP complex can alter the transcription of other antioxidant proteins such as SOD and catalase. Therefore, the translocation of TXNIP to the mitochondria under mild oxidative stress will not necessarily induce apoptosis and can actually promote cell survival through enhanced anti-oxidant capacity. The situation changes with more severe oxidative stress. In this case, the complex between Trx and TXNIP is broken in favor of intramolecular disulfide bonds. The free TXNIP in the mitochondria initiates formation of a complex known as the NLRP3 inflammasome. The release of ASK1 and the formation of the inflammasome both contribute to oxidative stress-induced apoptosis.⁶⁴

In this study, doxorubicin significantly increased ROS production. This induction of oxidative stress promoted the translocation of TXNIP to the mitochondria and the induction of apoptosis, as expected. Carvedilol alone moved TXNIP into the nucleus. However, in the combination, the TXNIP was translocated out of the nucleus and to the

mitochondria. However, this did not lead to induction of apoptosis; in fact, apoptosis markers were significantly decreased. This may be explained by the different responses to oxidative stress described above. Carvedilol significantly reduced the ROS produced by doxorubicin; however, the ROS level was still above that of control. This ROS production could be significant enough to cause the translocation of TXNIP to the mitochondria. In doxorubicin treated cells, the accumulation of TXNIP in the mitochondria was associated with apoptosis induction similar to what is observed with high levels of oxidative stress. The combination treatment exhibited an effect comparable to mild oxidative stress conditions with increased complexation of TXNIP-ASK1 and reduced cleaved PARP. This may be associated with induction of other antioxidant enzymes. This would be consistent with the observation that pretreatment with carvedilol was required for the improvement in cell viability and the reduction in ROS. If direct free radical scavenging was the primary mechanism, it would have been expected to see these effects without pretreatment. However, since the pretreatment was required, it is logical to consider that induction of antioxidant proteins by carvedilol is responsible for protective effect, similar to that observed with mild oxidative stress. Further study is needed to confirm the upregulation of antioxidant proteins. In addition, complexation of Trx2 and ASK1 in the mitochondria should be examined to verify the mild oxidative stress response.

In conclusion, carvedilol was able to protect against apoptosis and oxidative stress induced by doxorubicin. This effect required carvedilol pretreatment. It was accompanied by increased Trx2-ASK1 complexation in the presence of TXNIP in the mitochondria.

The observed data was consistent with that previously reported for a mild oxidative stress response.

CHAPTER 5. CONCLUSIONS

This dissertation presents the impact of carvedilol treatment on the thioredoxin system as well as the role of carvedilol and TXNIP in protecting H9c2 cells against oxidative stress produced by doxorubicin. In this study, carvedilol was found to be able to induce translocation of TXNIP, the negative regulator of Trx, to the nucleus. This compartmentalization of TXNIP from the cytoplasm to the nucleus was associated with an increase in TXNIP-PARP1 complexation in the nuclear fraction and a decrease in TXNIP-Trx1 complexation in the cytosol (figure 44).

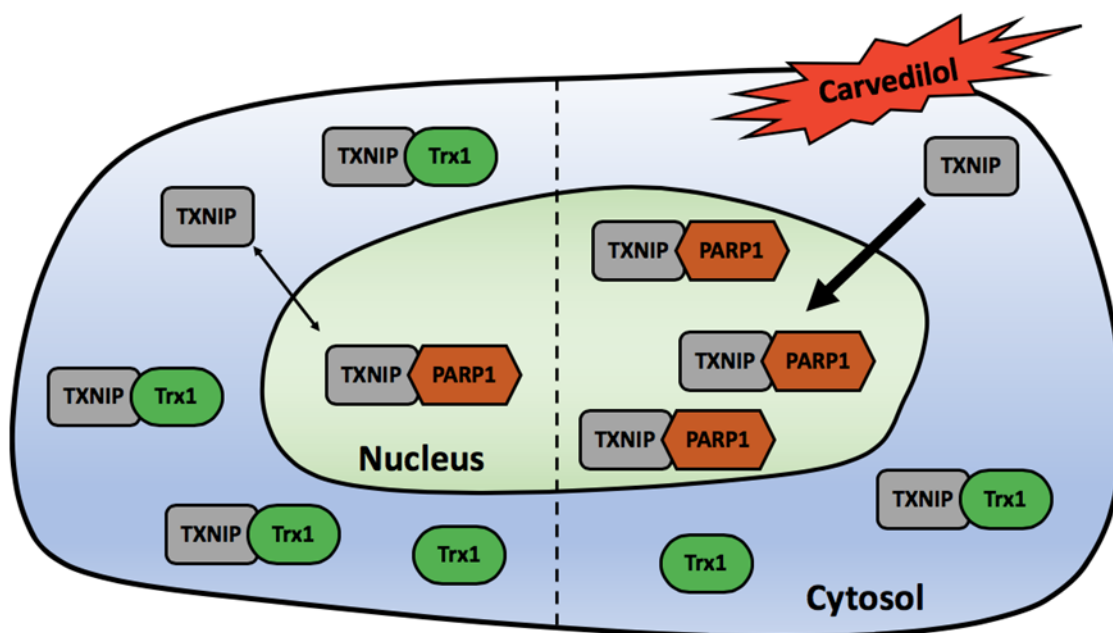


Figure 44. Effect of carvedilol in TXNIP localization under normal conditions.

Glucose levels have been found to change TXNIP expression in the cytosol. Cytosolic TXNIP increased with increasing glucose concentration in the H9c2 cells. This observation is consistent with the literature.¹¹³ Furthermore, TXNIP expression was decreased with different oxidative stress inducers. Doxorubicin and hypoxia-reoxygenation significantly decreased TXNIP expression. Both of those two methods generate ROS which suggests that TXNIP was moved to the mitochondria under those conditions. These findings suggest that modulating TXNIP translocation in the cell may be a potential target in diabetic cardiomyopathy and doxorubicin cardiac toxicity.

Doxorubicin increased ROS production after 12 and 24 hours of treatment at the 0.5 μ M concentration while the higher dose increased it at shorter time points. That proves that doxorubicin cardiotoxicity is time and dose dependent. Carvedilol was able to protect cardiomyocytes from doxorubicin toxicity. However, only cells pretreated with carvedilol were protected from toxicity from the doxorubicin treatment. This finding is supported by literature showing that pretreatment of carvedilol protected against doxorubicin damage in adult B6 mice.¹¹⁴ This is also consistent with our finding that carvedilol was able to prevent doxorubicin ROS production only in pretreated cells. The requirement for pretreatment indicates that a change in expression of endogenous antioxidant proteins may be involved in carvedilol's antioxidant effect. In fact, previous literature has shown that carvedilol plus doxorubicin resulted in an increase in expression and activity of other antioxidant proteins such as SOD and catalase.¹¹⁵ Further study should be conducted to determine the effect of carvedilol plus doxorubicin on expression of antioxidant proteins under the conditions used in this study.

Carvedilol and doxorubicin did not affect expression of any other protein in the thioredoxin family besides TXNIP. Doxorubicin translocated TXNIP to the mitochondria and decreased Trx2 complexation to ASK1, while carvedilol increased translocation to the nucleus. The combination caused a further reduction in cytosolic TXNIP, but carvedilol pretreatment did not prevent TXNIP translocation to the mitochondria. However, this was associated with restored Trx2-ASK1 complexation and reduced apoptosis. This finding is consistent with mild oxidative stress. In order to study this further, the complex of Trx1 and TXNIP in the cytosol and Trx2 and TXNIP in the mitochondria should be evaluated.

This study was conducted in the H9c2 rat cardiomyocytes model, and the main limitation of this model is that it is a non-contractile model. Thus, study in either an in vivo system or an ex vivo contractile system is needed to truly measure the effect of carvedilol treatment on the thioredoxin system and its role in protecting against doxorubicin toxicity. Another major limitation of this study is that it was difficult to determine the exact impact of TXNIP with the model used. In order to further study the role of TXNIP in cardioprotection by carvedilol, a TXNIP knockout mouse model or silencing the gene in a cell culture would be ideal. In addition, the mechanisms behind TXNIP movement within the cell are unclear. Importin alpha has been shown to be required for entry into the nucleus. However, export from the nucleus is not well understood. Also, the mechanisms for movement to the mitochondria are still unclear. Identifying these mechanisms of TXNIP movement to the mitochondria would be beneficial in finding a blocker to reduce doxorubicin toxicity.

Carvedilol is a non-selective β -adrenoceptor blocker and is used in the treatment of heart failure and hypertension. Unlike other β blocking drugs, carvedilol uniquely possesses antioxidant activity.^{65,66} In this study, carvedilol was able to translocate TXNIP to the nucleus while propranolol, atenolol and metoprolol did possess this effect. Carvedilol pretreatment protected H9c2 cells from doxorubicin toxicity while propranolol failed in that. These results suggest that carvedilol has unique off-target effects that should be further investigated for clinical significance. The previous literature has shown the ability of other agents such as verapamil, ramipril, and insulin to reduce TXNIP mRNA expression or degradation. Interestingly, carvedilol's effect on TXNIP is unique from these agents. Carvedilol does not decrease the overall TXNIP pool while verapamil, ramipril, and insulin actually decrease total cellular TXNIP. It is unclear which of these approaches would be most advantageous. Since TXNIP is a tumor suppressor gene, decreasing its expression could have a negative impact on cell growth. Therefore, carvedilol's mechanism might make it safer to use without increasing the risk of carcinogenesis. On the other hand, as was observed in this study, the TXNIP is still capable of moving within the cell with carvedilol treatment while this effect might be reduced with agents that decrease transcription or increase degradation of TXNIP; this could limit carvedilol's impact compared to other approaches. However, in this study, no negative impact of TXNIP translocation to the mitochondria with doxorubicin and carvedilol was observed.

In conclusion, this study shows for the first time that carvedilol impacts TXNIP localization and complexation and that the thioredoxin pathway may be involved in carvedilol's observed cardioprotective effect. Carvedilol succeeded in protecting against

doxorubicin toxicity through decreases activation of cell apoptotic signaling and reduction of oxidative stress. Carvedilol is currently used for the treatment of heart failure and hypertension. Multiple reports have shown its ability to work as an antioxidant, though the exact mechanism of antioxidant activity is not known. This dissertation study reported its ability to modulate the cardiac cells' antioxidants activity through modulating the TXNIP protein. This mechanism might explain carvedilol's antioxidant activity and how it contributes to cardioprotection. This knowledge may also lead to expanded therapeutic uses of carvedilol such as in other cardiovascular diseases, diabetes, and diabetes complications.

BIBLIOGRAPHY

- [1] M.A. Comini, Measurement and meaning of cellular thiol:disulfide redox status, *Free Radic Res* 50(2) (2016) 246-71.
- [2] L.B. Poole, The basics of thiols and cysteines in redox biology and chemistry, *Free Radic Biol Med* 80 (2015) 148-57.
- [3] S. Lee, S.M. Kim, R.T. Lee, Thioredoxin and thioredoxin target proteins: from molecular mechanisms to functional significance, *Antioxid Redox Signal* 18(10) (2013) 1165-207.
- [4] M.K. Ahsan, I. Lekli, D. Ray, J. Yodoi, D.K. Das, Redox regulation of cell survival by the thioredoxin superfamily: an implication of redox gene therapy in the heart, *Antioxid Redox Signal* 11(11) (2009) 2741-58.
- [5] D.L. Kirkpatrick, M. Kuperus, M. Dowdeswell, N. Potier, L.J. Donald, M. Kunkel, M. Berggren, M. Angulo, G. Powis, Mechanisms of inhibition of the thioredoxin growth factor system by antitumor 2-imidazolyl disulfides, *Biochem Pharmacol* 55(7) (1998) 987-94.
- [6] G. Bulaj, T. Kortemme, D.P. Goldenberg, Ionization-reactivity relationships for cysteine thiols in polypeptides, *Biochemistry* 37(25) (1998) 8965-72.
- [7] R.E. Hansen, H. Ostergaard, J.R. Winther, Increasing the reactivity of an artificial dithiol-disulfide pair through modification of the electrostatic milieu, *Biochemistry* 44(15) (2005) 5899-906.
- [8] A.T. Setterdahl, P.T. Chivers, M. Hirasawa, S.D. Lemaire, E. Keryer, M. Miginiac-Maslow, S.K. Kim, J. Mason, J.P. Jacquot, C.C. Longbine, F. de Lamotte-Guery, D.B.

Knaff, Effect of pH on the oxidation-reduction properties of thioredoxins, *Biochemistry* 42(50) (2003) 14877-84.

[9] G. Bulaj, D.P. Goldenberg, Mutational analysis of hydrogen bonding residues in the BPTI folding pathway, *J Mol Biol* 313(3) (2001) 639-56.

[10] R.B. Myers, G.M. Fomovsky, S. Lee, M. Tan, B.F. Wang, P. Patwari, J. Yoshioka, Deletion of thioredoxin-interacting protein improves cardiac inotropic reserve in the streptozotocin-induced diabetic heart, *Am J Physiol Heart Circ Physiol* 310(11) (2016) H1748-59.

[11] D. Mustacich, G. Powis, Thioredoxin reductase, *Biochem J* 346 Pt 1 (2000) 1-8.

[12] V.N. Gladyshev, K.T. Jeang, T.C. Stadtman, Selenocysteine, identified as the penultimate C-terminal residue in human T-cell thioredoxin reductase, corresponds to TGA in the human placental gene, *Proc Natl Acad Sci U S A* 93(12) (1996) 6146-51.

[13] C. Johansson, C.H. Lillig, A. Holmgren, Human mitochondrial glutaredoxin reduces S-glutathionylated proteins with high affinity accepting electrons from either glutathione or thioredoxin reductase, *J Biol Chem* 279(9) (2004) 7537-43.

[14] J. Lundstrom, A. Holmgren, Protein disulfide-isomerase is a substrate for thioredoxin reductase and has thioredoxin-like activity, *J Biol Chem* 265(16) (1990) 9114-20.

[15] K. Becker, S. Gromer, R.H. Schirmer, S. Muller, Thioredoxin reductase as a pathophysiological factor and drug target, *Eur J Biochem* 267(20) (2000) 6118-25.

[16] R. Brigelius-Flohe, M. Muller, D. Lippmann, A.P. Kipp, The yin and yang of nrf2-regulated selenoproteins in carcinogenesis, *Int J Cell Biol* 2012 (2012) 486147.

- [17] K.S. Chen, H.F. DeLuca, Isolation and characterization of a novel cDNA from HL-60 cells treated with 1,25-dihydroxyvitamin D-3, *Biochim Biophys Acta* 1219(1) (1994) 26-32.
- [18] H. Yamawaki, S. Pan, R.T. Lee, B.C. Berk, Fluid shear stress inhibits vascular inflammation by decreasing thioredoxin-interacting protein in endothelial cells, *J Clin Invest* 115(3) (2005) 733-8.
- [19] H.H. Ting, F.K. Timimi, K.S. Boles, S.J. Creager, P. Ganz, M.A. Creager, Vitamin C improves endothelium-dependent vasodilation in patients with non-insulin-dependent diabetes mellitus, *J Clin Invest* 97(1) (1996) 22-8.
- [20] M. Valko, C.J. Rhodes, J. Moncol, M. Izakovic, M. Mazur, Free radicals, metals and antioxidants in oxidative stress-induced cancer, *Chem Biol Interact* 160(1) (2006) 1-40.
- [21] M. Saitoh, H. Nishitoh, M. Fujii, K. Takeda, K. Tobiume, Y. Sawada, M. Kawabata, K. Miyazono, H. Ichijo, Mammalian thioredoxin is a direct inhibitor of apoptosis signal-regulating kinase (ASK) 1, *Embo j* 17(9) (1998) 2596-606.
- [22] K. Hensley, R.A. Floyd, Reactive oxygen species and protein oxidation in aging: a look back, a look ahead, *Arch Biochem Biophys* 397(2) (2002) 377-83.
- [23] N.R. Webster, J.F. Nunn, Molecular structure of free radicals and their importance in biological reactions, *Br J Anaesth* 60(1) (1988) 98-108.
- [24] D. Harman, Aging: a theory based on free radical and radiation chemistry, *J Gerontol* 11(3) (1956) 298-300.
- [25] P.S. Rao, S. Kalva, A. Yerramilli, S. Mamidi, Free radicals and tissue damage: role of antioxidants, *Free radicals and antioxidants* 1(4) (2011) 2-7.

- [26] F.L. Muller, Y. Liu, H. Van Remmen, Complex III releases superoxide to both sides of the inner mitochondrial membrane, *J Biol Chem* 279(47) (2004) 49064-73.
- [27] J.F. Turrens, Mitochondrial formation of reactive oxygen species, *The Journal of physiology* 552(2) (2003) 335-344.
- [28] M.J. Morgan, Z.G. Liu, Crosstalk of reactive oxygen species and NF-kappaB signaling, *Cell Res* 21(1) (2011) 103-15.
- [29] S. Puntarulo, A.I. Cederbaum, Production of reactive oxygen species by microsomes enriched in specific human cytochrome P450 enzymes, *Free Radic Biol Med* 24(7-8) (1998) 1324-30.
- [30] B. Poljsak, D. Suput, I. Milisav, Achieving the balance between ROS and antioxidants: when to use the synthetic antioxidants, *Oxid Med Cell Longev* 2013 (2013) 956792.
- [31] S. Di Meo, T.T. Reed, P. Venditti, V.M. Victor, Role of ROS and RNS Sources in Physiological and Pathological Conditions, *Oxid Med Cell Longev* 2016 (2016) 1245049.
- [32] L. He, T. He, S. Farrar, L. Ji, T. Liu, X. Ma, Antioxidants Maintain Cellular Redox Homeostasis by Elimination of Reactive Oxygen Species, *Cell Physiol Biochem* 44(2) (2017) 532-553.
- [33] WHO, Cardiovascular Diseases, https://www.who.int/cardiovascular_diseases/en/ Accessed January 20, 2019.
- [34] A.A. Inamdar, A.C. Inamdar, Heart Failure: Diagnosis, Management and Utilization, *J Clin Med* 5(7) (2016).

- [35] H. Tsutsui, S. Kinugawa, S. Matsushima, Oxidative stress and heart failure, *American Journal of Physiology-Heart and Circulatory Physiology* 301(6) (2011) H2181-H2190.
- [36] K. Sugamura, J.F. Keaney Jr, Reactive oxygen species in cardiovascular disease, *Free Radical Biology and Medicine* 51(5) (2011) 978-992.
- [37] Y. Liu, W. Min, Thioredoxin promotes ASK1 ubiquitination and degradation to inhibit ASK1-mediated apoptosis in a redox activity-independent manner, *Circ Res* 90(12) (2002) 1259-66.
- [38] J.P. Sanchez-Villamil, V. D'Annunzio, P. Finocchietto, S. Holod, I. Rebagliati, H. Perez, J.G. Peralta, R.J. Gelpi, J.J. Poderoso, M.C. Carreras, Cardiac-specific overexpression of thioredoxin 1 attenuates mitochondrial and myocardial dysfunction in septic mice, *Int J Biochem Cell Biol* 81(Pt B) (2016) 323-334.
- [39] M. Conrad, C. Jakupoglu, S.G. Moreno, S. Lippl, A. Banjac, M. Schneider, H. Beck, A.K. Hatzopoulos, U. Just, F. Sinowatz, W. Schmahl, K.R. Chien, W. Wurst, G.W. Bornkamm, M. Brielmeier, Essential role for mitochondrial thioredoxin reductase in hematopoiesis, heart development, and heart function, *Mol Cell Biol* 24(21) (2004) 9414-23.
- [40] T.Y. Hui, S.S. Sheth, J.M. Diffley, D.W. Potter, A.J. Lusis, A.D. Attie, R.A. Davis, Mice lacking thioredoxin-interacting protein provide evidence linking cellular redox state to appropriate response to nutritional signals, *J Biol Chem* 279(23) (2004) 24387-93.
- [41] J.L. Witztum, D. Steinberg, Role of oxidized low density lipoprotein in atherogenesis, *J Clin Invest* 88(6) (1991) 1785-1792.

- [42] J.W. Gofman, F. Lindgren, H. Elliott, W. Mantz, J. Hewitt, B. Strisower, V. Herring, T.P. Lyon, The role of lipids and lipoproteins in atherosclerosis, *Science* 111(2877) (1950) 166-186.
- [43] L. Kautz, V. Gabayan, X. Wang, J. Wu, J. Onwuzurike, G. Jung, B. Qiao, A.J. Lusis, T. Ganz, E. Nemeth, Testing the iron hypothesis in a mouse model of atherosclerosis, *Cell Rep* 5(5) (2013) 1436-42.
- [44] T. Sousa, S. Oliveira, J. Afonso, M. Morato, D. Patinha, S. Fraga, F. Carvalho, A. Albino-Teixeira, Role of H₂O₂ in hypertension, renin-angiotensin system activation and renal medullary dysfunction caused by angiotensin II, *British journal of pharmacology* 166(8) (2012) 2386-2401.
- [45] A. Baradaran, H. Nasri, M. Rafieian-Kopaei, Oxidative stress and hypertension: Possibility of hypertension therapy with antioxidants, *J Res Med Sci* 19(4) (2014) 358-67.
- [46] J. Rybka, D. Kupeczyk, K. Kedziora-Kornatowska, J. Motyl, J. Czuczejko, K. Szewczyk-Golec, M. Kozakiewicz, H. Pawluk, L.A. Carvalho, J. Kedziora, Glutathione-related antioxidant defense system in elderly patients treated for hypertension, *Cardiovasc Toxicol* 11(1) (2011) 1-9.
- [47] N. Munoz-Durango, C.A. Fuentes, A.E. Castillo, L.M. Gonzalez-Gomez, A. Vecchiola, C.E. Fardella, A.M. Kalergis, Role of the Renin-Angiotensin-Aldosterone System beyond Blood Pressure Regulation: Molecular and Cellular Mechanisms Involved in End-Organ Damage during Arterial Hypertension, *Int J Mol Sci* 17(7) (2016).

- [48] Y. Wang, G.W. De Keulenaer, R.T. Lee, Vitamin D₃-up-regulated protein-1 is a stress-responsive gene that regulates cardiomyocyte viability through interaction with thioredoxin, *Journal of Biological Chemistry* 277(29) (2002) 26496-26500.
- [49] J. Yoshioka, K. Imahashi, S.A. Gabel, W.A. Chutkow, A.A. Burds, J. Gannon, P.C. Schulze, C. MacGillivray, R.E. London, E. Murphy, R.T. Lee, Targeted deletion of thioredoxin-interacting protein regulates cardiac dysfunction in response to pressure overload, *Circ Res* 101(12) (2007) 1328-38.
- [50] T. Ago, T. Liu, P. Zhai, W. Chen, H. Li, J.D. Molkenin, S.F. Vatner, J. Sadoshima, A redox-dependent pathway for regulating class II HDACs and cardiac hypertrophy, *Cell* 133(6) (2008) 978-93.
- [51] T. Bedarida, S. Baron, F. Vibert, A. Ayer, D. Henrion, E. Thioulouse, C. Marchiol, J.L. Beaudoux, C.H. Cottart, V. Nivet-Antoine, Resveratrol Decreases TXNIP mRNA and Protein Nuclear Expressions With an Arterial Function Improvement in Old Mice, *J Gerontol A Biol Sci Med Sci* 71(6) (2016) 720-9.
- [52] W.A. Chutkow, A.L. Birkenfeld, J.D. Brown, H.Y. Lee, D.W. Frederick, J. Yoshioka, P. Patwari, R. Kursawe, S.W. Cushman, J. Plutzky, G.I. Shulman, V.T. Samuel, R.T. Lee, Deletion of the alpha-arrestin protein Txnip in mice promotes adiposity and adipogenesis while preserving insulin sensitivity, *Diabetes* 59(6) (2010) 1424-34.
- [53] J. Chen, H. Cha-Molstad, A. Szabo, A. Shalev, Diabetes induces and calcium channel blockers prevent cardiac expression of proapoptotic thioredoxin-interacting protein, *Am J Physiol Endocrinol Metab* 296(5) (2009) E1133-9.

- [54] G. Xu, J. Chen, G. Jing, A. Shalev, Preventing beta-cell loss and diabetes with calcium channel blockers, *Diabetes* 61(4) (2012) 848-56.
- [55] S.T. Hui, A.M. Andres, A.K. Miller, N.J. Spann, D.W. Potter, N.M. Post, A.Z. Chen, S. Sachithanatham, D.Y. Jung, J.K. Kim, R.A. Davis, Txnip balances metabolic and growth signaling via PTEN disulfide reduction, *Proc Natl Acad Sci U S A* 105(10) (2008) 3921-6.
- [56] A.H. Minn, C. Hafele, A. Shalev, Thioredoxin-interacting protein is stimulated by glucose through a carbohydrate response element and induces beta-cell apoptosis, *Endocrinology* 146(5) (2005) 2397-405.
- [57] J. Chen, G. Saxena, I.N. Mungrue, A.J. Lusic, A. Shalev, Thioredoxin-interacting protein: a critical link between glucose toxicity and beta-cell apoptosis, *Diabetes* 57(4) (2008) 938-44.
- [58] A.L. Sverdlov, W.P. Chan, N.E. Procter, Y.Y. Chirkov, D.T. Ngo, J.D. Horowitz, Reciprocal regulation of NO signaling and TXNIP expression in humans: impact of aging and ramipril therapy, *Int J Cardiol* 168(5) (2013) 4624-30.
- [59] M. Shaked, M. Ketzinel-Gilad, Y. Ariav, E. Cerasi, N. Kaiser, G. Leibowitz, Insulin counteracts glucotoxic effects by suppressing thioredoxin-interacting protein production in INS-1E beta cells and in *Psammomys obesus* pancreatic islets, *Diabetologia* 52(4) (2009) 636-44.
- [60] H. Parikh, E. Carlsson, W.A. Chutkow, L.E. Johansson, H. Storgaard, P. Poulsen, R. Saxena, C. Ladd, P.C. Schulze, M.J. Mazzini, C.B. Jensen, A. Krook, M. Bjornholm, H. Tornqvist, J.R. Zierath, M. Ridderstrale, D. Altshuler, R.T. Lee, A. Vaag, L.C. Groop,

- V.K. Mootha, TXNIP regulates peripheral glucose metabolism in humans, *PLoS Med* 4(5) (2007) e158.
- [61] N. Wu, B. Zheng, A. Shaywitz, Y. Dagon, C. Tower, G. Bellinger, C.H. Shen, J. Wen, J. Asara, T.E. McGraw, B.B. Kahn, L.C. Cantley, AMPK-dependent degradation of TXNIP upon energy stress leads to enhanced glucose uptake via GLUT1, *Mol Cell* 49(6) (2013) 1167-75.
- [62] W. Shao, Z. Yu, I.G. Fantus, T. Jin, Cyclic AMP signaling stimulates proteasome degradation of thioredoxin interacting protein (TxNIP) in pancreatic beta-cells, *Cell Signal* 22(8) (2010) 1240-6.
- [63] M. Shaked, M. Ketzinel-Gilad, E. Cerasi, N. Kaiser, G. Leibowitz, AMP-activated protein kinase (AMPK) mediates nutrient regulation of thioredoxin-interacting protein (TXNIP) in pancreatic beta-cells, *PLoS One* 6(12) (2011) e28804.
- [64] L.P. Singh, Thioredoxin Interacting Protein (TXNIP) and Pathogenesis of Diabetic Retinopathy, *J Clin Exp Ophthalmol* 4 (2013).
- [65] P. Dandona, H. Ghanim, D.P. Brooks, Antioxidant activity of carvedilol in cardiovascular disease, *J Hypertens* 25(4) (2007) 731-41.
- [66] S. Ayashi, A.R. Assareh, M.T. Jalali, S. Olapour, H. Yaghooti, Role of antioxidant property of carvedilol in mild to moderate hypertensive patients: A prospective open-label study, *Indian J Pharmacol* 48(4) (2016) 372-376.
- [67] D.A. Sica, Current concepts of pharmacotherapy in hypertension. Carvedilol: new considerations for its use in the diabetic patient with hypertension, *J Clin Hypertens (Greenwich)* 7(1) (2005) 59-64.

- [68] P.A. Poole-Wilson, K. Swedberg, J.G. Cleland, A. Di Lenarda, P. Hanrath, M. Komajda, J. Lubsen, B. Lutiger, M. Metra, W.J. Remme, C. Torp-Pedersen, A. Scherhag, A. Skene, Comparison of carvedilol and metoprolol on clinical outcomes in patients with chronic heart failure in the Carvedilol Or Metoprolol European Trial (COMET): randomised controlled trial, *Lancet* 362(9377) (2003) 7-13.
- [69] E. Saltiel, W. McGuire, Doxorubicin (adriamycin) cardiomyopathy—a critical review, *Western Journal of Medicine* 139(3) (1983) 332.
- [70] K. Chatterjee, J. Zhang, N. Honbo, J.S. Karliner, Doxorubicin cardiomyopathy, *Cardiology* 115(2) (2010) 155-162.
- [71] R.D. Olson, R.C. Boerth, J.G. Gerber, A.S. Nies, Mechanism of adriamycin cardiotoxicity: evidence for oxidative stress, *Life Sci* 29(14) (1981) 1393-401.
- [72] T. Simunek, M. Sterba, O. Popelova, M. Adamcova, R. Hrdina, V. Gersl, Anthracycline-induced cardiotoxicity: overview of studies examining the roles of oxidative stress and free cellular iron, *Pharmacol Rep* 61(1) (2009) 154-71.
- [73] B. Kalyanaraman, J. Joseph, S. Kalivendi, S. Wang, E. Konorev, S. Kotamraju, Doxorubicin-induced apoptosis: implications in cardiotoxicity, *Molecular and cellular biochemistry* 234(1) (2002) 119-124.
- [74] Y. Octavia, C.G. Tocchetti, K.L. Gabrielson, S. Janssens, H.J. Crijns, A.L. Moens, Doxorubicin-induced cardiomyopathy: from molecular mechanisms to therapeutic strategies, *J Mol Cell Cardiol* 52(6) (2012) 1213-25.
- [75] A. Kumar, R. Mittal, Mapping Txnip: Key connexions in progression of diabetic nephropathy, *Pharmacol Rep* 70(3) (2018) 614-622.

- [76] Y. Nishinaka, H. Masutani, S. Oka, Y. Matsuo, Y. Yamaguchi, K. Nishio, Y. Ishii, J. Yodoi, Importin alpha1 (Rch1) mediates nuclear translocation of thioredoxin-binding protein-2/vitamin D(3)-up-regulated protein 1, *J Biol Chem* 279(36) (2004) 37559-65.
- [77] H. Tsutsui, S. Kinugawa, S. Matsushima, Oxidative stress and heart failure, *Am J Physiol Heart Circ Physiol* 301(6) (2011) H2181-H2190.
- [78] Q. Liu, S. Wang, L. Cai, Diabetic cardiomyopathy and its mechanisms: Role of oxidative stress and damage, *J Diabetes Investig* 5(6) (2014) 623-34.
- [79] D.N. Granger, P.R. Kvietys, Reperfusion injury and reactive oxygen species: The evolution of a concept, *Redox Biol* 6 (2015) 524-51.
- [80] M. Yamamoto, G. Yang, C. Hong, J. Liu, E. Holle, X. Yu, T. Wagner, S.F. Vatner, J. Sadoshima, Inhibition of endogenous thioredoxin in the heart increases oxidative stress and cardiac hypertrophy, *J Clin Invest* 112(9) (2003) 1395-406.
- [81] Q. Huang, H.J. Zhou, H. Zhang, Y. Huang, F. Hinojosa-Kirschenbaum, P. Fan, L. Yao, L. Belardinelli, G. Tellides, F.J. Giordano, G.R. Budas, W. Min, Thioredoxin-2 inhibits mitochondrial reactive oxygen species generation and apoptosis stress kinase-1 activity to maintain cardiac function, *Circulation* 131(12) (2015) 1082-97.
- [82] G. Xiang, T. Seki, M.D. Schuster, P. Witkowski, A.J. Boyle, F. See, T.P. Martens, A. Kocher, H. Sondermeijer, H. Krum, S. Itescu, Catalytic degradation of vitamin D up-regulated protein 1 mRNA enhances cardiomyocyte survival and prevents left ventricular remodeling after myocardial ischemia, *J Biol Chem* 280(47) (2005) 39394-402.
- [83] H. Su, L. Ji, W. Xing, W. Zhang, H. Zhou, X. Qian, X. Wang, F. Gao, X. Sun, H. Zhang, Acute hyperglycaemia enhances oxidative stress and aggravates myocardial

ischaemia/reperfusion injury: role of thioredoxin-interacting protein, *J Cell Mol Med* 17(1) (2013) 181-91.

[84] B.F. Wang, J. Yoshioka, The Emerging Role of Thioredoxin-Interacting Protein in Myocardial Ischemia/Reperfusion Injury, *J Cardiovasc Pharmacol Ther* 22(3) (2017) 219-229.

[85] J. Yoshioka, P.C. Schulze, M. Cupesi, J.D. Sylvan, C. MacGillivray, J. Gannon, H. Huang, R.T. Lee, Thioredoxin-interacting protein controls cardiac hypertrophy through regulation of thioredoxin activity, *Circulation* 109(21) (2004) 2581-6.

[86] W.M. Book, Carvedilol: a nonselective beta blocking agent with antioxidant properties, *Congest Heart Fail* 8(3) (2002) 173-7, 190.

[87] R.J. Zepeda, R. Castillo, R. Rodrigo, J.C. Prieto, I. Aramburu, S. Brugere, K. Galdames, V. Noriega, H.F. Miranda, Effect of carvedilol and nebivolol on oxidative stress-related parameters and endothelial function in patients with essential hypertension, *Basic Clin Pharmacol Toxicol* 111(5) (2012) 309-16.

[88] J.B. Bartholomeu, A.S. Vanzelli, N.P. Rolim, J.C. Ferreira, L.R. Bechara, L.Y. Tanaka, K.T. Rosa, M.M. Alves, A. Medeiros, K.C. Mattos, M.A. Coelho, M.C. Irigoyen, E.M. Krieger, J.E. Krieger, C.E. Negrao, P.R. Ramires, S. Guatimosim, P.C. Brum, Intracellular mechanisms of specific beta-adrenoceptor antagonists involved in improved cardiac function and survival in a genetic model of heart failure, *J Mol Cell Cardiol* 45(2) (2008) 240-9.

[89] K. Kawai, F. Qin, J. Shite, W. Mao, S. Fukuoka, C.S. Liang, Importance of antioxidant and antiapoptotic effects of beta-receptor blockers in heart failure therapy, *Am J Physiol Heart Circ Physiol* 287(3) (2004) H1003-12.

- [90] H. Huang, J. Shan, X.H. Pan, H.P. Wang, L.B. Qian, Q. Xia, Carvedilol improved diabetic rat cardiac function depending on antioxidant ability, *Diabetes Res Clin Pract* 75(1) (2007) 7-13.
- [91] C. Xu, Y. Hu, L. Hou, J. Ju, X. Li, N. Du, X. Guan, Z. Liu, T. Zhang, W. Qin, N. Shen, M.U. Bilal, Y. Lu, Y. Zhang, H. Shan, beta-Blocker carvedilol protects cardiomyocytes against oxidative stress-induced apoptosis by up-regulating miR-133 expression, *J Mol Cell Cardiol* 75 (2014) 111-21.
- [92] M. Wang, X. Wang, C.B. Ching, W.N. Chen, Proteomic profiling of cellular responses to Carvedilol enantiomers in vascular smooth muscle cells by iTRAQ-coupled 2-D LC-MS/MS, *J Proteomics* 73(8) (2010) 1601-11.
- [93] H. Hernan Gomez Llambi, G. Cao, M. Donato, D. Suarez, G. Ottaviano, A. Muller, B. Buchholz, R. Gelpi, M. Otero-Losada, J. Milei, Left ventricular hypertrophy does not prevent heart failure in experimental hypertension, *Int J Cardiol* 238 (2017) 57-65.
- [94] Y. Zhao, Y. Xu, J. Zhang, T. Ji, Cardioprotective effect of carvedilol: inhibition of apoptosis in H9c2 cardiomyocytes via the TLR4/NF-kappaB pathway following ischemia/reperfusion injury, *Exp Ther Med* 8(4) (2014) 1092-1096.
- [95] O.N. Spindel, C. Yan, B.C. Berk, Thioredoxin-interacting protein mediates nuclear-to-plasma membrane communication: role in vascular endothelial growth factor 2 signaling, *Arterioscler Thromb Vasc Biol* 32(5) (2012) 1264-70.
- [96] R.R. Poudel, N.K. Kafle, Verapamil in Diabetes, *Indian J Endocrinol Metab* 21(5) (2017) 788-789.

- [97] O.N. Spindel, C. World, B.C. Berk, Thioredoxin interacting protein: redox dependent and independent regulatory mechanisms, *Antioxid Redox Signal* 16(6) (2012) 587-96.
- [98] G. Saxena, J. Chen, A. Shalev, Intracellular shuttling and mitochondrial function of thioredoxin-interacting protein, *J Biol Chem* 285(6) (2010) 3997-4005.
- [99] A. Brunyanszki, G. Olah, C. Coletta, B. Szczesny, C. Szabo, Regulation of mitochondrial poly(ADP-Ribose) polymerase activation by the beta-adrenoceptor/cAMP/protein kinase A axis during oxidative stress, *Mol Pharmacol* 86(4) (2014) 450-62.
- [100] E. Yoshihara, S. Masaki, Y. Matsuo, Z. Chen, H. Tian, J. Yodoi, Thioredoxin/Txnip: redoxisome, as a redox switch for the pathogenesis of diseases, *Front Immunol* 4 (2014) 514.
- [101] T. Lane, B. Flam, R. Lockey, N. Kolliputi, TXNIP shuttling: missing link between oxidative stress and inflammasome activation, *Front Physiol* 4 (2013) 50.
- [102] G. Schevzov, A.J. Kee, B. Wang, V.B. Sequeira, J. Hook, J.D. Coombes, C.A. Lucas, J.R. Stehn, E.A. Musgrove, A. Cretu, R. Assoian, T. Fath, T. Hanoch, R. Seger, I. Pleines, B.T. Kile, E.C. Hardeman, P.W. Gunning, Regulation of cell proliferation by ERK and signal-dependent nuclear translocation of ERK is dependent on Tm5NM1-containing actin filaments, *Mol Biol Cell* 26(13) (2015) 2475-90.
- [103] K. Gao, Y. Chi, W. Sun, M. Takeda, J. Yao, 5'-AMP-activated protein kinase attenuates adriamycin-induced oxidative podocyte injury through thioredoxin-mediated suppression of the apoptosis signal-regulating kinase 1-P38 signaling pathway, *Mol Pharmacol* 85(3) (2014) 460-71.

- [104] K. Nagaraj, L. Lapkina-Gendler, R. Sarfstein, D. Gurwitz, M. Pasmanik-Chor, Z. Laron, S. Yakar, H. Werner, Identification of thioredoxin-interacting protein (TXNIP) as a downstream target for IGF1 action, *Proc Natl Acad Sci U S A* 115(5) (2018) 1045-1050.
- [105] H. Li, C. Xu, Q. Li, X. Gao, E. Sugano, H. Tomita, L. Yang, S. Shi, Thioredoxin 2 Offers Protection against Mitochondrial Oxidative Stress in H9c2 Cells and against Myocardial Hypertrophy Induced by Hyperglycemia, *Int J Mol Sci* 18(9) (2017).
- [106] L. Cai, Y. Wang, G. Zhou, T. Chen, Y. Song, X. Li, Y.J. Kang, Attenuation by metallothionein of early cardiac cell death via suppression of mitochondrial oxidative stress results in a prevention of diabetic cardiomyopathy, *J Am Coll Cardiol* 48(8) (2006) 1688-97.
- [107] B.L. Mau, G. Powis, Inhibition of cellular thioredoxin reductase by diaziquone and doxorubicin. Relationship to the inhibition of cell proliferation and decreased ribonucleotide reductase activity, *Biochem Pharmacol* 43(7) (1992) 1621-7.
- [108] B. Liao, R. Chen, F. Lin, A. Mai, J. Chen, H. Li, S. Dong, Z. Xu, Imperatorin protects H9c2 cardiomyoblasts cells from hypoxia/reoxygenation-induced injury through activation of ERK signaling pathway, *Saudi Pharm J* 25(4) (2017) 615-619.
- [109] L. Nonn, R.R. Williams, R.P. Erickson, G. Powis, The absence of mitochondrial thioredoxin 2 causes massive apoptosis, exencephaly, and early embryonic lethality in homozygous mice, *Mol Cell Biol* 23(3) (2003) 916-22.
- [110] K. Shioji, C. Kishimoto, H. Nakamura, H. Masutani, Z. Yuan, S. Oka, J. Yodoi, Overexpression of thioredoxin-1 in transgenic mice attenuates adriamycin-induced cardiotoxicity, *Circulation* 106(11) (2002) 1403-9.

- [111] S. Kylarova, D. Kosek, O. Petrvalska, K. Psenakova, P. Man, J. Vecer, P. Herman, V. Obsilova, T. Obsil, Cysteine residues mediate high-affinity binding of thioredoxin to ASK1, *Febs j* 283(20) (2016) 3821-3838.
- [112] K. Min, O.S. Kwon, A.J. Smuder, M.P. Wiggs, K.J. Sollanek, D.D. Christou, J.K. Yoo, M.H. Hwang, H.H. Szeto, A.N. Kavazis, S.K. Powers, Increased mitochondrial emission of reactive oxygen species and calpain activation are required for doxorubicin-induced cardiac and skeletal muscle myopathy, *J Physiol* 593(8) (2015) 2017-36.
- [113] H. Cha-Molstad, G. Saxena, J. Chen, A. Shalev, Glucose-stimulated expression of Txnip is mediated by carbohydrate response element-binding protein, p300, and histone H4 acetylation in pancreatic beta cells, *J Biol Chem* 284(25) (2009) 16898-905.
- [114] Y.L. Chen, S.Y. Chung, H.T. Chai, C.H. Chen, C.F. Liu, Y.L. Chen, T.H. Huang, Y.Y. Zhen, P.H. Sung, C.K. Sun, S. Chua, H.I. Lu, F.Y. Lee, J.J. Sheu, H.K. Yip, Early Administration of Carvedilol Protected against Doxorubicin-Induced Cardiomyopathy, *J Pharmacol Exp Ther* 355(3) (2015) 516-27.
- [115] Q.L. Zhang, J.J. Yang, H.S. Zhang, Carvedilol (CAR) combined with carnosic acid (CAA) attenuates doxorubicin-induced cardiotoxicity by suppressing excessive oxidative stress, inflammation, apoptosis and autophagy, *Biomed Pharmacother* 109 (2019) 71-83.